Unveiling metabolomic and transcriptomic responses to waterlogging in spring wheat at different developmental stages

Dissertation

zur Erlangung des

Doktorgrades der Naturwissenschaftlichen (Dr. rer. nat.)

der

Naturwissenschaftlichen Fakultät I

- Biowissenschaften -

der Martin-Luther-Universität Halle-Wittenberg

vorgelegt von

Frau Geeisy Angela Cid Valdés

geboren am 17.12.1992 in Ciego de Avila (Kuba)

Gutachter: 1. Prof. Dr. Nicolaus von Wirén

2. Prof. Dr. Edgar Peiter

3. Prof. Dr. Philipp Franken

Verteidigung am: 24.10.2023

Halle (Saale)

To my loving parents Angela and Carlos,
whose endless love and support accompany me always

A mis queridos padres Angela y Carlos,
cuyo amor y apoyo infinitos me acompañan siempre

TABLE OF CONTENTS

1. SUMMARY

Among the extreme weather conditions caused by climate change, flooding has a particular strong impact on crop productivity and global food security. Excessive water in the soil limits oxygen transport to the roots, impairing respiration, nutrient uptake and metabolism. Roots have developed adaptive mechanisms against hypoxia, such as changes in root morphology or ATP production via fermentation. However, the dynamics of metabolic and transcriptomic responses of flooding-susceptible crop species, such as wheat, to waterlogging and the subsequent recovery are still not fully understood.

This study investigated temporally coordinated changes in metabolism and gene regulation in leaves and roots of wheat plants (*Triticum aestivum*) during and after waterlogging at different developmental stages, using ionomic, metabolomic, and transcriptomic approaches. A 12-day waterlogging period during tillering or booting, significantly affected the nutrient status of wheat plants, causing a decrease in the concentrations of nitrogen, phosphorus, potassium, and magnesium, and an increase in manganese and iron. This effect was more evident in the leaves and roots of waterlogged plants at tillering and booting respectively. At tillering stage, primary metabolites, including non-structural carbohydrates, organic acids, and amino acids, were accumulating in roots under waterlogging, while leaves of the same plants showed only increasing concentrations of glucose but reduction of the rest of metabolites. Opposite effect was observed at booting, as the same metabolites increased more in the leaves than in the roots. Either of these changes resulted in decreased plant height, root biomass, and enhanced leaf chlorosis, with negative impacts on grain yield parameters.

At tillering stage, waterlogging strongly decreased xylem exudation and hormone translocation rates, but these effects were temporary and reversed after draining excess water. Wheat plants accumulated alanine in the roots and increased its translocation in the xylem as the most predominant metabolic changes under waterlogging. This regulation was interpreted as a strategy of plants to re-program carbon and nitrogen metabolism in leaves to meet energy requirements in roots. It was then hypthesised that alanine plays a dual role as an amino-nitrogen form for long-distance transport as well as carbon source for pyruvate recycling, facilitating glucose biosynthesis.

Gene expression in waterlogged plants was found to be tissue and stage specific and reflected major changes in carbon and nitrogen metabolisms. Notably, hypoxia-responsive genes were activated in the roots at tillering only. However, nutrient-transport-related genes were de-regulated in either tissue and growth stage. Finally, this study compared also transcriptional and metabolic responses between waterlogging and drought. Although these opposing stresses were largely characterised by different changes in the transcriptome and metabolome, some responses including the accumulation of sugars and of particular amino acids were common to both stresses.

In conclusion, this study demonstrates that wheat plants respond to waterlogging by initiating metabolic and transcriptomic changes starting in the roots. Through enhanced alanine translocation to leaves this metabolic acclimation leads to a systemic response that balances the differential demands of roots and leaves for carbon and nitrogen under waterlogging, and allows plants to overcome prolonged periods of hypoxia.

2. ZUSAMMENFASSUNG

Unter den Klimawandel-bedingten Extremwetterereignissen haben Überschwemmungen einen erheblichen Einfluss auf die Ernteerträge und die globale Ernährungssicherheit. Überschüssiges Wasser im Boden verringert den Sauerstoffgehalt in den Wurzeln und verringert die Respiration sowie die Aufnahme und den Metabolismus von Nährstoffen. Pflanzen haben Anpassungsmechanismen an Sauerstoffmangel entwickelt, einschließlich Veränderungen in der Wurzelmorphologie oder ATP-Produktion über Fermentation. Die Dynamik der metabolischen und transkriptomischen Reaktionen von überstau-sensitiven Kulturarten wie Weizen während und nach der Überflutung sind jedoch noch nicht vollständig verstanden.

Diese Studie untersuchte zeitlich koordinierte Veränderungen im Stoffwechsel und in der Genregulation in Blättern und Wurzeln von Weizenpflanzen (*Triticum aestivum*) während und nach Wasserüberstau in zwei Entwicklungsstadien. Ionom, Metabolom und Transkriptom Analysen durchgeführt. Eine 12-tägige Wasserstau-Periode während des Bestockens oder Schossens hatte signifikante Auswirkungen auf den Ernährungszustand der Weizenpflanzen mit verringerten Konzentrationen von Stickstoff, Phosphor, Kalium und Magnesium und einer Zunahme von Mangan und Eisen. Dieser Effekt war bei den Blättern und Wurzeln der überschwemmten Pflanzen während des Bestockens bzw. Schossens deutlicher erkennbar. In der Bestockungsphase primäre Metabolite, wie nicht-strukturelle Kohlenhydrate, organische Säuren und Aminosäuren, sammelten sich in den Wurzeln an, während die Blätter nur eine erhöhte Konzentration von Glucose aufwiesen, jedoch eine Verringerung der übrigen Metabolite zeigten. In der Ährenbildungsphase wurde hingegen der entgegengesetzte Effekt beobachtet, da die gleichen Stoffwechselprodukte in den Blättern stärker anstiegen als in den Wurzeln. Diese Veränderungen führten zu einer Verringerung der Pflanzenhöhe, der Wurzelbiomasse und zu verstärkter Blattchlorose, was sich negativ auf die Kornausbeute auswirkte.

In der Bestockungsphase verringerte Wasserüberstau stark die Xylem-Exsudation und die Hormontranslokation, aber diese Effekte waren vorübergehend und kehrten nach Entfernen des überschüssigen Wassers um. Die Weizenpflanzen akkumulierten Alanin in den Wurzeln und erhöhten dessen Translokation im Xylem als vorherrschende Stoffwechselveränderung bei Wasserüberstau. Diese Regulation wurde als eine Strategie der Pflanzen interpretiert, um den Kohlenstoff- und Stickstoffstoffwechsel in den Blättern umzuprogrammieren, um den Energiebedarf in den Wurzeln zu decken. Es wurde vermutet, dass Alanin eine doppelte Rolle als Amino-Stickstoff-Form für die Translokation und als Kohlenstoffquelle für das Recycling von Pyruvat und die Glucose-Biosynthese spielt. Die Genexpression bei wasserstauenden Pflanzen war gewebespezifisch und stadienspezifisch verändert und spiegelte die wesentlichen Veränderungen im Kohlenstoff- und Stickstoffstoffwechsel wider. Insbesondere Hypoxie-responsive Gene wurden nur in den Wurzeln während der Bestockungsphase aktiviert. Allerdings waren Gene des Nährstofftransports in beiden Geweben und Wachstumsphasen dereguliert. Schließlich verglich diese Studie auch die transkriptionellen und metabolischen Veränderungen zwischen Wasserüberstau und Trockenheit. Obwohl diese entgegengesetzten Stressbedingungen hauptsächlich durch unterschiedliche Veränderungen im Transkriptom und Metabolom charakterisiert waren, wiesen einige Reaktionen, wie der Akkumulation von Zuckern und bestimmten Aminosäuren Gemeinsamkeiten auf.

Zusammenfassend zeigt diese Studie, dass Weizenpflanzen auf Wasserüberstau mit metabolischen und transkriptomischen Veränderungen reagieren, die von den Wurzeln ausgehen. Über eine

erhöhte Translokation von Alanin in die Blätter führt diese metabolische Akklimation zu einer systemischen Antwort, die Kohlenstoff und Stickstoff zwischen Wurzeln und Blättern ausgewogen verteilt und es den Pflanzen ermöglicht, längere Phasen von Sauerstoffmangel zu überwinden.

3. INTRODUCTION

3.1 Waterlogging impacts important agricultural ecosystems globally

The ongoing global warming has become one of the most pressing challenges, as it significantly affects weather patterns with serious consequences for existing agriculture in terms of plant development and productivity. The alteration of weather conditions has led to various disruptions, with floods accounting for the highest percentage of occurrences globally. The frequency of floods has been increasing, causing significant damage to agricultural crop-production systems. According to the Ecological Threat Report 2022 (ETR, 2022), between 1981 and 2022, flood events accounted for 41.5% of natural disasters worldwide. In 2022, Asian countries, such as Indonesia, China, and the Philippines, recorded the highest frequency of floods, followed by countries in the Americas, including the United States, Colombia, and Brazil. Yet, floods constituted the second natural disaster after drought in terms of the number of affected people and the same position after extreme temperatures in terms of the number of deaths (CRED, 2022). In addition, the impact of climate change on forced migration is increasing, as tens of millions of people worldwide are displaced from their homes every year due to flooding (Mousavi *et al.,* 2011; Paterson, Wright and Harris, 2018). This migratory displacement will eventually affect the infrastructure and economies of less affected regions such as Europe, as more and more people are displaced (ETR, 2022). Notably, floods are also increasingly occurring in northeastern and western Europe, with the timing of floods shifting to earlier in the year (Blöschl *et al.,* 2017; Shirzaei *et al.,* 2021).

The subtypes of floods, namely flash floods, river floods, and coastal floods, are characterised by different impact profiles in space and time, as reported by Kruczkiewicz *et al.* (2022). A historical analysis of natural hazards in Europe by the HANZE database revealed that 1564 flood events were recorded from 1870 to 2016, of which 879 (56%) were flash floods, 606 (39%) were river floods, 56 (4%) were coastal floods, and the remaining 23 (1.5%) were floods caused by the coincidence of storm surge and high river water (Paprotny *et al.,* 2018). Unfortunately, these events have been sufficient to cause the destruction of agricultural lands, crops, livestock, critical agricultural infrastructure, and household food reserves. The impact of flooding on agricultural production systems worldwide is significant, being the second gravest disaster responsible for a total of USD 21 billion of crop and livestock production losses incurred between 2008 and 2018, mainly in least developed and middle-income countries (FAO, 2021). These losses have severe implications for food security, particularly for the most vulnerable communities that rely heavily on agriculture for their livelihoods.

Floods of agricultural fields is typically caused by prolonged rainfall (Fukao *et al.,* 2019). The distribution of crops and species is often directly influenced by the annual timing of rainfall and the

depth of the groundwater table. The latter, in turn, affects the hydrology of the soil and the physiological conditions to which plants must adapt in response to changes in water availability (D'Odorico *et al.,* 2013; Fukao *et al.,* 2019). An imbalance of water in the soil not only changes the physical and chemical properties of the ecosystem but also has harmful effects on plants and animals (www.fao.org). Flooding can have detrimental effects on plant growth and productivity, depending on the depth of the water table in agricultural lands (Nishiuchi *et al.,* 2012; Fukao *et al.,* 2019). It can cause submergence or waterlogging stress, both of which can lead to the emergence of new plant diseases and a reduction in agricultural productivity, with long-term negative economic and social impacts. When plants are exposed to waterlogging, only root tissues are directly affected by the excess water, whereas submergence affects the entire plant with all above-ground tissues being under water leading to disruptions in photosynthesis and respiration (Schulze *et al.,* 2019; Kaur *et al.,* 2020).

In general, waterlogging is a serious problem that can have a significant impact on agricultural ecosystems worldwide, and have economic and social impacts, particularly in agricultural regions. Therefore, addressing waterlogging is crucial to develop sustainable and productive agricultural systems globally.

3.2 Economic losses in crop productivity due to waterlogging

Worldwide, 20% of irrigated land is affected by waterlogging (den Besten *et al.,* 2021). However, its impacts on crop yields depends on many factors such as variations in the climatic conditions, soil type, crop species and genotype (Kaur *et al.,* 2020). To illustrate the economic losses associated to waterlogging, a recent report stated that waterlogging has a significantly negative effect on winter wheat and winter barley of up to 1.50 Euros/ha across Germany, mainly in the southern area. One day of waterlogging during tillering and flowering resulted in a yield reduction of 0.28% for winter wheat and 0.23% during seed formation and ripening. The same was true for winter barley yields, which decreased by 0.40 % per day during tillering and flowering and by 0.24 % during seed formation and ripening (Schmitt *et al.,* 2022).

Seed production of field peas declined to 6%, and in the United States the loss of crop production between 2010 and 2016 amounted to about USD 360 million per year. In the Argentine Pampas, a vast plain of about 50 million ha, about 31% of the land has been repeatedly affected by waterlogging since 2002 (Ploschuk *et al.,* 2018). Depending on the duration of waterlogging, soil type and genotypes, wheat and barley yield losses ranged from 15 to 25% (Setter and Waters, 2003; Herzog *et al.,* 2016). Furthermore, annual losses in wheat production due to waterlogging in Australia are estimated at EUR 180 million (den Besten *et al.,* 2021). Waterlogging events are projected to increase also in the United Kingdom, the Netherlands and Denmark by 2060 (Mäkinen

et al., 2018), and according to the NASA dynamic-crop models, it is predicted that corn production losses in the United States due to waterlogging will be about USD 3 billion per year by 2030 (Rosenzweig *et al.,* 2002). It is therefore an important task to develop strategies over the next decades to either avoid further climate change and subsequent waterlogging, and/or to select for new adaptive traits in crops to cope with this stress.

3.3 Oxygen depletion in plant cells as a major consequence of waterlogging

Waterlogging induces significant changes in soil structure and porosity, which in part are directly correlated with the oxygen (O_2) concentration in the soil. However, when soil pores are occupied by water, the diffusion of oxygen becomes significantly slower, approximately 10 000 times slower than in air-filled soil pores (Wongs-Aree and Noichinda, 2018). This ultimately limits the availability of oxygen to the plants, leading to a negative impact on cellular metabolism. Additionally, waterlogged soils experience a reduction in redox potential (Eh), which results in a highly competitive demand for oxygen (Wongs-Aree and Noichinda, 2018).

The most significant impact of waterlogging is the decreasing availability of oxygen (Parent *et al.,* 2008). In well-aerated soils, i.e. under normoxia, oxygen concentrations in plant cells are typically around 8-8.5 mg $O_2 \cdot l^{-1}$ (Wongs-Aree and Noichinda, 2018) as root cells profit from oxygen diffusion through the air-filled pores in the soil matrix. However, during waterlogging oxygen diffusion decreases, and gas exchange between the soil and root is restricted, leading to partial or complete oxygen deficiency (Pan *et al.,* 2021). This oxygen deficiency negatively impacts all metabolic reactions that require oxygen as a terminal electron acceptor, which are essential for plant growth and survival.

Oxygen deficiency in plant cells can result in two distinct levels of stress, hypoxia or anoxia, depending on the concentration of available oxygen. Hypoxia occurs when oxygen decrease to a point where oxidative damage becomes the limiting factor, while anoxia occurs when there is no longer any oxygen available, and ATP can only be generated through fermentative glycolysis (Wongs-Aree and Noichinda, 2018). Hypoxia or anoxia stress can lead to changes in gene transcription and mRNA translation (Bailey-Serres and Voesenek, 2008), as well as altered cellular metabolism, which promotes anaerobic metabolism for ATP production in a less efficient manner. Furthermore, the lack of oxygen can also inhibit the electron transport chain of chloroplasts and mitochondria, leading to the production of reactive oxygen species (Sachdev *et al.,* 2021). However, the effect of oxygen deprivation on plants can vary depending on factors such as cell type, tissue type, developmental stage, and genotype, as well as the severity and duration of the stress (Fukao and Bailey-Serres, 2004). Therefore, it is important to consider these factors when studying the effects of waterlogging stress on plant growth and development.

3.4 Phenology and morphology of waterlogged plants

Waterlogging stress has a significant negative impact on plant growth and development, resulting in reduced yields and decreased plant health. Recent studies have conducted tissue-specific investigations to better understand the morphological and physiological acclimation of plants in different organs, such as roots, shoots, or whole seedlings under flooding (Ellis, Dennis and James-Peacock, 1999; Kreuzwieser *et al.,* 2009; Hsu *et al.,* 2011; Mustroph *et al.,* 2014; Lothier *et al.,* 2020). The degree of sensitivity to waterlogging in plants depends on multiple factors, including the stage of development, the duration of the event, and external conditions (Setter and Waters, 2003). Furthermore, different plant species exhibit varying physiological, morphological, and growth responses to waterlogging. For instance, wheat and barley may experience reduced root growth, chlorosis, premature leaf senescence, tiller reduction, reduced dry matter accumulation, decreased number and weight of kernels, and increased flower sterility due to waterlogging (Marti *et al.,* 2015; Ploschuk *et al.,* 2018). However, wheat can tolerate early and late waterlogging, while barley and rapeseed are more susceptible to late waterlogging, and field pea is strongly affected at both timings (Ploschuk *et al.,* 2020). Different oat varieties may display chlorosis and early senescence, reduced nitrogen concentration in shoots, and a decrease in grain yield of up to 42% under waterlogging, but the physiological processes involved in dry matter accumulation and mineral uptake can be resumed after drainage (Arduini, Baldanzi and Pampana 2019a). Similarly, waterlogging-exposed cucumber plants may exhibit impaired growth, biomass, and photosynthesis (Barickman, Simpson and Sams 2019). The inhibition of leaf emergence, a reduced number of terminal leaves, yellowing of basal leaves, and delay of flowering and maturity are typical phenological changes observed in plants exposed to waterlogging. Nonetheless, phenological delay under waterlogging has been linked to greater waterlogging tolerance when comparing different plant genotypes (Liu *et al.,* 2020).

Roots are the first target of waterlogging stress in plants, and the impact is mainly reflected in reduced root growth and rooting depth, leading to decreased nutrient uptake and overall plant growth (Ploschuk *et al.,* 2020). Fine roots and root meristems are particularly sensitive to oxygen deficiency. In species that cannot tolerate flooding, the parts of the root system responsible for water and ion uptake die off when the oxygen partial pressure falls below 0.5-5 kPa, leading to responses similar to drought stress, even though the plant is in water. This is indicated by stomata closure, decreases in photosynthesis and growth and stunted plant growth with severe epinasty or modifications in leaf traits to reduce transpiration and conserve water (Schulze *et al.,* 2019). However, plants have evolved various mechanisms to cope with waterlogging and prevent damage to their tissues. Aerenchyma formation plays a crucial role in internal long-distance oxygen transport from shoot to root in waterlogged soil (Arduini, Kokubun and Licausi 2019b). Adventitious

roots can grow towards air to access oxygen from the above-ground. After drainage, survival of root tips, lateral root initiation, and restoration of tillering are considered crucial developmental processes to ensure recovery (Herzog *et al.,* 2016).

Waterlogged plants have evolved various strategies to cope with the stress, with three main adaptive mechanisms that can come into play: escape, quiescence, or self-regulation compensation (Zhang *et al.,* 2021). The escape strategy involves accelerating growth and elongation of internodes to "escape" the hypoxic environment, often seen in complete submergence. However, plants can also apply an escape strategy under waterlogging by increasing adventitious root growth and/or producing aerenchyma (Guan *et al.,* 2019; Zhang *et al.,* 2021). Alternatively, the quiescence strategy allows plants to survive temporary flooding in an energy-saving manner with reduced carbohydrate metabolism, ATP consumption, and lower biomass formation (Parlanti *et al.,* 2011; Nishiuchi *et al.,* 2012; Bailey-Serres, Lee and Brinton, 2012; Voesenek and Sasidharan, 2013; Zaman *et al.,* 2019; Loreti and Perata, 2020). This is more commonly observed in the context of waterlogging, where a series of metabolic changes occur. The self-regulating compensation mechanism allows plants to accelerate growth and development and exploit their indeterminate growth habit and compensatory growth ability (Zhang *et al.,* 2021). Understanding these adaptive mechanisms can aid in the development of crops with improved waterlogging tolerance and in better management practices for flooded areas.

In general, the effect of waterlogging on plant phenology and morphology varies depending on the specific circumstances and the severity of the stress, which can differ among plant species. Certain plants have developed effective mechanisms to adapt to waterlogging, while others are more vulnerable to the negative effects of this stress. Thus, it is crucial to conduct research on different plant species to enhance our understanding of ecosystem functioning and improve agricultural productivity under waterlogging conditions.

3.5 Nutrient uptake and translocation in plants under waterlogging

Nutrient uptake in waterlogging conditions is commonly reduced by several factors, such as lower root surface area, inhibition of root elongation, and impaired root hydraulic conductivity. For instance, in wheat roots exposed to short-term hypoxia, the hydraulic conductivity of root cortical cells was reduced by 45%, as reported by Bramley *et al.* (2010). This limitation in water transport ultimately affects nutrient uptake and distribution. Similarly, Qiu *et al.* (2007) observed that maize roots that were waterlogged for six days were unable to absorb nutrients from the soil, resulting in nutrient deficiency and yellowing of the leaves.

Waterlogging stress can cause a decrease in the redox potential of the soil due to the low oxygen partial pressure, leading to the growth of anaerobic microorganisms. These microorganisms in a

state of negative O_2 concentration, utilize nitrate (NO_3^-) as an electron acceptor, which is then rapidly reduced to nitrite (NO_2^-), and eventually to molecular nitrogen (N_2) or other oxygenated forms of nitrogen (NO, N_2O) as part of the denitrification process. The reduction of N concentration can be significant, estimated at 61% per day of waterlogging. Meanwhile, N losses from soils due to nitrous oxide (N_2O) emissions can range from 1.1-2.6% (Zurweller *et al.,* 2015). Nitrate leaching is also a concern as it becomes more dislocated from the top soil, contributing to approximately 11% of the total NO_3^- loaded to the groundwater (Huber *et al.,* 2012). However, the degree of N losses in different forms varies depending on the type and structure of the soil. Simultaneously, ammonium (NH_4^+) accumulates due to the suppression of nitrification. Ammonification rates depend on several conditions such as the N requirements of the anaerobic microbial community, pH, temperature, and nutrient availability (Reddy, Patrick and Broadbent, 1984). As the redox potential decreases dramatically, soil redox reactions occur, such as the reduction of iron (Fe (III)) and manganese (Mn (IV)) to their respective divalent ions Fe^{2+} and Mn^{2+} making these nutrients more available for higher uptake than their oxidized forms. Under these conditions, the concentration of theses nutrients reaches toxic levels to the plants. Additionally, waterlogging can result in the complete consumption of sulfate (SO_4^{2-}) and the formation of methane (CH_4), leading finally to soil alkalization as these reactions mostly consume protons (Schulze *et al.,* 2019).

In waterlogged roots, inhibition of H^+-ATPase activity due to low ATP can lead to a reduced proton motive force across the plasma membrane, and a less negative membrane potential leading to the inhibition of most nutrient uptake and xylem transport processes (Mancuso and Shabala, 2010; Colmer and Greenway, 2011). In addition, ion uptake can be further inhibited by the down-regulation of transport systems, which is a common energy-saving strategy to preserve essential processes (Elzenga and van Veen, 2010). Altered nutrient availabilities under waterlogging can lead to lower levels of phosphorus (P), potassium (K), magnesium (Mg), copper (Cu) and zinc (Zn) uptake. For example, in barley net K^+ uptake decreased even within a few minutes of waterlogging (Steffens *et al.,* 2005; Shabala and Pottosin, 2014). When wheat plants were waterlogged, decreases in nutrient concentrations in their shoots resulted from less nutrient uptake and translocation from the roots, as well as continued growth of the shoots, which further dilutes the nutrient pool in these tissues (Herzog *et al.,* 2016). Nutrient acquisition is also negatively affected by the disruption of symbiosis between plant roots and mycorrhiza fungi in waterlogged soils (Schulze *et al.,* 2019). However, in the case of P uptake, it is often observed that its availability is increasing with the availability of some transition metals, such as Fe (Elzenga and van Veen, 2010).

Waterlogged plants can adapt to nutrient shortages by redistributing endogenous nutrients. For example, early leaf senescence under waterlogging remobilises N from older to younger leaves (Tong *et al.,* 2021). Previous studies have also shown that supplying additional nutrients to

waterlogged barley leaves increases N and K concentrations in roots, suggesting that nutrients are translocated from leaves to roots to compensate for losses in root uptake and support root growth under flooding conditions (Tong *et al.,* 2021). Studies conducted in rapeseed indicated a reduction in N accumulation in plants exposed to waterlogging at the five-leaf stage in pot and field trials (Men *et al.,* 2020). However, the same authors reported that the application of N fertilisers to the same plants increased N accumulation in shoots at different stages of development.

In general, the nutrient uptake and transport of plants under waterlogging can be influenced by various factors, such as soil type, plant species, and the duration and intensity of waterlogging. Waterlogging can trigger severe deficiencies in essential nutrients, while also leading to the accumulation of Fe and Mn in toxic levels, which can adversely affect plant growth and development. Therefore, a comprehensive understanding of the nutrient uptake and transport of plants under waterlogging can help in identifying processes that are more crucial under this stress condition and in developing strategies to mitigate its negative impacts on crop productivity.

3.6 Biochemical modifications as an acclimative response of plants to cope with waterlogging

Plants, being sessile organisms, have developed the ability to sense flooding and readjust their metabolism to survive. However, this acclimation often comes at the cost of reduced growth and reproduction. Biochemical readjustments include switching from glycolysis to lactate and ethanol production in their roots. This allows them to compensate for the reduction of the electron flow through the respiratory pathway, which leads to lower rates of ATP production (Parent *et al.,* 2008), but helps the plants to maintain cell viability in the short term.

The ability of plants to tolerate waterlogging is related to their molecular, metabolic, and physiological characteristics, which determine how they convert their metabolism under strong environmental influences (Waters *et al.,* 1991). However, this acclimation comes with a reduction in cellular energy, cytoplasmic pH, and the production and accumulation of toxic metabolites and reactive oxygen species. Waterlogging can lead to the accumulation of soluble sugars, polyols, and starch in the leaves of various plant species, including *Medicago truncatula* (Lothier *et al.,* 2020) and others (Irfan *et al.*, 2010). This accumulation suggests that the transportation of assimilates to the roots may be hindered by waterlogging. Lothier *et al.* (2020) reported an increased imbalance between sugar loading in the phloem by shoots and unloading by roots as the sugar pool increased in the phloem. However, they also observed a significant decrease in sucrose levels in the roots of waterlogged plants. This disruption in phloem unloading under waterlogging can be attributed to the low energy charge of the plant tissues caused by the Pasteur effect, which maintains a low energy charge during waterlogging (Schulze *et al.,* 2019). However, alternative pathways are required to maintain a constant flow of assimilates. Sugars and amino acids produced in the shoots

have been shown to play an important role in carbohydrate delivery to the roots allowing them to maintain glycolytic metabolism (De Sousa and Sodek, 2003; Lothier *et al.,* 2020). For example, wheat (Herzog *et al.,* 2016), tomato (Mignolli, Barone and Vidoz, 2021), and waterlogged trees (Kreuzwieser & Rennenberg, 2014) have been reported to experience an increased demand for soluble carbohydrates, leading to higher sugar transport to the waterlogged roots than in control plants. Furthermore, waterlogging has also an impact on the concentration of amino acids in plants. Studies by Kreuzwieser *et al.* (2009) and Kreuzwieser and Rennenberg (2014) have shown increased concentrations of certain amino acids derived from glycolysis in the roots and xylem exudates of waterlogged plants, while the levels of most amino acids decreased in the leaves. However, amino acids derived from tricarboxylic cycle (TCA) intermediates, such as glutamine (Gln) are generally negatively affected by waterlogging in the roots and xylem exudates (Oliveira, Freschi and Sodek, 2013). Decreased concentration of these amino acids can be attributed to inhibited biosynthesis of the intermediates in the TCA cycle that provides the carbon skeletons for their synthesis. Alternatively, certain amino acids may serve also as signaling molecules between roots and shoots. During the inhibition of mitochondrial respiration and switch to a fermentative metabolism, it is required an increased throughput of energy sources, in particular glucose, must be maintained, as the metabolic energy yield is much lower, i.e. 2 moles of ATP per mole of glucose by glycolysis compared to 34-36 moles of ATP per mole of glucose by oxidative phosphorylation. Under these conditions, metabolic reserves are quickly depleted (Schulze *et al.,* 2019). Such reserves comprise also alanine (Ala), resulting from alternative metabolic routes in order to prevent carbon loss in the form of ethanol that readily permeates through cell membranes and gets lost. The transamination of pyruvate (Pyr) via glutamate (Glu), catalysed by the enzyme alanine aminotransferase (ALAT), is induced under waterlogging and thought to be the main source of Ala production in waterlogged rice roots (Reggiani 1999; Reggiani *et al.,* 2000). Interestingly, high concentrations of Ala have also been found in the xylem sap of soybean under hypoxia, suggesting that this amino acid is an important compound translocated from roots to shoots (De Sousa and Sodek, 2003). Extensive studies have addressed the function of Ala production under oxygen depletion by ALATs (Miyashita and Good, 2008; Rocha *et al.,* 2010a; Rocha *et al.,* 2010b; Bailey-Serres *et al.,* 2012b). The readily reversible activity of this enzyme and its numerous isoforms play an important role in Ala production to recover the carbon that otherwise may be lost through ethanol production (Watson *et al.,* 1992; Orzechowski, Socha-Hanc and Paszkowski, 1999). Other amino acids, such as Gln, gamma-aminobutyric acid (GABA) and putrescine have also been frequently identified as dominant amino acids during waterlogging (Reggiani 1999). However, it is still poorly understood how and to what extent Ala is translocated and further degraded to meet energy needs in energy-deficient plants. Interestingly, in humans other ALAT homologues with glyoxylate aminotransferase (AGT) activity

use alanine: glyoxylate as substrates to produce pyruvate and glycine (Gly) (Liepman and Olsen 2003). Despite the well-documented functions of different types of AGTs in humans, the function of this enzyme in plants for Ala degradation remains poorly understood, esp. in scenarios such as flooding that provoke metabolic changes. Further clarification is needed to understand the function of Ala metabolism in roots, Ala translocation to shoots, and Ala degradation in leaves for recycling C-N forms.

Studies have shown that hormones also play a crucial role in the ability of plants to regulate their response to waterlogging. For example, Arbona and Gómez-Cadenas (2008) found that different Citrus genotypes exposed to waterlogging exhibited a progressive increase of abscisic acid (ABA) and a rapid increase of jasmonic acid (JA) in the leaves. However, the same authors observed a rapid decrease in ABA and JA while indole acetic acid (IAA) increased in the waterlogged roots of the same plants. The balance between ethylene (ET) and ABA is also important for plant adaptation to waterlogging, as both hormones have partly opposite effects on the growth and development of plants (Bailey-Serres and Voesenek, 2008). These results suggested that not only the increase of hormones indicates their role in regulating down-stream responses to stress, but also the reduction of the same.

In general, plants have evolved a range of intricate acclimative responses to withstand waterlogging stress. One such acclimation involves modifications of carbohydrate and amino acid metabolism to sustain glycolysis and maintain energy production at a reduced rate, thus allowing the plant to conserve energy and enhance survival. However, differences in the response of tolerant and sensitive species underscore the complexity of the metabolic adjustments that plants undertake to cope with waterlogging stress.

3.7 Core-hypoxia-responsive genes as molecular markers in waterlogged plants

The transition of plants from aerobic respiration to lactic acid fermentation requires the expression of lactate dehydrogenases (LDH) (Kreuzwieser *et al.,* 2009). As the accumulation of lactic acid leads to acidification of the cytoplasm, the activity of LDH is reduced, which favors alcoholic fermentation (Kreuzwieser and Rennenberg, 2014). The activities of the enzymes required for alcoholic fermentation, which include pyruvate decarboxylase (PDC) and alcohol dehydrogenase (ADH), are elevated in waterlogged roots (Atkinson, Harrison-Murray and Taylor, 2008). Sucrose synthase (SUS), is also important for survival in hypoxia (Santaniello *et al.,* 2014). Among the signalling molecules moving from roots to shoots, ethylene has been shown to play a crucial role in the above-mentioned acclimative response of plant organs to hypoxia, including the formation of aerenchyma, the appearance of adventitious roots and epinasty (Schulze *et al.,* 2019). Inhibitors of the synthesis of 1-aminocylopropane-1-carboxylic acid (ACC), the precursor of ethylene biosynthesis, have been

reported to also inhibit the synthesis of the latter expressing in petiole epinasty in tomato plants exposed to waterlogging (Bradford, Hsiao and Yang, 1982).

A specific subfamily of transcription factors (TF), the ethylene response factors of the VII group (ERF-VIIs), plays an important role in regulating the activation of fermentation-related genes (Bailey-Serres and Voesenek, 2008). In plants, ERF-VII-related genes have been found to play a role in the oxygen-sensing mechanism through the N-end rule pathway of proteolysis (Gibbs *et al.,* 2011; Licausi *et al.,* 2011). Under hypoxia, ERF-VIIs are induced and activate the expression of hypoxia-responsive genes, including the genes *PDC1* and *ADH1* required for fermentation.

Occasional hypoxia can be compensated by the expression of so-called "core hypoxia-responsive genes". Such a genetic response leads to a re-orchestration of primary root metabolism, including (i) the induction of ethanolic fermentation by up-regulation of *PDC1* and *ADH1*, (ii) an increase in sucrose synthase to metabolise sugars, by up-regulation of sucrose synthase1 (*SUS1*) and *SUS4*, and (iii) the accumulation of metabolites from alternative pathways (Lee *et al.,* 2011; Herzog *et al.,* 2016; Lothier *et al.,* 2020). In different waterlogging-tolerant and susceptible wheat varieties, *TaERFVII.1* has been reported to play an important role in response to waterlogging, exhibiting differential expression patterns between varieties (Wei *et al.,* 2019). The same authors demonstrated that the expression of this TF in wheat increased the expression of waterlogging-responsive genes that enhance grain weight per plant, survival rate, and chlorophyll content of leaves, and may be a candidate for improving tolerance to waterlogging in crops. Short- and long-term studies in tomato plants have also shown that hypoxia regulates the expression of genes involved in carbon and amino acid metabolism and affects the link between N metabolism and the formation/scavenging of nitric oxide (NO) (Safavi-Rizi, Herde and Stöhr, 2020). The same authors also reported up-regulation of genes involved in glycolysis (*ENO2, PPC4* and *TPI*), fermentation (*PDC2, ADH1*), amino acid synthesis and degradation (*ALAT, GAD4*), while genes encoding nitrite reductase 1 (*NIR1*), nitrate transporters (*NRT2.4, NRT1.1, NRT1.2*) and an uncharacterised nitrate transporter were down-regulated.

Overall, hypoxia-responsive genes are regulated by a complex network of molecular pathways, including the activation of transcription factors, and changes in gene expression. These genes can play critical roles in the regulation of plant growth and development, and provide valuable insights into the molecular mechanisms underlying plant responses to waterlogging.

3.8 Aim of the dissertation

Individual mechanisms of physiological, biochemical, and molecular readjustments that occur as a result of waterlogging have been extensively described in several plant species. However, the understanding of how these changes interact and build a systemic response in waterlogged plants,

and finally allow the plants to cope with this stress is still limited. This holds true particularly for wheat, one of the most important crop species being threatened by waterlogging.

Against this background, the present dissertation has been built on the hypothesis that waterlogging stress triggers a systemic response in wheat plants, involving coordinated changes that occur in roots and leaves and thus throughout the plant. It is assumed that a coordinated response is required to enable plants to cope with the stress and maintain growth and survival. However, such a systemic response may depend on the developmental stage, and involve a complex interplay between physiological, biochemical, and molecular processes that occur in roots as a local response. Furthermore, it would be beneficial for the identification of waterlogging-tolerant genotypes, if certain N-C carriers that orchestrate metabolism under waterlogging can be identified as biochemical markers. Therefore, this study aimed to identify key metabolic processes and their biochemical markers at various stages of plant development that play an important role in the local and/or systemic response to waterlogging stress. Additionally, this study investigated transcriptome changes underlying root and leaf such responses, and focused on responsive genes in waterlogged wheat at different stages of development. For this purpose, several experiments were conducted in a soil-based system, in which the waterlogging and control treatments were conducted under controlled conditions.

The first chapter of this dissertation describes changes in plant growth, development and metabolism of spring wheat under waterlogging at the stage of tillering or booting. To this end, a pot experiment was conducted to investigate the effects of a period of 12 days of waterlogging on the physiological status and development of the plants. Results are presented for fully developed leaves and roots by a comparison between waterlogging and control treatments, and within developmental stages (DS). In addition, the effect of waterlogging on the accumulation of nutrients, soluble sugars, amino acids and key metabolites from glycolysis and the TCA cycle are described. Furthermore, a dynamic experiment was conducted over 12 days to evaluate the short- and long-term effects of waterlogging and the metabolic adjustments to investigate an eventual systemic response of wheat. To this end, the dynamic profile of major metabolites and nutrients, as well as the main changes in amino acid and hormone translocation rates in the xylem of the stressed plants have been documented.

The following chapter constitutes an evaluation of the transcriptomic response of spring wheat to waterlogging at different growth stages. For this purpose, differentially expressed genes (DEGs) were analysed and compared between leaves or roots of stressed plants and the respective controls. Gene Ontology (GO) enrichment analysis of the DEGs in response to water stress and identification of functional categories related to metabolic responsive mechanisms of wheat are summarised.

To describe the unique and common patterns in waterlogging-responsive metabolic pathways as compared to those under other types of water stress such as drought, an assessment was made of the contrasting effects of the two opposite conditions of the soil water gradient. Changes in global metabolite profiles in leaves and roots are expressed in terms of common functional categories when wheat plants were exposed to waterlogging or drought. The final section of this thesis summarises the results and discusses the observed metabolic and transcriptomic responses of wheat to waterlogging. A link is made between the metabolic acclimative responses that take place in the below-ground and above-ground tissues, and interpreted in the light of a systemic response mechanism in wheat.

4. MATERIAL AND METHODS

4.1 Plant growth conditions

4.1.1 Central experiment

To investigate the metabolic and transcriptomic changes of spring wheat exposed to 12 days of uninterrupted waterlogging or drought stress, a pot experiment referred as "**central experiment**" was conducted in the greenhouse of the Leibniz-Institute of Plant Genetics and Crop Plant Research (IPK-Gatersleben, Germany) (Figure 1A). Seeds of wheat (*Triticum aestivum* L. var. Chinese spring) were propagated and obtained by Prof. Dr. Andreas Börner, Head of the Resource Genetics and Reproduction group from the same Institute. The soil used for the experiment, including for the seed germination, was a loamy sandy/medium silty sandy soil (S3/Su3 - according to the German Texture Classification; Ad-hoc Soil Working Group) with 65% sand, 27% silt and 8% clay obtained from the experimental station in Dedelow, Germany. Seeds germinated under controlled conditions, i.e. day/night temperature of 14/12 °C, humidity of 85%, and light intensity of 250-300 µE until the appearance of the third leaf three weeks after sowing. The seedlings were transferred individually into 7.5-liter pots filled with 5 kg soil, and kept under controlled conditions, i.e. day/night temperature of 18/16°C, humidity of 70%, light intensity of 250-300 µE and photoperiod of 16 h light/8 h dark during the entire experiment.

4.1.2 Dynamics experiment

A second experiment referred to as the "**dynamics experiment**" was conducted to study the dynamics of growth and metabolism of wheat plants at shorter time intervals during 12-days exposure to waterlogging and 12 days of recovery (Figure 1B). The same growth conditions as in the previous experiment were used and only plants at tillering stage and under waterlogging were observed. Different time points during waterlogging were considered, i.e. 0, 3, 6, 9 and 12 days, and fully developed leaves and roots were collected from the corresponding plants. After day 12, the stress was terminated from half of the initially exposed plants by allowing them to drain the excess water. Then followed a recovery phase in which the plant material was collected from the corresponding plants at days 2, 6 and 12 during recovery. 24 days after the onset of waterlogging, the excess of water was removed from the remaining waterlogged plants.

Plants from control treatment (never exposed to waterlogging), waterlogging 1 (terminated at day 12), and waterlogging 2 (terminated at day 24) were considered during the recovery period of the experiment. After this period, plants form all treatments continued their growth under well-irrigated and well-drained conditions until they reached the ripening stage, and yield parameters,

e.g. spike and grain weight and spike and grain number, were monitored for all treatments. A final assessment of the germination rate of representative seeds from each treatment was carried out.

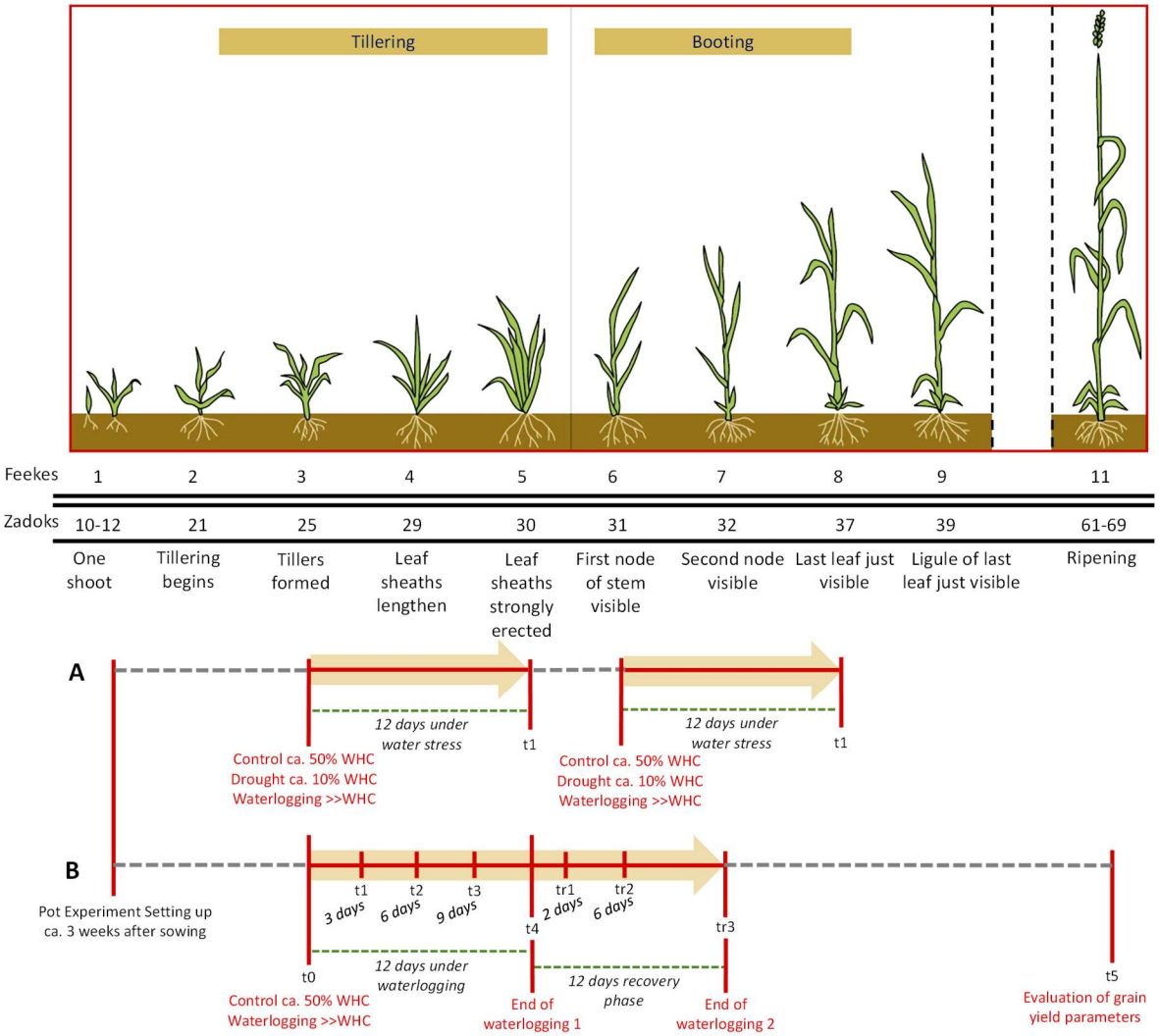

Figure 1. Representative scheme of the experimental design of the two experiments. Seeds of spring wheat germinated under controlled conditions, i.e. day/night temperature of 14/12 °C, humidity of 85%, and light intensity of 250-300 µE until the appearance of the third leaf three weeks after sowing. (A) refers to the **central experiment** to evaluate the metabolic and transcriptomic changes of spring wheat subjected to 12 days of uninterrupted waterlogging or drought stress at tillering (Z, 25) or booting (Z, 31) stage. (B) refers to the **dynamics experiment** to evaluate the short- and long-term effects of waterlogging on wheat growth and metabolism at tillering stage. Leaf samples and xylem exudates were taken at 0, 3, 6, 9 and 12 days during waterlogging, and at 2, 6 and 12 days during the recovery period. Root samples were collected only in the central experiment on day 12 after the onset of the stress.

4.2 Set-up of water stress

The main focus of this study was to investigate the effects of waterlogging on the metabolic and transcriptomic response of wheat at different stages of plant development. Initially, drought stress was also investigated to establish a comparative analysis of effects of the two types of stress in wheat at different stage of development.

For the central experiment, the establishment of well-drained conditions as control, of waterlogging or of drought was performed only once for an uninterrupted period of 12 days starting either at tillering (Z, 25) or booting (Z, 31) stage according to the Zadok's scale (Figure 1A). Eight biological replicates for each treatment were considered, and placed in the greenhouse in a completely randomised design. The severity of water stress in wheat plants was established after determining the water holding capacity (WHC) of the soil used in the experiment (Appendix 1) according to Pauwels *et al.* (2020). WHC was previously determined based on the mass of soil (5 kg) before over-irrigation and after drainage overnight. Control plants were monitored at 50 % WHC (Volumetric Water Content (VWC) 20.26 - 15.77 % v/v and Soil Water Tension (SWT) 1.8 $\log_{10}$ hPa), while waterlogging was maintained at >> 50 % WHC (VWC 38.24 v/v % and SWT 1.5 $\log_{10}$ hPa) by keeping excess water about 5 cm above the soil surface. For drought stress, WHC was set to 10 % (VWC: 9.96 - 8.6 %, SWT: 3.2 $\log_{10}$ hPa) of the control conditions. To ensure reproducibility among biological replicates, pots of control and drought-exposed plants were weighed daily until day 12.

4.3 Collection of plant material and phenotypic characterisation

To evaluate the phenotypic response of wheat plants to waterlogging or drought, fresh and dry shoot and root biomass, plant height, root length, number of tillers and number of spikes/size-ratio were recorded for all plants at tillering or booting stage. All above-ground parameters were recorded in both experiments using the same procedure. For the fresh biomass, the plants were decapitated and weighed immediately. In the central experiment, the roots were washed carefully, removing the remaining soil particles as much as possible, and thoroughly blotted dry with thin paper towels. Root biomass and length were then documented.

For the dynamics experiment, the root harvest was omitted and replaced by the collection of xylem sap. The xylem exudate was collected at the time points previously described in section 3.1.2. The collection procedure was carried out according to Aguirre (2020) under control conditions at 21°C, 98 % humidity and ambient light. In each treatment and at each time point, eight biological replicates were taken, which consisted of three individual plants grown in the same pot. Silicone tubes with a diameter of 2 - 2.5 mm and a length of 4 - 5 cm (Rotilabo®-Silikonschlauch, Carl Roth GmbH + Co. KG, Karlsruhe, Germany) were placed on the hypocotyl to match to the corresponding cut diameter. The accumulated sap was collected periodically from the top of the silicon tubes using a 20 µl pipette until completing a collection time of 4 hours. During xylem accumulation, the silicone tubes were covered with aluminum foil (Rotilabo®-Typ R 100, Carl Roth GmbH + Co. KG, Karlsruhe, Germany) to protect the exudates from contamination and UV light. The estimated total volume collected was registered by the difference in weight of the collection tubes before and after collection. All samples from all experiments were immediately stored at -80°C until further analysis.

Yet in the dynamics experiment, some yield parameters, e.g. spike and grain weight and number of spikes and grains, were monitored in all treatments when the plants had reached the ripening stage (Z61-69). A final assessment of the germination rate of representative seeds from each treatment was carried out.

4.4 Determination of chlorophyll concentration

For the extraction of total chlorophyll in the central experiment, 10 mg of fresh material from fully expanded leaves harvested on day 12 of waterlogging, either at tillering or booting stage, were used. Samples were incubated in 80 % acetone at 80 °C for 60 minutes, followed by cooling for 15 minutes and centrifugation at 14 000 rpm for 5 minutes. Samples were analysed photometrically at 663 and 645 nm. Quantification of chlorophyll *a, b* and *total* was performed according to Roca, Chen and Pérez-Gálvez (2016), using the following formulae:

1. *Chl a* = 12.7 x (A663) - 2.69 x (A645)
2. *Chl b* = 22.9 x (A645) - 4.68 x (A663)
3. *Total Chl* = 20.2 x (A645) + 8.02 x (A663)

4.5 Analysis of macro- and micronutrients

Fresh, fully developed leaves or roots of plants from the control and waterlogging treatments in the central experiment were homogenised and a representative amount was transferred to Eppendorf tubes and dried for 24 hours. For the analysis of total carbon and nitrogen concentration, 1.5 mg of dried plant material were weighed into the corresponding tin (Sn) capsules. The analysis was performed using a EuroEA3000 (EuroVector SpA, Redavalle, Italy) and Callidus 5.1 software. The standard 2,5-bis(5-tert-butyl-benzoxazol-2-yl) thiophene with 72.52% carbon and 6.51% nitrogen from HEKAtech GmbH (Wegberg, Germany) was used for calibration. For the analysis of other macro- and microelements, approx. 30 mg of the same dry plant material were weighed into PTFE digestion tubes and 1 ml concentrated nitric acid (67-69 %, Bernd Kraft, Duisburg, Germany) was added to each tube. After 4 hours of incubation, the samples were digested under pressure in a high-performance microwave reactor (Ultraclave 4; MLS, Leutkirch, Germany). The digested samples were transferred to Greiner centrifuge tubes and diluted with deionised (Milli-Q®) water to a final volume of 15 ml. For the analysis of the same mineral composition in xylem exudates collected from the corresponding treatments in the dynamics experiment, 0.05 ml of the samples were directly diluted with 5% nitric acid to a final volume of 5 ml. The analysis was performed using inductively coupled plasma optical emission spectroscopy (ICP-OES) (iCAP 7400 duo OES spectrometer; Thermo Fisher Scientific, Dreieich, Germany) coupled to a 4DX preFAST automated in-line dilution system (Elemental Scientific™ (ESI), Mainz, Germany). An external three-point

calibration curve was generated from a certified multiple standard solution (Bernd Kraft, Duisburg, Germany). The element yttrium (Y) was used as an internal standard for matrix correction.

4.5.1 Determination of soil mineral composition

Soil samples were collected from the control and waterlogged treatments on day 12 after the onset of the stress in the central experiment. The analysis of the soil mineral composition was carried out at the Leibniz-Center for Agricultural Landscape Research (ZALF). Total organic carbon (TOC) and total nitrogen (Nt) contents were determined in triplicates by dry combustion using a Vario EL III C/H/N analyser (Elementar, Hanau, Germany). Since the carbonate concentration of the soils was negligible (< 2%), the measured total C concentration was considered as TOC. Plant-available P (PDL) was extracted from fresh soil using the double lactate method (1:50 w/v, pH 3.6, 1.5 h) (Riehm 1943). After filtration of the suspension (Whatman Schleicher and Schuell 595 1/5 Ø 270 mm), the extracted P was quantified colorimetrically using the molybdenum blue method (Murphy and Riley, 1962). The oxalate-extractable Fe (Feox) and Mn (Mnox) was extracted by acid ammonium oxalate solution adjusted to pH 3. The concentration of Mn, Ca, Na, K, Mg, Feox and Mnox in the soil was measured with an inductively coupled plasma optical emission spectrometer ICP-OES (ICP-iCAP 6300 DUO, ThermoFisher Scientific, Germany).

4.6 Extraction and quantification of carbohydrates

Soluble sugars and starch were determined in fully expanded leaves and roots according to Tula *et al.* (2020) with slight modifications. 50 mg of frozen fully developed leaves and roots from control, waterlogged or drought plants were homogenised in liquid nitrogen, dissolved in 0.7 ml of 80 % (v/v) ethanol and shaken at 600 rpm at 80 °C for 60 min. The resulting crude extracts were centrifuged at 14 000 rpm and 4°C for 5 minutes and the supernatant was transferred to a new Eppendorf tube. The remaining pellet was washed twice with 1 ml each of 100 % ethanol for starch determination. To break down starch into glucose moieties, 0.2 ml of 0.2 N KOH was added and the samples were incubated overnight at 4°C and neutralised with 0.07 ml of 1 N acetic acid, pH 6.5-7.5. Samples were digested with 0.1 ml of a buffer containing 7 $U \cdot mg^{-1}$, i.e. 2 $mg \cdot ml^{-1}$ amyloglucosidase in 50 mM NaAc, pH 5.2, and incubated overnight at 37°C. Starch was calculated from the glucose concentration present in the samples after starch breakdown. Glucose, fructose and sucrose were determined by a coupled photometric assay in the presence of the auxiliary enzymes hexokinase, phosphoglucoisomerase and invertase respectively, and the oxidation of NADH to NAD^+ was monitored at a maximum wavelength of 340 nm.

4.7 Analysis of soluble amino acids

For the analysis of amino acids, the same plant extracts were used as for the sugar analysis. In addition, xylem exudates (0.01 ml) collected in the dynamics experiment were also used. The extracts were derivatised with the NMR-purified fluorescent reagent AQC (6-aminoquinolyl-N hydroxysuccinimidyl carbamate) (BIOSYNTH AG, Switzerland). 3 mg AQC was dissolved in 1 ml acetonitrile and incubated at 55°C for 10 minutes. Derivatisation was performed for 0.01 ml plant extract, xylem exudate or standard mixture containing 0.01 ml AQC and 0.08 ml 0.2 M boric acid, pH 8.8 at 55°C for 10 minutes. Soluble amino acids were separated by ultra-pressure reversed phase chromatography (UPLC), Acquity H-Class, (Waters GmbH, Germany) coupled with a fluorescence detector (FLR Detector) (Waters GmbH, Germany). Separation was performed on a C18 reversed-phase column (Luna Omega, 1.6 µm, 2.1x100 mm, Phenomenex, Germany) at a flow rate of 0.6 $ml \cdot min^{-1}$ for 6 minutes. The column was heated to 40°C throughout the run. The gradient consisted of B (Millipore, FA0.1%), C (50/50 Acetonitirle/Water), and D (Acetonitrile 100%) as follows: 0-3.66 min, 32.4% B, 65.5% C, 2.1%D; 3.66-3.73 min, 84.5% B, 5.5%C, 10.0% D; 3.73-4.13 min, 26.6%B, 47.9% C, 25.5% D; 4.13-4.32 min 7.8% B, 60.9% C, 31.3% D; 4.32-4.79 min, 4.0% B, 36.3% C, 59.7% D; 4.79-6.00 min, 32.4% B, 65.6% C, 2.0%D. The wavelengths for detection were 266 nm for excitation and 473 nm for emission. Empower 3 Software (Waters GmbH, Germany) was used for instrumentation settings, data acquisition and processing. The quantification of the amino acids in the samples was carried out using a calibration curve from a mixture of 19 different amino acids in the range of 0.5 to 20 $nmol \cdot ml^{-1}$ reaching a correlation of $R^2 > 0.98$ in all cases.

4.8 Extraction and quantification of metabolites

The extraction of metabolites followed the protocol described by Tognetti *et al.* (2007) with some modifications. 100 mg of frozen, fully expanded leaves and roots collected at day 12 in the central experiment were used. The samples were thoroughly homogenised at 4°C by gentle shaking for at least 20 minutes. Then 0.3 ml of HPLC-grade water was added to each sample and centrifuged at 14 000 rpm for 10 minutes at 4°C. The supernatant was transferred to a new Eppendorf tube and dried in a Speed-Vac (Christ RVC2-33IR, Germany) at 35°C for about 2 hours. The resulting pellet was resuspended in 0.3 ml HPLC-water and immediately used for the measurement of the desired compounds. Separation and detection of metabolites was performed according to Ghaffari *et al.* (2016) using an ion chromatography system (IC)-coupled MS/MS connected to a conductivity detector (Dionex, Thermofisher Germany) and a QQQ6490 triple quadrupole mass spectrometer (Agilent Technologies, Waldbronn Germany). The gradient was prepared from ultrapure water (buffer A, Millipore) and a concentrated potassium solution EGCIII KOH (Dionex, Germany, buffer B) using an eluent generator EG-SP (Dionex Germany). The column was equilibrated under the same

conditions at 0.32 ml·min^{-1} and 37°C throughout the measurement. Electrospray Ionisation ESI-MS /MS analysis was performed in negative ionisation mode using nitrogen gas at 720 l·h^{-1}, at a heating temperature of 250°C, a capillary voltage 3.5 KV and different dwell times between 40 and 200 seconds. The collision energy (CE) was between 6 and 50 for different masses. Multiple Reactions Monitoring (MRM) was performed to accurately identify each compound. Quantification was performed considering 30 different compounds and a calibration curve of the same with concentrations ranging from 25 to 500 pmol·µl^{-1}. Data acquisition and quantification were performed using Chromeleon software, version 7.3 (Dionex GmbH, Germany) and MassHunter software, version B.07.01 (Agilent Technology, Waldbronn Germany).

4.9 Analysis of hormone translocation in xylem exudates

For phytohormone analysis in xylem exudates, 0.03 ml of the samples were mixed with internal standards (OlChemim s.r.o, Czech Republic) at a final concentration of 100 nM. Samples were homogenised for 30 seconds and centrifuged for 30 minutes at 14 000 rpm at 4°C (CT 15 RE centrifuge, Himac, Japan). Auxins and cytokinins were analysed by ultra-high-performance liquid chromatography UHPLC-ESI-MS /MS as described in Eggert and von Wirén (2017). 10 µl of the samples were injected into an ultra-performance LC system (Acquity) coupled with a Xevo TQ mass spectrometer (Waters, Milford, MA, USA). The sample analytes were separated on an Acquity UPLC® BEH C18 1.7-µm, 2.1 x 100 mm column coupled with a VanGuard pre-column BEH C18 1.7 µm, 2.1 x 5 mm. The column temperature was set to 40°C and the autosampler temperature was set to 4°C. Gibberellins were determined using ultra-high-performance liquid chromatography coupled to high resolution mass spectrometer Orbitrap UHPLC-HESI-HRMS equipped with a heated electrospray ionization (HESI) probe operating in negative ion mode. An Acquity UPLC HSS T3 reversed-phase column (10 Å, 2.1 × 150 mm, 1.8 µm, Waters) (45°C, 0.3 ml·min^{-1}) coupled to a guard column (130 Å, 2.1 × 5 mm, 1.8 µm, Waters) was used. The gradient consisted of A (Water, 0.1% FA) and B (MeOH, 0.1% FA) as follows: 0-0.3 min, 10% B; 0.3-0.7 min, 10% to 30% B; 0.7-2 min, 30% to 50% B; 2-4 min, 50% to 60% B; 4-8 min, 60% to 80% B; 8-9.5 min, 80% to 99% B; 9.5-10.4 min, 99% B. Source values were set as follows: spray voltage 2.5 kV; capillary temperature 255°C; S-lens RF Level 40; aux gas heating temperature 320°C; sheath gas flow rate 47; aux gas flow rate 11. Spectra acquisition was performed using a Full MS /dd-MS² experiment. The resolution of Full Scan was set to 70 000. The resolution of the MS /MS experiments was 17 500 and NCE 40V was used. Data acquisition and processing was done with Trace Finder software (v. 4.1, Thermo Scientific, San Jose, CA, USA). To generate the calibration curve, the peak area was measured on the extracted ion chromatogram (XIC) of the deprotonated molecular ion $[M-H]^-$. Compounds were identified by their retention times, high resolution m/z spectrum and isotopic pattern compared to the standards. In

addition, the MS2 spectra generated were searched in a custom spectral library to confirm the identification of the compounds.

4.10 RNA isolation, cDNA synthesis and gene expression analysis

Total RNA was extracted from fully expanded leaves and roots collected on day 12 under waterlogging or drought stress using the NuceloSpin RNA Kit for extraction and NanoDropTM2000c for RNA quality as described in Beier *et al.* (2022). Library preparation for transcriptome sequencing was performed by Novogene Co. using the NEBNext® UltraTM RNA Library Prep Kit for Illumina® (NEB, USA) according to the manufacturer's recommendations and considering three biological replicates for each plant material and treatment. mRNA was purified from total RNA using magnetic beads bound to poly-T oligos and then fragmented. Random hexamer primer and M-MuLV reverse transcriptase (RNase H-) were used for first-strand cDNA synthesis, while second-strand cDNA synthesis was performed with DNA polymerase I and RNase H. cDNA fragments of 150~200 bp were selected by purification of library fragments using AMPure XP system (Beckman Coulter, Beverly, USA).

PCR was performed using Phusion High-Fidelity DNA Polymerase, Universal PCR primers and Index (X) primer. Library quality was assessed using the Agilent Bioanalyzer 2100 system. After cluster generation, library preparations were sequenced on an Illumina platform and paired-end reads were generated. Reference genome and gene model annotation files were downloaded from the genome website browser (NCBI/UCSC/Ensembl) and paired-end clean reads were mapped to the reference genome using HISAT2 software. The number of mapped reads for each gene, including known and new genes, was determined using feature counts. The number of reads per kilobase million (RPKM) of each gene was then calculated. Differential expression analysis was performed using the DESeq2 R package. The resulting P values were adjusted using the Benjamini and Hochberg approach to control for false discovery rate (FDR).

Gene Ontology (GO) was implemented by the clusterProfiler R package and the $P_{adj} < 0.05$ and $\log_2$ fold-change ≥ |2| were classified as differentially expressed. For the Kyoto Encyclopedia of Genes and Genomes (KEGG) enrichment analysis, the clusterProfiler R package was used to test the statistical enrichment of differentially expressed genes in KEGG pathways.

4.11 Determination of yield-related parameters

Twenty-four days after the onset of the waterlogging stress in the dynamics experiment, i.e. on day 12 after the termination of waterlogging in one group of plants (waterlogging 1), the remaining waterlogged plants were also restored (waterlogging 2), and able to continue their growth in parallel with the control and waterlogging 1 treatments (Figure 1B). In this way, it was possible to

register yield-related parameters at the ripening stage (Z61-69) of control (well-drained), waterlogging 1 (terminated on day 12) and waterlogging 2 (terminated on day 24). Size and weight of spikes and number of grains were monitored for each treatment. To assess the seed viability of the plants from control and waterlogging, a germination rate assessment was also conducted.

4.12 Statistical analysis

In all greenhouse experiments eight biological replicates were arranged in a complete randomised experimental design. Statistical analyses were performed using R Studio version 4.2.1. The normal distribution of the data was checked using Shapiro-Wilk's normality test considering $p < 0.05$. To determine the difference between groups, a Student's t-test or one-way ANOVA analysis was performed for the data that passed the normality test. For data that did not pass the normality test, the Mann-Whitney U-test or Kruskal-Wallis test was performed instead. In all cases, a 95% confidence interval ($P \leq 0.05$) was considered. For treatments with unequal sample numbers, Dunn's test was used. Different letters indicate significant differences among treatments based on Tukey's HSD. Heatmaps were created using the versatile online visualisation and analysis software MORPHEUS, https://software.broadinstitute.org/morpheus.

5. RESULTS

Chapter 1: Characterisation of acclimative physiological and biochemical traits in spring wheat in response to waterlogging

5.1 Influence of prolonged waterlogging on plant growth and metabolism at different stages of development

To study the effects of prolonged uninterrupted waterlogging on plant physiology and metabolism, an experiment was conducted in which plants were waterlogged for 12 days at tillering or booting stage. After the 12th day, various phenotypic characteristics of above- and below-ground tissues of waterlogged and control plants were recorded and all fully developed leaves and roots were collected.

5.1.1 Influence of waterlogging on phenotypic traits and chlorophyll concentration in wheat

In general, the waterlogging treatment resulted in smaller plants with fewer leaves than those in the control treatment. In addition, chlorosis symptoms occurred, but the effects were more pronounced at the booting than at the tillering stage (Figure 2A, B). Compared to the control, waterlogged plants showed a decrease in Chl *a, b* and total chlorophyll by a factor of two, both at tillering and booting stage (Figure 2C, D). However, at both stages the Chl *a/b* ratio remained unchanged (Figure 2E).

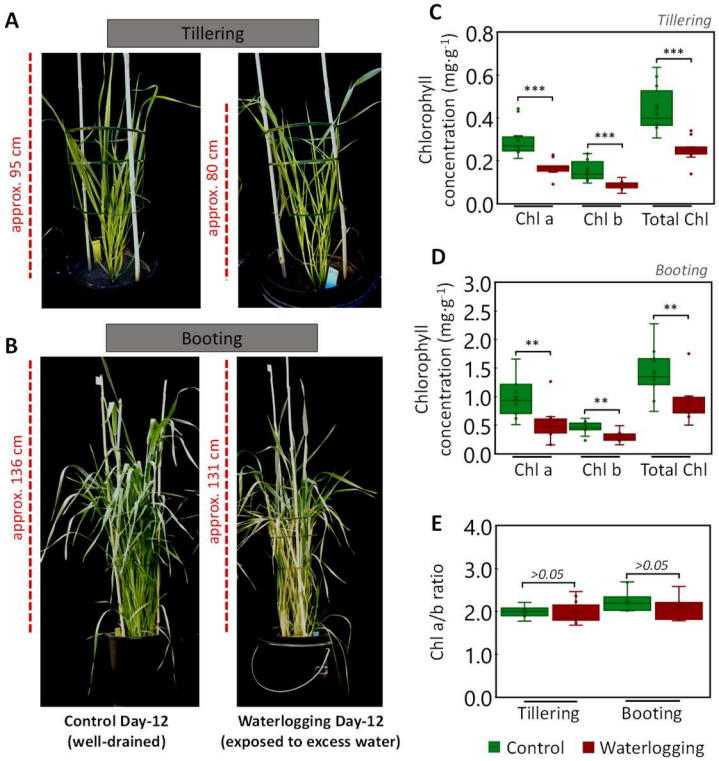

Figure 2. Wheat growth and chlorophyll concentration at different developmental stages. (A) Above-ground appearance of wheat at tillering (B) or booting stage. (C) Chlorophyll concentration in fully developed leaves of wheat plants on day 12 under waterlogging at tillering (D) or booting stage. (E) Chlorophyll a/b ratio at

tillering or booting. After 12 days of waterlogging, either at tillering or booting stage, the plant height was noted and a pool of all fully developed leaves from plants of control or waterlogging treatments were collected. Box limits indicate the 25th and 75th percentiles, horizontal lines show medians and whiskers extend to 1.5 times the interquartile range from the 25th and 75th percentiles. Different asterisks indicate significant differences at ** $P < 0.01$ and *** $P < 0.001$ according to Student's *t*-test or Mann-Whitney *U*-test, $P \leq 0.05$, n = 8.

Notably, shoot biomass and tiller number did not differ significantly between the stressed and control plants in both stages (Figure 3A, B). Notably, plant height was lowered in stressed plants at tillering stage and did not differ at booting (Figure 3C). Below-ground plant parameters showed that 12 days of waterlogging reduced root biomass at both DS (Figure 3D), while root length was unaffected (Figure 3E). At booting stage, the development of the spikes was also documented in terms of units per plant and size (Figure 3F) in addition to the root-to-shoot ratio (Figure 3G). None of these values showed significant differences compared to the control plants.

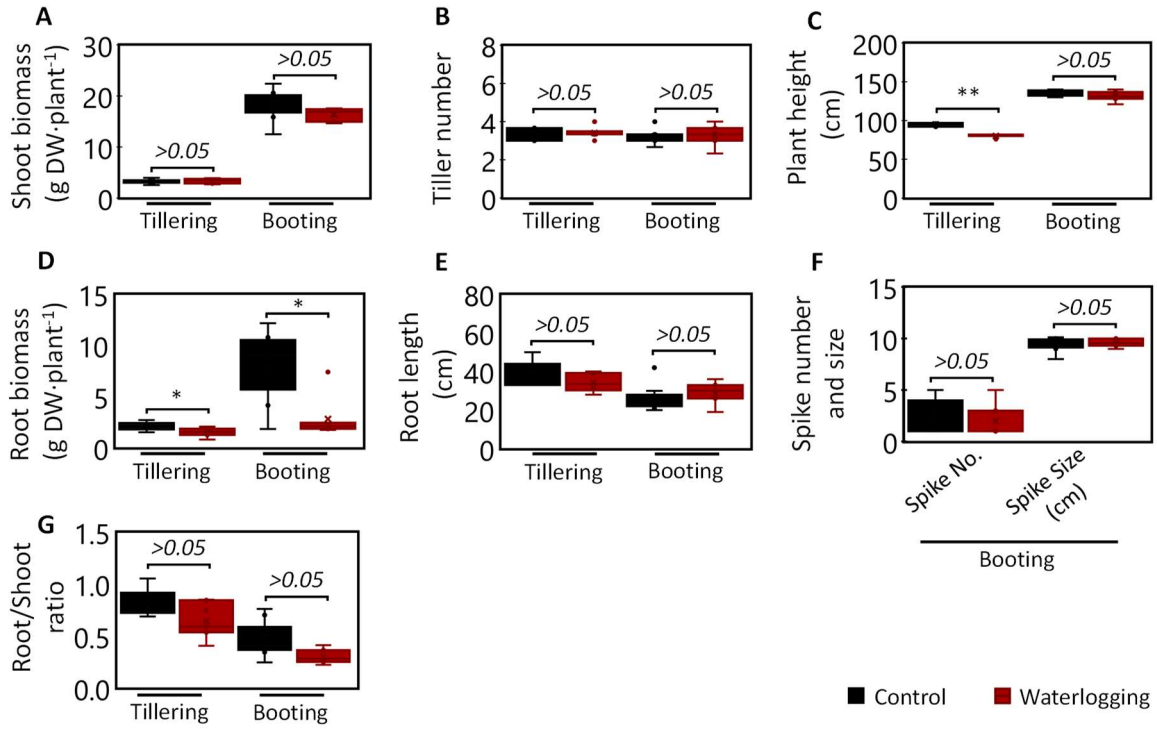

Figure 3. Effect of waterlogging on root and shoot phenotypic traits. (A) Shoot biomass, (B) number of tillers, (C) plant height, (D) root biomass, (E) root length, (F) spike number and size, and (G) root to shoot ratio. After 12 days of waterlogging, the phenotypic characteristics of the control and waterlogged plants were recorded at either tillering or booting stage. Box limits indicate the 25th and 75th percentiles, horizontal lines show medians and whiskers extend to 1.5 times the interquartile range from the 25th and 75th percentiles. Different asterisks indicate significant differences at * $P < 0.05$ and ** $P < 0.01$ according to Student's *t*-test or Mann-Whitney *U*-test, $P \leq 0.05$, n = 8.

In summary, waterlogging had significant effects on phenotypic traits and chlorophyll concentration in wheat. The most apparent effects were reduced plant height, root biomass, and leaf chlorosis. However, the severity of these effects was influenced by the stage of development as waterlogged plants at tillering showed a stronger response than those at booting stage.

5.1.2 Influence of waterlogging on the mineral composition in wheat plants

On the 12th day after the start of the water treatments, soil, fully expanded leaves and roots were collected from well-drained (control) and waterlogged treatments to determine the effects of these treatments on the macro- and micronutrient composition, either at tillering or booting stage. Samples of the original soil, which had not been exposed to any of the treatments, were also analysed to assess the changes in the physico-chemical properties of the soil when wheat plants grew under control or waterlogged conditions. The comparison between the original soil and the soil from the control treatment at tillering and booting showed no significant differences for any of the elements measured (Appendix 2). In contrast, the comparison between control and waterlogged soil showed that PDL concentration increased significantly in the waterlogged soil regardless of the DS (Appendix 2A and B). The other variables measured in the soil were unaffected by the stress.

At tillering stage, waterlogged plants showed a reduction in nitrogen (N) concentration of about 35% in leaves and about 22% in roots compared to control plants (Figure 4A). At the time of booting, only the N concentration in the roots had decreased by about 26% compared to the control. Waterlogging had no significant effect on the N concentration in the leaves. In contrast, the total carbon (C) concentration in the leaves of stressed plants did not differ significantly compared to the control and was independent of the developmental stage of the plants (Figure 4B). However, it was increased by about 45 % in the roots of waterlogged plant at the time of tillering. The C:N ratio in the leaves and roots of waterlogged plants in the tillering stage increased by about twofold compared to the control (Figure 4C). The same was true for the roots of the stressed plants when booting. However, no significant difference was found in the leaves at the same stage.

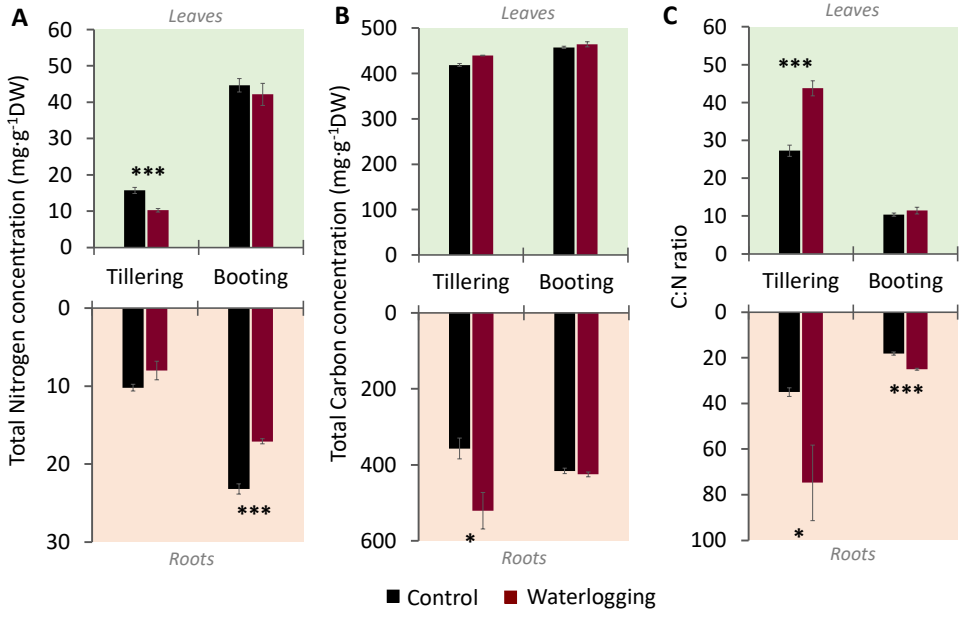

Figure 4. Influence of waterlogging on nitrogen and carbon concentrations in wheat plants. (A) Total nitrogen concentration, (B) total carbon concentration, (C) C:N ratio. After 12 days of waterlogging, the fully developed

leaves and roots of the control or waterlogging treatments were collected at tillering or booting stage. The bars show means ± SE. Different asterisks indicate significant differences at * $P < 0.05$ and *** $P < 0.001$ according to Student's *t*-test or Mann-Whitney *U*-test, $P \leq 0.05$, n = 8.

In general, the concentration of other macronutrients in the leaves of stressed plants was reduced regardless of the stage of development (Figure 5A). However, the most obvious effect of waterlogging was seen in the concentration of phosphorus (P), sulphur (S), and magnesium (Mg) regardless of the developmental stage. In addition, a significant reduction of potassium (K) of about twofold in the leaves of stressed plants was observed at tillering stage. A similar observation was made for Ca in the leaves of stressed plants at booting (Figure 5A). However, the greatest decrease in roots occurred for Mg and Ca at both stages. P and K were significantly reduced in the same tissue of plants at booting stage, whereas S was reduced in waterlogged plants at tillering.

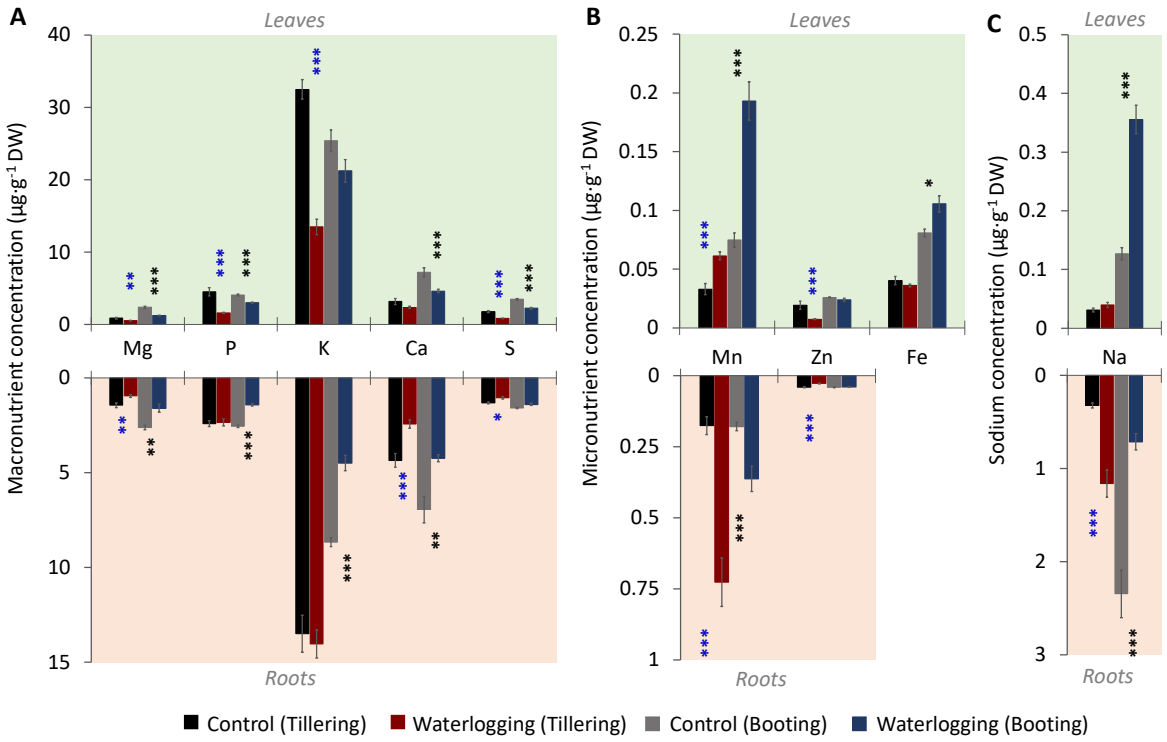

Figure 5. Effect of waterlogging on the composition of macro- and microelements. (A) Macronutrient concentration, (B) micronutrient concentration and (C) sodium concentration in leaves and roots of control and waterlogged plants. After 12 days of waterlogging, the fully developed leaves and roots of the control or waterlogging treatments were collected at tillering or booting stage. The bars show means ± SE. Different asterisks indicate significant differences at * $P < 0.05$, ** $P < 0.01$, and *** $P < 0.001$ according to Student's *t*-test or Mann-Whitney *U*-test, $P \leq 0.05$, n = 8. Blue asterisks indicate the significance at tillering, and black asterisks indicate the significance at booting.

An opposite effect was observed with micronutrients (Figure 5B). Waterlogging increased the concentration of manganese (Mn) in leaves and roots by about twofold at both developmental stages (Figure 5B). The concentration of iron (Fe) remained unchanged in the leaves at the tillering stage, while it increased slightly at booting. Zinc (Zn) concentration was reduced by twofold in both tissues of the plants at tillering stage, while it remained unchanged at booting. Na concentration

did not differ in the leaves of waterlogged plants at tillering, while it increased about threefold in the roots of the same plants (Figure 5C). The same was true for leaves of stressed plants at booting, whereas Na decreased sharply in the roots of the same plants.

Taken together, waterlogging had a significant negative impact on the mineral composition in wheat plants, resulting in reduced uptake of essential nutrients and increased uptake of non-essential elements. These effects were observed across different developmental stages of the plants, with similar nutrient patterns detected during tillering and booting stages, despite the different nutrient requirements and uptake rates at these stages.

5.1.3 Influence of waterlogging on carbohydrate assimilation in wheat

To assess the effects of waterlogging on carbohydrate assimilation, glucose, fructose, sucrose and starch were determined in the fully developed leaves and roots at day 12 after the onset of waterlogging in the central experiment. The concentrations of glucose and fructose in the leaves of stressed plants increased significantly at both DS (Figure 6A, B, upper panel). In contrast, sucrose concentration tended to decrease in the same tissues. However, no significant differences were observed relative to control plants (Figure 6C, upper panel). In addition, a strong starch accumulation was observed in the leaves of waterlogged plants at tillering stage, while it did not change in plants at booting (Figure 6D, upper panel).

The same parameters were measured in the roots. Glucose and fructose increased significantly at tillering (Figure 6A, B, lower panel), while they decreased dramatically at booting. Interestingly, sucrose and starch were also significantly enriched in waterlogged roots at tillering (Figure 6C, D, lower panel), whereas they were reduced and not significantly different in plants at booting stage.

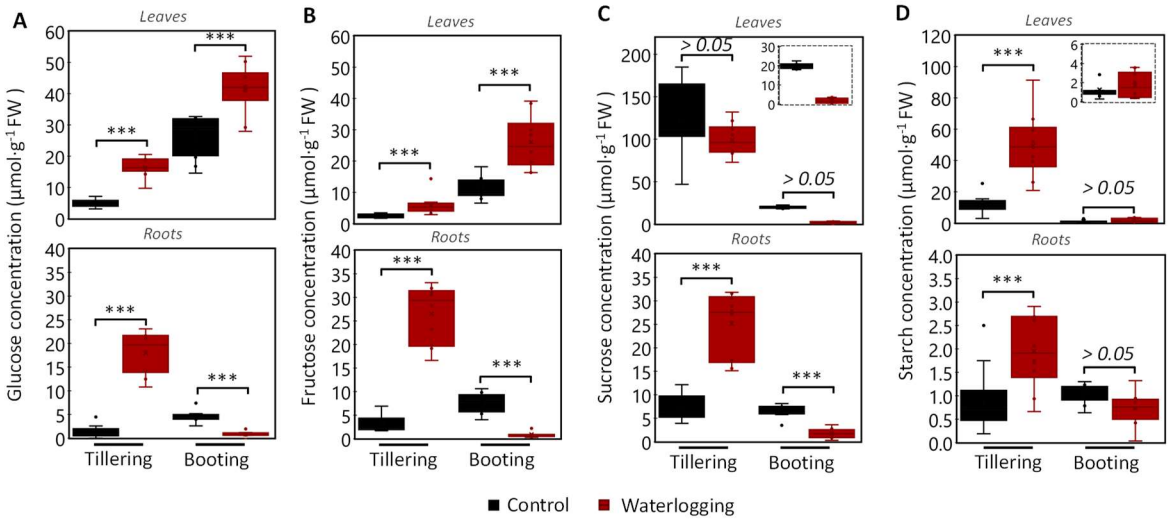

Figure 6. Changes in non-structural carbohydrates in wheat plants exposed to waterlogging at tillering or booting. (A) Glucose concentration, (B) fructose concentration, (C) sucrose concentration, and (D) starch concentration in fully developed leaves and roots of waterlogged plants. Soluble sugars were determined on the 12th day after the onset of waterlogging in wheat plants at tillering or booting stage. Box limits indicate the 25th and 75th percentiles, horizontal lines show medians and whiskers extend to 1.5 times the interquartile

range from the 25th and 75th percentiles. Different asterisks indicate significant differences at *** $P < 0.001$ according to Student's *t*-test or Mann-Whitney *U*-test, $P \leq 0.05$, n = 10 leaves or 9 roots.

Overall, 12 days of waterlogging had a significant impact on carbohydrate accumulation in the leaves and roots of wheat plants. Soluble sugars and starch strongly accumulated in the leaves of wheat plants regardless of the DS. However, waterlogging had a contrasting effect on carbohydrate concentration in the roots of plants at tillering and booting. Sugars strongly accumulated in the roots of plants during the tillering stage, whereas they decreased in the roots of plants during booting. Thus, carbohydrate metabolism in waterlogged wheat appeared to differ between developmental stages.

5.1.4 Influence of waterlogging on primary metabolites in wheat plants

Major metabolites from glycolysis and the TCA cycle were analysed in fully developed leaves and roots of plants exposed to waterlogging for 12 days, either at the tillering or booting stage (Figure 7). In general, most metabolites measured in the leaves did not differ significantly between the control and the waterlogging treatments. Of all metabolites, glucose-1-phosphate (Glc-1P), pyruvate, 3-phosphoglyceric acid (3-PGA), citrate/isocitrate, and oxoglutarate were significantly decreased in leaves of waterlogged plants at tillering. However, most metabolites increased slightly in the leaves of stressed plants at booting but without showing significant differences. The only exception accounted for oxoglutarate, which increased significantly in the same tissue. Besides lactate and fumarate, Glc-1P and succinate were not detected in the leaves of plants at booting.

The concentrations of metabolites in the roots responded differently to those in the leaves of the same stressed plants. At the tillering stage, citrate/isocitrate, succinate, oxoglutarate, *cis*-aconitate, *trans*-aconitate, Glc-1P, and glucose -6-phosphate / fructose-6-phosphate (Glc/Frc-6P) accumulated strongly in the roots of the stressed plants (Figure 7). Interestingly, the same metabolites responded differently at the booting stage. Malate, oxoglutarate, *cis*-aconitate, *trans*-aconitate, Glc-1P, and Glc/Frc-6P were strongly decreased in the roots of stressed plants. However, other metabolites such as lactate, succinate, and pyruvate were significantly increased under the same conditions. The other metabolites remained unaffected, at either stage of development.

Altogether, these results suggest that waterlogging induced metabolic changes in wheat plants that varied depending on the tissue and developmental stage. Glycolytic metabolites and TCA-intermediates were either decreased at tillering or not affected in the leaves of waterlogged plants, regardless of the DS. However, there was a tendency for these metabolites to have a contrasting effect in the roots of stressed plants at both stages. Most of them decreased in concentration in the roots of plants during the tillering stage, whereas the opposite occurred in the roots of plants during booting. Interestingly, the accumulation of fermentative products, such as lactate, was only

observed in the roots of plants at the booting stage. However, other indications of metabolic shifts to alternative pathways to produce energy, such as succinate accumulation, were observed in the roots of plants at both stages. The accumulation of succinate was more pronounced at the booting stage.

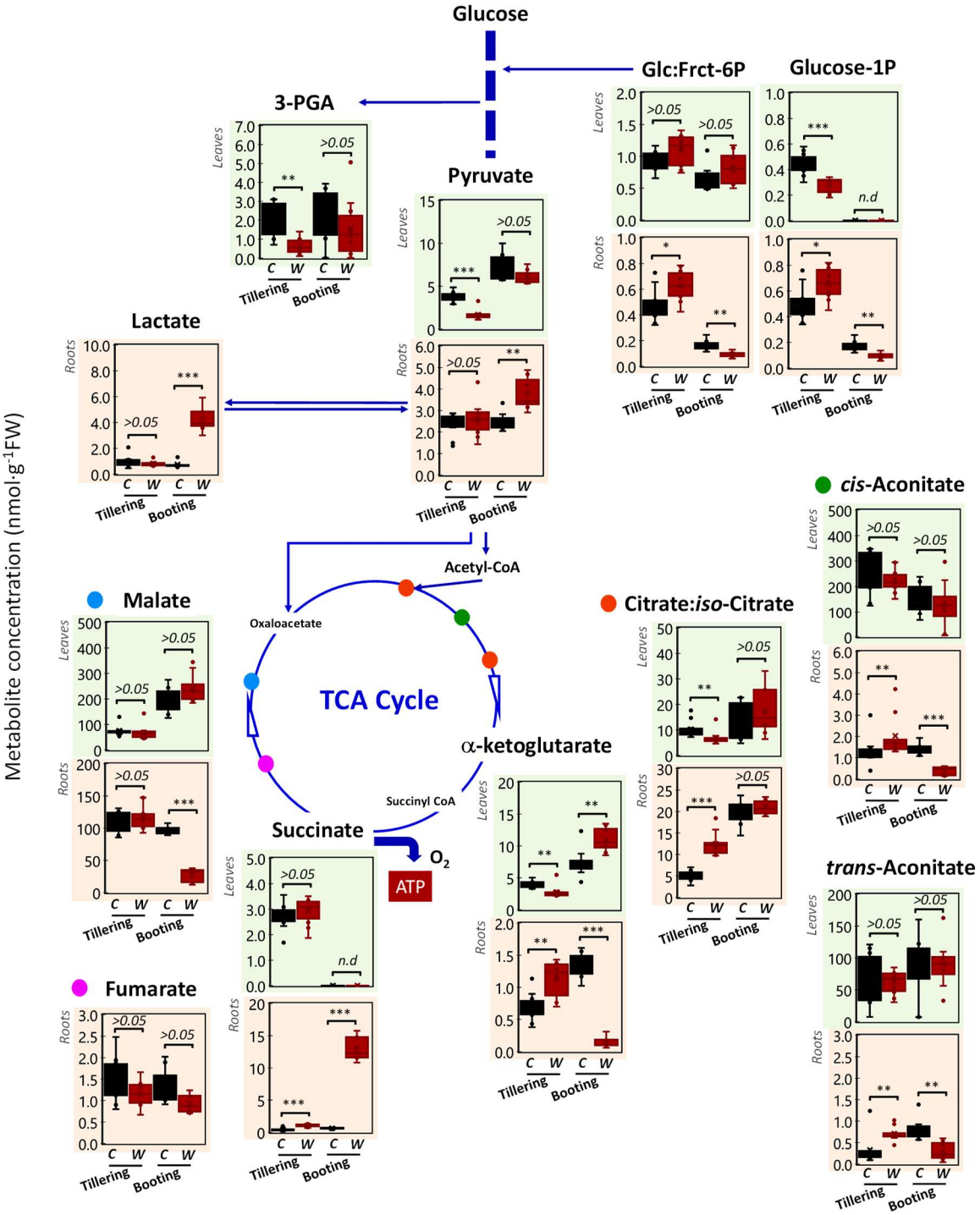

Figure 7. Primary metabolite profile in leaves and roots of wheat plants under waterlogging. After 12 days of waterlogging, fully developed leaves and roots were collected from control (C) or waterlogged (W) plants being either at tillering or booting stage. Box limits indicate the 25th and 75th percentiles, horizontal lines show medians and whiskers extend to 1.5 times the interquartile range from the 25th and 75th percentiles. Different

asterisks indicate significant differences at * $P < 0.05$; ** $P < 0.01$; *** $P < 0.001$ according to Student's *t*-test or Mann-Whitney *U*-test, $P \leq 0.05$, n = 10 leaves or 9 roots. Not-detected metabolites are identified as n.d.

5.1.5 Influence of waterlogging on the concentration of essential amino acids in wheat

Changes in the concentration of 19 different amino acids were determined in fully expanded leaves and roots of control and waterlogged plants in the central experiment (Figure 8, Appendix 3). In general, a decrease in amino acid concentrations was observed in the leaves of the stressed plants at tillering stage. In particular Ala, glutamate (Glu), GABA, proline (Pro), tyrosine (Tyr), serine (Ser) (Figure 8, upper panel), histidine (His), and lysine (Lys) (Appendix 3) decreased significantly. Only methionine (Met) and Gln increased significantly (Figure 8B, upper panel), while the other amino acids remained unchanged (Appendix 3). In addition, the waterlogging treatment increased most amino acids in the leaves of the stressed plants at booting stage. However, no statistical differences were found except for asparagine (Asn), Tyr, phenylalanine (Phe), Gln, and valine (Val), which were strongly increased (Figure 8, upper panel). Only Glu decreased significantly (Figure 8B, upper panel), and the rest did not change (Appendix 3).

Interestingly, an opposite effect was observed in the roots of waterlogged plants (Figure 8, lower panel, Appendix 3). At tillering stage, waterlogging increased the concentration of amino acids in the roots in particular of Ser, glycine (Gly), Ala, aspartate (Asp), Met, Val, Glu, GABA (Figure 8 lower panel), leucine (Leu), and arginine (Arg) (Appendix 3). Only Asn decreased significantly (Figure 8B, lower panel), while the others did not change (Appendix 3). An opposite effect was observed in the roots of the stressed plants at booting stage. Significant decreases in Ser, Asn, Asp, Gln, Glu, Pro (Figure 8, lower panel), and Arg were registered (Appendix 3), while Gly, Ala, GABA, Phe, and Tyr increased strongly under the same conditions (Figure 8, lower panel).

Overall, waterlogging had a significant impact on the concentration of amino acids, with varying effects depending on the type of plant tissue and its developmental stage. While some amino acids showed a sharp decrease in concentration, others accumulated strongly. During the tillering stage, most amino acids tended to decrease in the leaves, while they increased or remained constant in the roots of the same plants. In contrast, most amino acids increased in the leaves of plants during the booting stage. However, a clear distinction was observed in the roots between amino acids derived from glycolysis and those derived from TCA-cycle intermediates. Amino acids derived from glycolysis tended to increase, while those derived from TCA-cycle intermediates tended to decrease. Among all the differences observed in amino acids, Ala showed the strongest response, accumulating significantly in the roots of plants at both developmental stages.

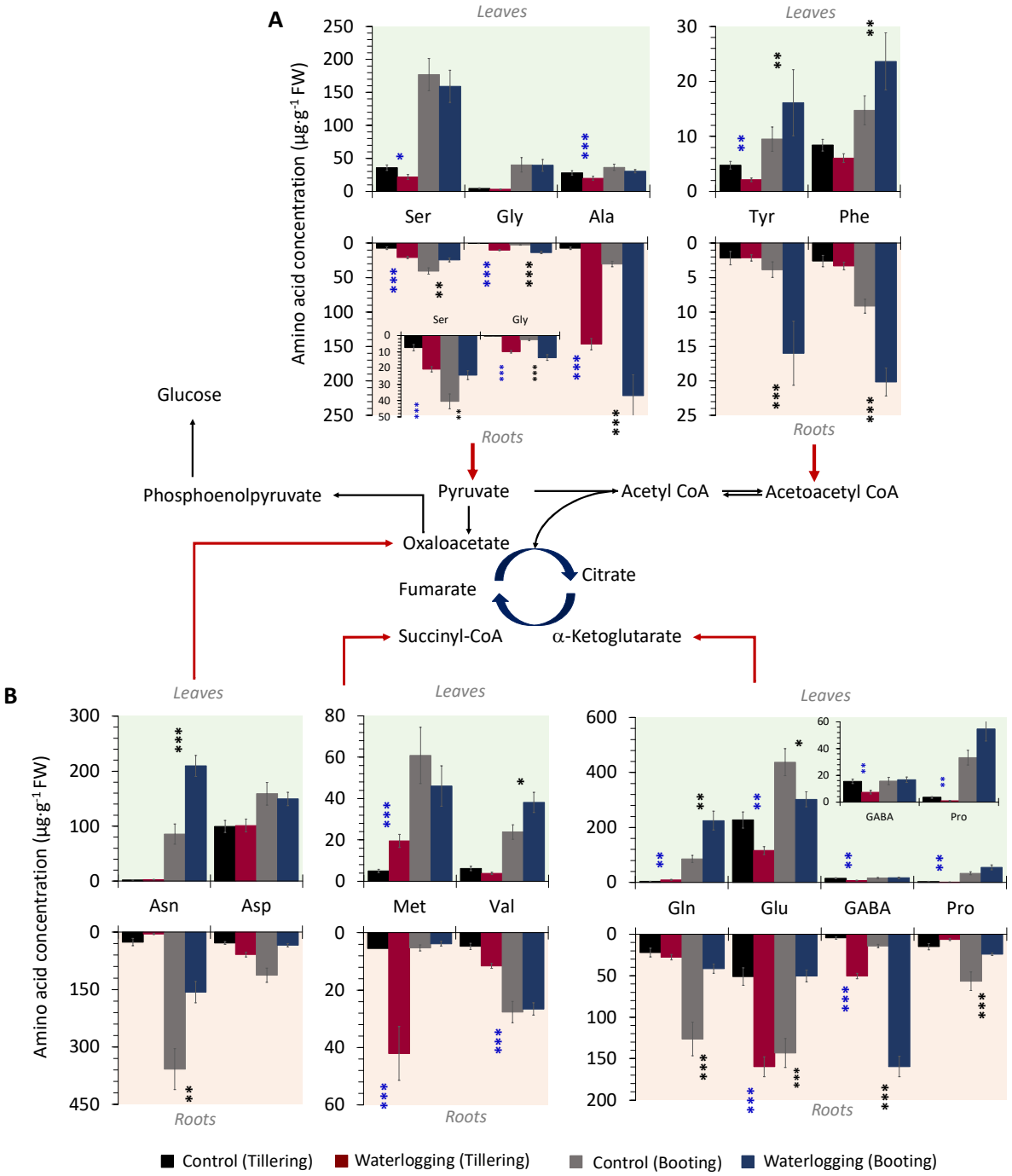

Figure 8. Changes in the amino acid concentrations in waterlogged wheat at tillering or booting. (A) Glycolysis- and (B) TCA-derived amino acid concentrations. After 12 days of waterlogging, fully developed leaves and roots were collected from control or waterlogged plants. The bars show the mean ± SE. Different asterisks indicate significant differences at * $P < 0.05$, ** $P < 0.01$, and *** $P < 0.001$ according to Student's *t*-test or Mann-Whitney *U*-test, $P \leq 0.05$, n = 8. Blue: significance at tillering, black: significance at booting.

5.1.6 Influence of waterlogging on metabolite and nutrient distribution in leaves and roots of wheat plants

To discriminate the profile of metabolites and elements between leaves and roots of the control and waterlogged plants, a Principal Component Analysis (PCA) was performed (Figure 9). Normalised data of 28 metabolites and 8 elements were combined to show the relationships

between these variables and the scores in the different plant tissues and treatments. For example, at the tillering stage, the PC1 captured 32.5% of the variation among leaves and roots (Figure 9A). Additionally, PC2 described 21.5% of the second largest variation in the data between control and waterlogging. Interestingly, the observations made in the roots of waterlogged plants clustered separately from those in the roots of control plants. Notably, the variables in the leaves clustered with a larger scattering, and variables from control and waterlogged plants clustered rather close to each other.

Additionally, the loading plots showed how strongly each of the characteristic influenced a principal component. As expected, most of the variables strongly influenced the separation between leaves and roots along PC1, as these vectors were further away from the origin, especially those ones representing Mn, Na, Gln, malate, starch, and *cis*- and *trans*-aconitate. However, the direction of a large number of characteristics were towards the cluster of variables from roots of waterlogged plants. This indicated that these variables, including a large number of amino acids, glycolysis-derived compounds, and Mn and Na, had the strongest influence on the separation into that cluster. Additionally, other characteristics including TCA intermediates had the strongest influence on the separation of the observations into the cluster representing leaves of control plants. Notably, the characteristics influencing the separation of roots of waterlogged plants and those influencing the separation of leaves of controls showed a negative correlation, as indicated by a wide angle between them. All characteristics separated by a narrow angle like Mn and Gln, or sucrose and succinate, implied to be positively correlated.

At the booting stage (Figure 9B), PC1 captured 38.2% of the variation in metabolite and nutrient concentrations between leaves and roots, whereas PC2 described 19.1% of the variation between control and waterlogging. Interestingly, the observations made in the leaves and roots of waterlogged plants clustered separately to those in the control plants, as observed at tillering. Notably, most of the characteristics had again the strongest influence on the separation along PC1. However, at this stage of development, the loading of most variables, including glycolysis- and TCA-derived compounds, had the strongest influence on the separation of the observations into the leaves of waterlogged plants. Interestingly, only a few characteristics including Mn, Ala, and GABA showed a strong influence on the separation of the observations into the cluster representing roots of waterlogged plants, with a strong correlation among them.

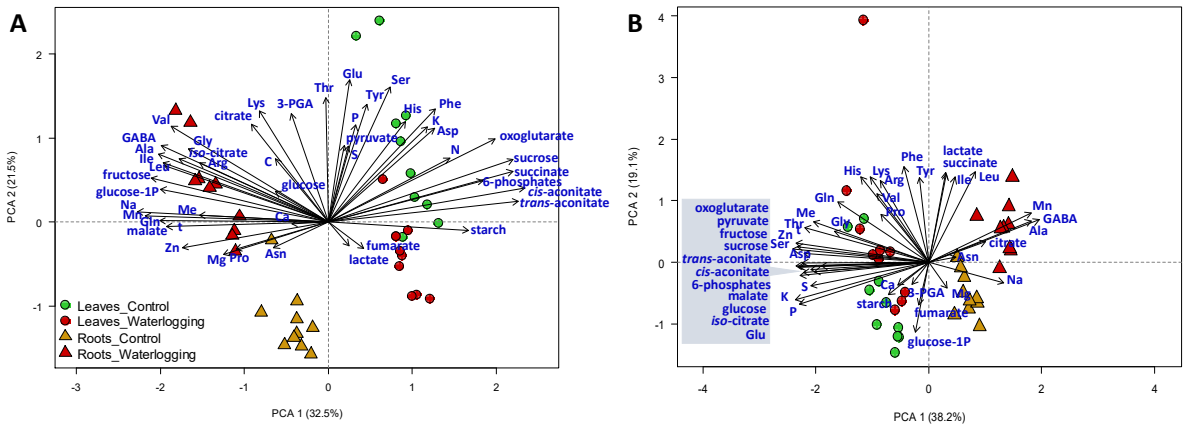

Figure 9. Principal Component Analysis of metabolites and nutrients in fully developed leaves and roots of control or waterlogged plants at (A) tillering or (B) booting stage. After 12 days of waterlogging, the fully developed leaves and roots were collected from the control and waterlogging treatments. The variance captured by the first and second principal components (PCA1 and PCA2, respectively) is given in brackets. Each vector represents one characteristic determined in all plant tissues and treatments. The direction and length of the vectors represent the influence of the variables on the separation of the data into the different clusters.

Taken together, these results indicate that metabolite and nutrient profiles were able to differentiate waterlogging from control, and such differences depended on the developmental stage. At tillering stage, most of the variables explained the variation in the data that separated the cluster of waterlogged roots form the rest of the observations, suggesting roots as the more responsive organ under waterlogging. However, an opposite effect was observed at booting, when most of the characteristics influenced the separation of leaves of waterlogged plants from the rest of the observations. At this stage, the leaves of waterlogged plants were more responsive to the stress than the roots of the same plants.

5.2 Comparative analysis of metabolite profiles in waterlogged and drought-stressed wheat

The present study aimed to investigate the impact of waterlogging and drought stress on the metabolomic and ionomic profiles of fully developed leaves and roots. To achieve this, plants were subjected to 12 days of stress exposure and compared to control conditions. To comprehensively analyze the dataset, PCA was employed, allowing for the reduction of dimensionality and the identification of underlying patterns and distinct features associated with each treatment. Notably, when considering the type of tissue separately, an interesting finding emerged. At the tillering stage, the variance between waterlogging, drought, and control in the roots was primarily displayed in PC1, with no discernible PC2. Similarly, for the dataset corresponding to leaves from either treatment at the booting stage, the same trend was observed. Therefore, for the PCA analysis, both plant tissues were displayed together at either growth stage (Figure 10).

At the tillering stage (Figure 10A), the PC1 captured 30% of the variation among plant tissues, whereas PC2 described 22% of variations between control, waterlogging and drought. Independent

of the type of tissue, the observations made for waterlogging clustered separetly to those ones made for control and drought. These two observations clustered rather together in either plant tissue with a larger dispertion in the leaves. Additionally, the loading plots showed how strongly each of the characteristic influenced mostly the separation between plant tissue in the PC1. Among them, sucrose, succinate, oxoglutarate, and *cis*- and *trans*-aconitate were the characterisitics with the strongest influence in the separation along PC1, especially in the leaves. Interestingly, almost half of the variables measured, including Ala, GABA, Ile, Leu, Arg, and Val indicated a strong effect on the observations made in roots of waterlogging plants, whereas the other half, including Thr, Glu, Tyr, Ser, Phe, His, P, S and to a lesser extent pyruvate influenced the observations made in leaves of drought and control plants.

At the booting stage (Figure 10B), the PC1 and PC2, also explained the variances given by the type of tissue and the treatments respectively. Interestingly, a rather opposite effect as the indicated at tillereing was observed in the clusters representing the leaves of all treatments. The observations made in the leaves of drought-stressed plants clustered further away from those ones made in the leaves of waterlogged and control plants, beign these two clustered rather together. However, the observations made in roots indicated that again, waterlogging exhibited the largest variation at booting stage.

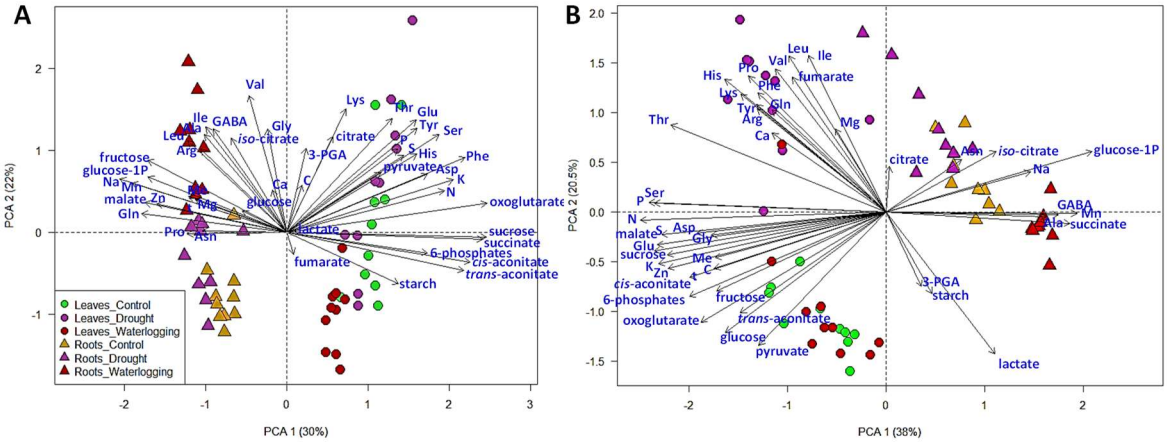

Figure 10. Principal Component Analysis of metabolites and nutrients in fully developed leaves and roots of control, waterlogged or drought-stressed plants at (A) tillering or (B) booting stage. After 12 days of waterlogging, the fully developed leaves and roots were collected from the control, waterlogging, and drought treatments. The variance captured by the first and second principal components (PC1 and PC2, respectively) is given in brackets. Each vector represents one characteristic determined in all plant tissues and treatments. The direction and length of the vectors represent the influence of the variables on the separation of the observations into the different clusters.

Notably, the loading plots clearly showed that most of the characterisitcs measured explained the variances displayed in the PC1, being positively influencing the observations made in the leaves of waterlogged and control plants. Additionally, some amino acids such as Ile, Leu, Val, Phe, Pro and His influenced the cluster made by the observations in leaves of drought-stressed plants. Yet, Ala,

GABA, Mn and succinate had the greatest effect on the separation of the root profile of the waterlogged plants.

Altogether, these results provided insights into the effects of waterlogging and drought stress on metabolomic and ionomic profiles in leaves and roots. Importantly, these effects varied depending on the growth stage of the plants. The PCA analysis revealed that distinct patterns and influential characteristics existed at each stage. At tillering stage, the largest variations were given by the observations made in the roots of waterlogged plants, whereas the observations made in the leaves of drought-stressed plants showed the largest variation at booting. These findings highlighted the stage-dependent responses of plants to waterlogging and drought stress, and provided valuable insights into the specific metabolic responses of plants under either stress. This was indicated by higher metabolic changes in the roots of waterlogged plants at tilleirng and in the leaves of drought-stressed plants at booting.

5.3 Effect of waterlogging on the dynamic response of plant growth and metabolism

In order to evaluate the effect of short- and long- term waterlogging on the dynamics of plant growth and metabolism, the wheat plants at tillering were chosen because they showed a more pronounced response to waterlogging than plants at booting stage. To better capture the dynamics of the physiological response, five time points were set during the 12-day exposure to waterlogging and three time points during the recovery period starting at day 12 until day 24 (Figure 1B). For the latter period, samples were taken from control, waterlogging 1 (terminated on day 12), and waterlogging 2 (terminated on day 24). To evaluate the yield performance at ripening stage, waterlogging was terminated on day 24 in all plants allowing an optimal drain off to field capacity as in control plants.

5.3.1 Effect of waterlogging on the dynamics of plant growth in wheat

Under waterlogging, no significant changes in shoot biomass were observed until day 6 (Figure 11A, green lines). However, from day 6 until day 12 this parameter decreased in waterlogged plants. Two days after the end of waterlogging 1, i.e. on day 14 after the onset of the stress, the biomass of plants recovered from waterlogging became again similar to that of the control plants. However, plants kept yet under waterlogging (waterlogging 2) showed less biomass at the same time point (Figure 11B, upper panel). In addition, on day 18, plants from the waterlogging 1 treatment had similar height and leaf number as the control plants, indicating that the effects of waterlogging for 12 days on shoot biomass were reversible. In contrast, root biomass responded earlier to the stress (Figure 11A, brown lines). Root biomass decreased by 32% on day 3 under waterlogging compared to control. Interestingly, from day 6 to day 9, the root biomass of the stressed plants did not differ

from that of the control plants. Furthermore, from day 9 on, the appearance of adventitious roots was observed (Figure 11B, lower panel). From day 9 throughout the whole recovery phase, root biomass was lower than that of control plants.

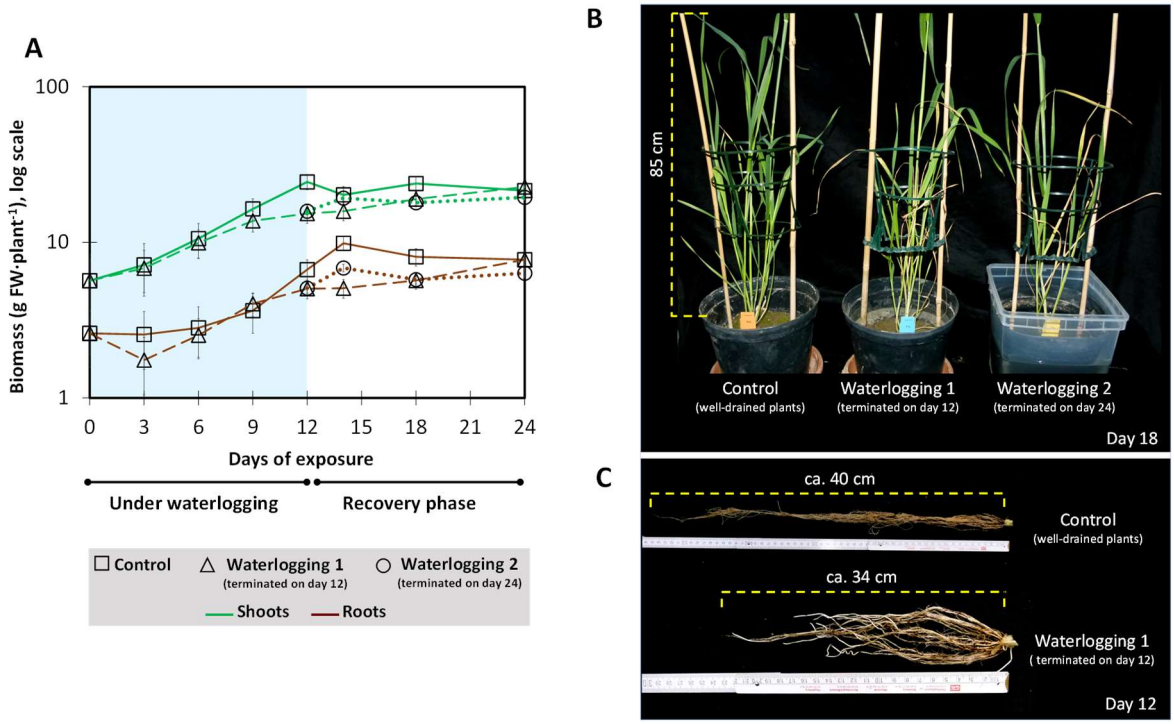

Figure 11. Growth and visual appearance of wheat plants during waterlogging and recovery from stress. (A) Dynamics of shoot (green lines, top) and root (brown lines, bottom) biomass during waterlogging and the recovery phase. (B) Shoot and (C) root appearance of wheat plants that were adequately water-drained (control) or waterlogged for either 12 or 24 days. Fully developed leaves and roots were collected at days 0, 3, 6, 9 and 12 (under waterlogging), and 14, 18 and 24 (during recovery phase). Symbols show means ± SE (n = 8).

In addition, other parameters, such as the tiller number, plant height, and root length were monitored. For these, only the period during waterlogging was considered, as day 12 corresponded with the end of the tillering stage (Z30). Tiller number was not significantly affected by waterlogging (Figure 12A), whereas plant height was negatively affected from day 6 after the onset of the stress (Figure 12B). In addition, the maximum root length of waterlogged plants was significantly reduced since the onset of the stress and remained lower than that of control plants during the 12-day stress period (Figure 12C).

Altogether, the results highlight the effect of waterlogging on various plant characteristics and how they recover after the stress period. The roots of waterlogged plants responded quickly with a reduction in biomass and length and the formation of adventitious roots, most likely due to impaired root respiration from the lack of oxygen. In contrast, above-ground parameters, such as shoot biomass, were not affected initially and only decreased after day 6 of the stress. When waterlogging persisted for longer, the low oxygen availability eventually affected shoot growth and development. During the recovery phase, shoot parameters were fully restored after the excess

water was removed, but the root parameters did not fully recover, indicating organ-specific effects of prolonged waterlogging on plant growth and development.

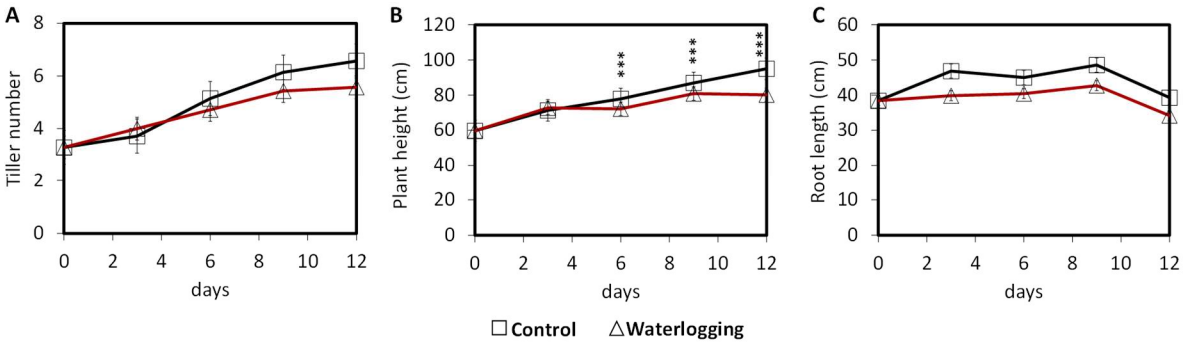

Figure 12. Dynamics of phenotypic traits of wheat plants during 12-day waterlogging at tillering stage. (A) Tiller number, (B) plant height and (C) root length at 0, 3, 6, 9 or 12 days under waterlogging. Above-ground parameters were measured at each indicated time point, and the length of the entire root system was measured immediately after sample collection. Symbols show means ± SE. Different asterisks indicate significant differences at *** $P < 0.001$ according to Student's *t*-test or Mann-Whitney *U*-test, $P \leq 0.05$, n = 7.

5.3.2 Effect of waterlogging on the dynamics of hormone translocation rates in wheat

In order to assess the nutritional and stress status of the roots, xylem exudates were collected from control and stressed plants at the same time points specified in the waterlogging and recovery phases. Due to the limited volume of xylem sap collected from the plants on day 24 under waterlogging, this time point was omitted and therefore, all data were presented in terms of translocation rates in the xylem up to day 18. Due to the absence of transpiration measurements during the experiment, the translocation rates of all metabolites and nutrients measured in the xylem exudates was interpreted as the "apparent translocation rate".

In general, xylem exudation rates (Appendix 4) kept rather constant in the control plants and were not yet compromised by excess water in stressed plants until day 3, so that sufficient exudate could be collected from each treatment. Thereafter, xylem exudation rate sharply decreased during waterlogging, with the lowest value registered on day 12. Once the stress was removed from the corresponding set of plants (waterlogging 1), xylem exudation rates recovered and reached a maximum on day 18. Notably, continuosly waterlogged plants (waterlogging 2) kept the lowest exudation rates.

To investigate whether waterlogging affects the communication between roots and shoots via hormone translocation, different species of phytohormones were determined in the xylem exudates by LC-MS/MS. Among all detected hormones, gibberellins (GA) accounted for the largest amount and diversity in the xylem (Figure 13). In both control and waterlogged plants, the translocation rates of GA53, GA44, GA19, GA5, GA15 and GA4 increased by two- or threefold during the first 3 days, followed by a sharper decrease under waterlogging in the following days. Only GA51 decreased steadily from day 0 to day 9. During the recovery phase, the translocation rates of all GAs

remained low in the control plants and in the plants from which the stress had not yet been removed on day 12 (waterlogging 2). However, by day 18, recovered plants (waterlogging 1) showed an increase of the translocation rate of about twofold compared with the other treatments.

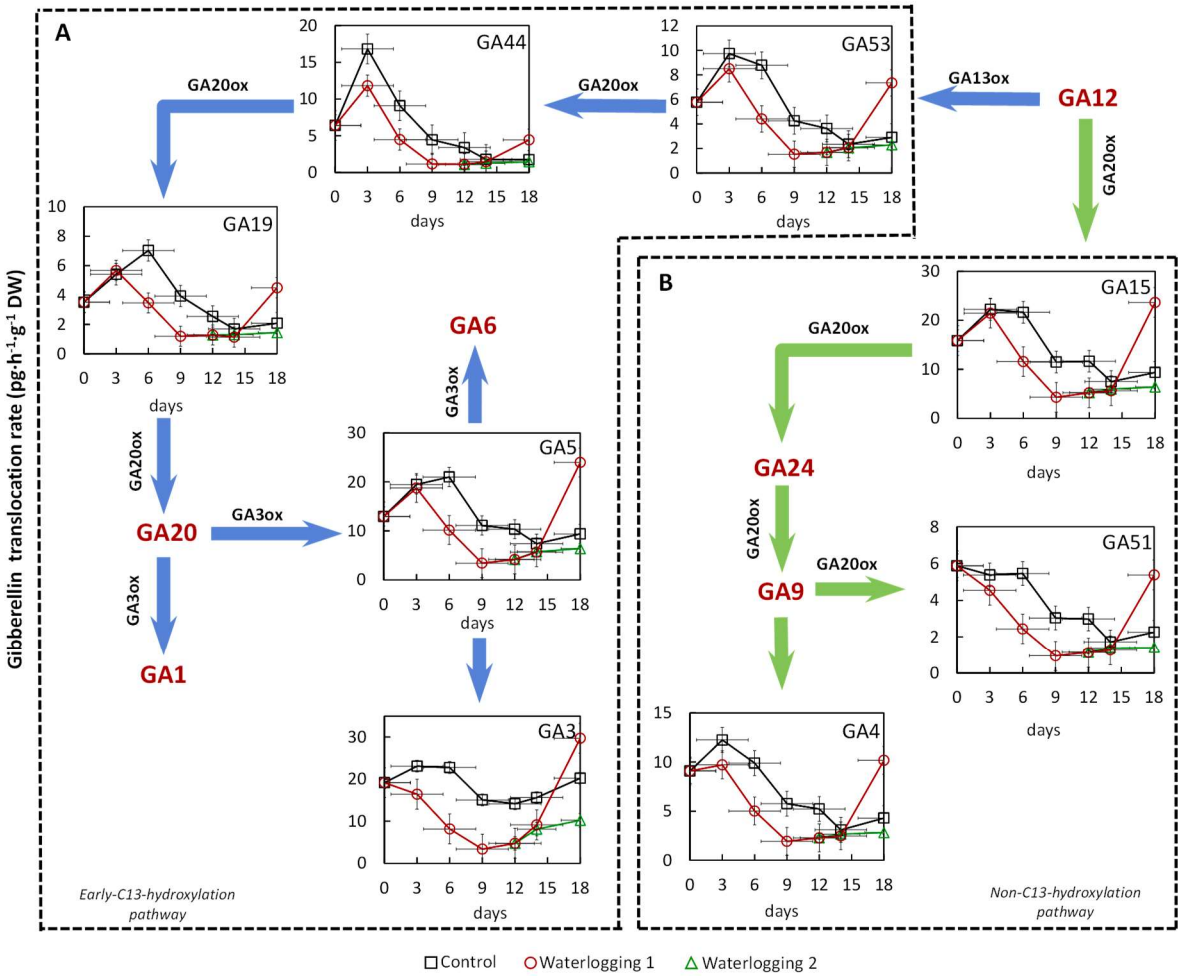

Figure 13. Influence of waterlogging on gibberellin translocation rates in the xylem of wheat plants. (A) Dynamics of gibberellin translocation rates (GA44, GA19, GA5, GA3, GA53) of the early C13 hydroxylation pathway and (B) the non-C13 hydroxylation pathway (GA4, GA15, GA51). GA species are graphically arranged according to their position in the metabolic pathway. Xylem exudates were collected at days 0, 3, 6, 9 and 12 under control conditions or waterlogging (waterlogging 1), and at days 14 and 18 during the recovery phase or continuous waterlogging (waterlogging 2). Symbols show means ± SE (n = 8).

Abscisic acid (ABA) and its degradation product phaseic acid (PA) were also found in xylem exudates of plants from different treatments (Figure 14A, B). Their translocation rates in control plants increased by threefold on day 6, followed by a decline on day 9. Stressed plants showed a steady decline until day 12 under waterlogging, as observed for gibberellins. Interestingly, translocation rates of salicylic acid (SA) increased on day 3 by twofold in waterlogged plants, followed by a sharp decline on day 9 (Figure 14C). During the recovery phase, the translocation rates of ABA, PA, and SA increased in plants from waterlogging 1 treatment. On day 18, the same group of plants reached maximum translocation rates of these hormones, similar as observed for gibberellins.

A similar pattern to ABA and PA was observed also for jasmonic acid (JA) and *cis*-zeatin riboside (cZR) (Figure 14D, E). Control plants showed a maximum of translocation rates on day 6 and a decrease from that day onwards. In stressed plants, the translocation rates decreased from day 0, followed by a recovery approx. to the levels of control plants by day 14. In contrast, jasmonic acid-isoleucine (JAIle) showed rather a progressive increase in control plants until the end of the experiment, whereas in stressed plants it decreased from day 6 after the onset of the stress (Figure 14F). The translocation rates increased again on day 12 after the end of waterlogging to similar levels than in control plants. Continuously waterlogged plants (waterlogging 2), remained with lower translocation rates of all hormones, except for JA-Ile. Other hormones such as N6-isopentenyladenosine (IPR), indoleacetic acid (IAA) and *trans*-zeatin riboside (tZR) showed no significant differences between the different treatments (Appendix 5).

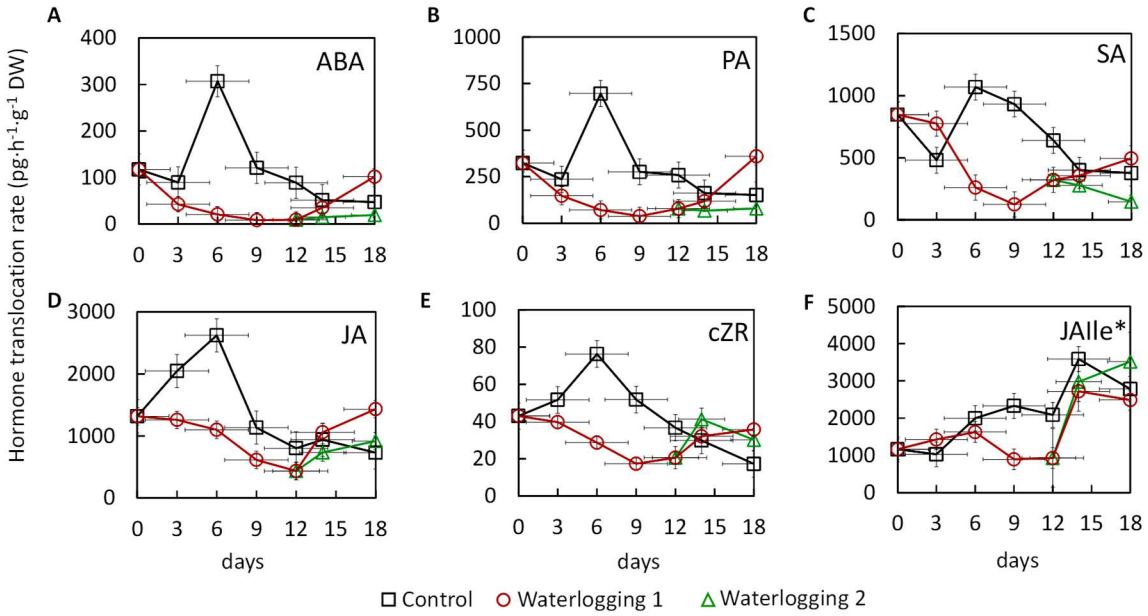

Figure 14. Influence of waterlogging on the translocation rates of hormones in the xylem of wheat plants. (A) Abscisic acid (ABA), (B) phaseic acid (PA), (C) salicylic acid (SA), (D) jasmonic acid (JA), (E) *cis*-zeatin riboside (cZR), and (F) jasmonic acid-isoleucine (JAIle) . Xylem exudates were collected at 0, 3, 6, 9 and 12 days under control conditions or waterlogging (waterlogging 1), and at days 14 and 18 during the recovery phase or continuous waterlogging (waterlogging 2). Symbols show means ± SE (n = 8). * The scale in (F) is expressed as peak area.

Overall, xylem exudation rates were interrupted from the early stages of exposure to waterlogging, and remained low throughout the 12-day period. However, once excess water was drained off, the plants were able to recover and return to their similar rates of xylem exudation as in control plants. This interruption in xylem exudation also affected hormone translocation rates, which saw a dramatic decrease from day 3 of waterlogging. After drainage, the hormone translocation rates in the plants were able to reach comparable values to those of the control group. Interestingly, the waterlogged and subsequently drained plants showed a strong increase in hormone translocation

rates on day 18, exceeding even those of the control group. This effect corresponded with recovered xylem translocation rates on the same day, probably due to reconstitution of the hydraulic properties of the soil and roots.

5.3.3 Effect of waterlogging on the dynamics of nutrient translocation rates in wheat

The tillering phase of wheat plants is critical for ensuring maximum tiller formation and subsequent spike development. In order to assess nutrient translocation rates during this stage of development, the dynamics of translocation rates of macro- and microelements in the xylem exudates were monitored over a 12-day waterlogging period and the subsequent recovery phase (Figure 15).

In control plants, translocation rates of macronutrients (Figure 15A) and also of Zn (Figure 15B) showed an initial increase before they dropped at day 9 to a rather constant low level. Such an initial transient increase was not recorded in waterlogged plants, in which translocation rates remained at a low level throughout the stress period. Only at day 18, translocation rates increased sharply in plants recovering from stress (waterlogging 1) to a level far above that of control plants. In continuously waterlogged plants (waterlogging 2), translocation rates of these elements, except for Ca, remained at a low level throughout the recovery period. On the other hand, translocation rates of Mn, Fe and Na showed an almost opposite pattern with a considerable increase soon after the onset of waterlogging (Figure 15B). When waterlogging was resumed, translocation rates remained at high levels and exceeded those of control plants. Continuously waterlogged plants (waterlogging 2) showed rather constant translocation rates for macroelements, and a sharp increase of microelements by day 14 followed by a strong decrease by day 18.

Overall, waterlogging strongly decreased the translocation rates of most macronutrients in wheat plants, but these rates recovered once the stress was removed. In contrast, the translocation rates of Fe, Mn and Na increased sharply throughout the stress period and remained high in particular when waterlogging was resumed. While this increase of Fe and Mn in waterlogged plants can be attributed to the reducing conditions in the waterlogged soil, the reason for the initial increase in translocation rates of macronutrients in control plants remains unknown. These findings underscore the importance of changing nutrient availabilities in ensuring optimal growth and development of wheat plants under waterlogging stress.

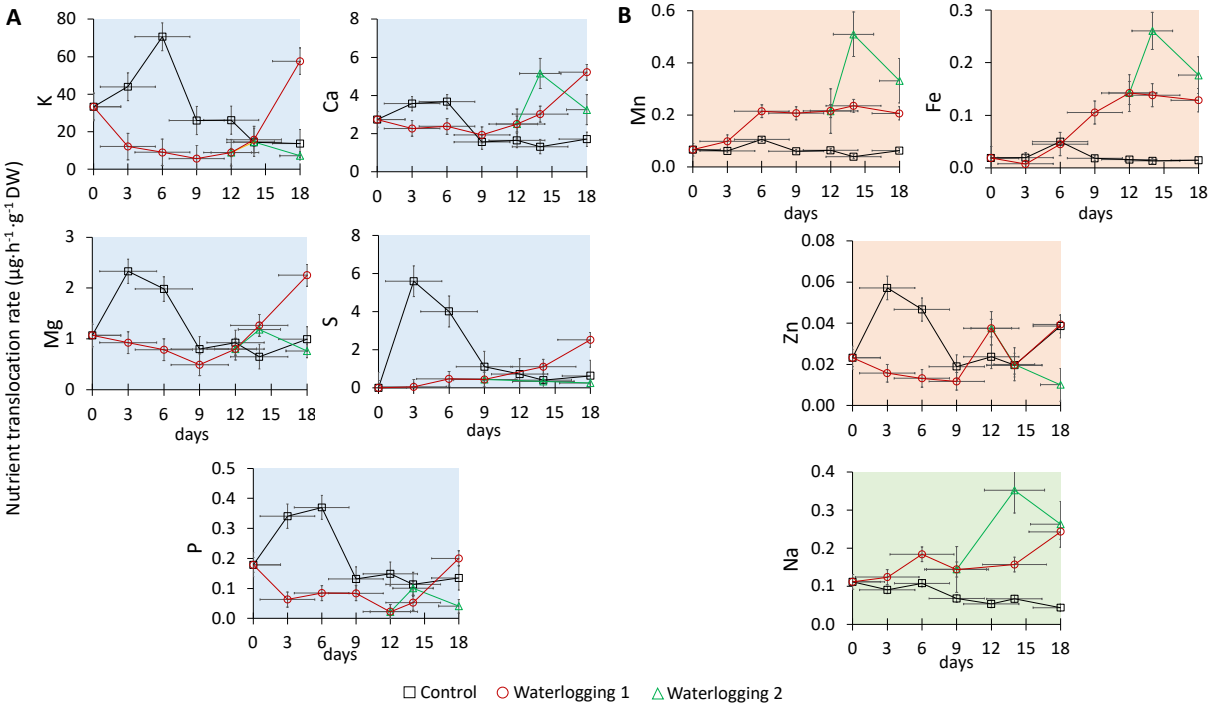

Figure 15. Influence of waterlogging on nutrient translocation rates in the xylem of wheat plants. (A) Translocation rates of macronutrients and (B) of micronutrients and of Na in the xylem of wheat plants at tillering stage. Xylem exudates were collected at 0, 3, 6, 9 and 12 days under control conditions or waterlogging (waterlogging 1), and at days 14 and 18 during the recovery phase or continuous waterlogging (waterlogging 2). Symbols show means ± SE (n = 8).

5.3.4 Effect of waterlogging on the dynamics of amino acid translocation rates in wheat

To investigate the effect of waterlogging on amino acid translocation rates in wheat at tillering stage, amino acid concentrations were determined in the xylem exudate of control and waterlogged plants. Quantification of total amino acids in the xylem exudate revealed a sharp increase in the amino acid translocation rate at day 3, which was higher in control than in waterlogged plants (Figure 16A). From day 6 onwards, aa translocation rates decreased to a similarly low level in all treatments until the end of the experiment.

To estimate the overall abundance of each individual amino acid in the xylem exudates, and considering a pool of all samples collected at each time point, the overall amino acid concentration in all treatments was calculated at the end of each evaluation phase, i.e. on day 12 under waterlogging, and on day 18 during the recovery phase (Figure 16B, Appendix 6). Notably, Asn and Gln were the most abundant amino acids translocated in the xylem of control plants (Figure 16B). Gln accounted for approx. 60% of the total amino acid concentration, followed by Asn with approx. 20% on day 12, and 8% on day 18. In contrast, Ala and GABA constituted the amino acids with the highest percentages present in the xylem exudates of waterlogged plants. Interestingly, on day 12 Ala accounted for approx. 54% of the total amino acid concentration, whereas GABA represented approx. 9%. In addition, the same plants exhibited a sharp decrease of Gln and Asn. Furthermore, on day 18 during the recovery phase, Ala and GABA concentration dropped again to the order of

control plants during the same evaluation period. Notably, plants kept under stress until day 24 (waterlogging 2) showed a sharp decrease of Asn and Gln and a strong increase of Ala and GABA by day 18 during the recovery phase.

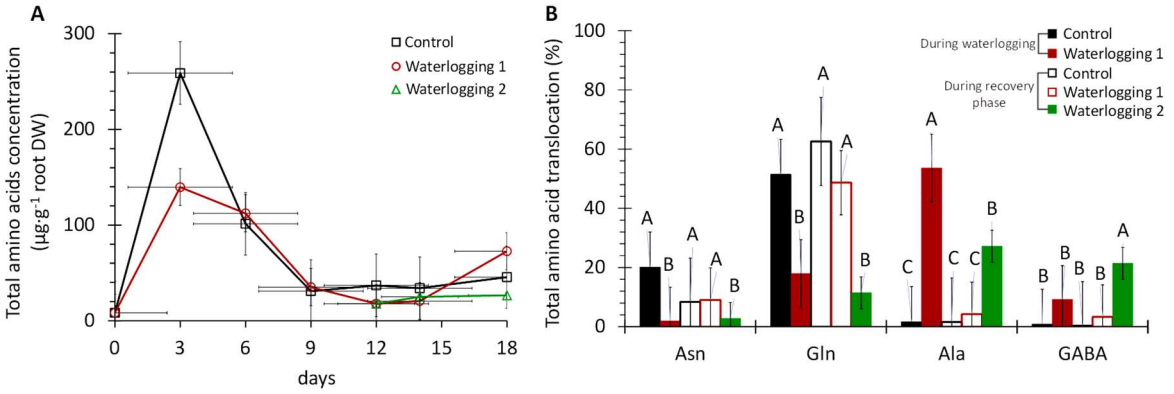

Figure 16. Influence of waterlogging on amino acid translocation rates in the xylem of wheat plants. (A) Translocation rates of total amino acids in the xylem of wheat plants at tillering stage. (B) Total percentage of major amino acids in the xylem exudate determined at the end of each phase of the experiment. Xylem exudates were collected at days 0, 3, 6, 9 and 12 days under control conditions or waterlogging (waterlogging 1), and at days 14 and 18 during the recovery phase or continuous waterlogging (waterlogging 2). Symbols in (A) show means ± SE (n = 8) and the bars in (B) show means ± SE. One-way ANOVA analysis determined the differences between groups. Different letters in (B) indicate significant differences according to Tukey's HSD or Dunn's test, $P \leq 0.05$, n = 8.

The comparison of individual amino acid translocation rates in the xylem of plants under the different treatments revealed that most of them were much lower in waterlogged than in control plants (Appendix 7). In the latter, some amino acids such as Gln (Figure 17A), showed a sharp increase until day 3 followed by a strong decline until day 9, keeping rather constant values until the end of the experiment. Among all amino acids, Gly, Ala and GABA exhibited a contrary trend In particular between day 3 and day 6, translocation rates of these were higher in waterlogged plants than in control (Figure 17B-D). After the end of the stress at day 12 in the corresponding plants, the same amino acids showed comparable values to those from control plants during the recovery phase. Interestingly, of all amino acids determined in waterlogged plants, Ala accounted for the most abundant during the 12 days of stress, representing about 65% of the total amino acid determined in this study.

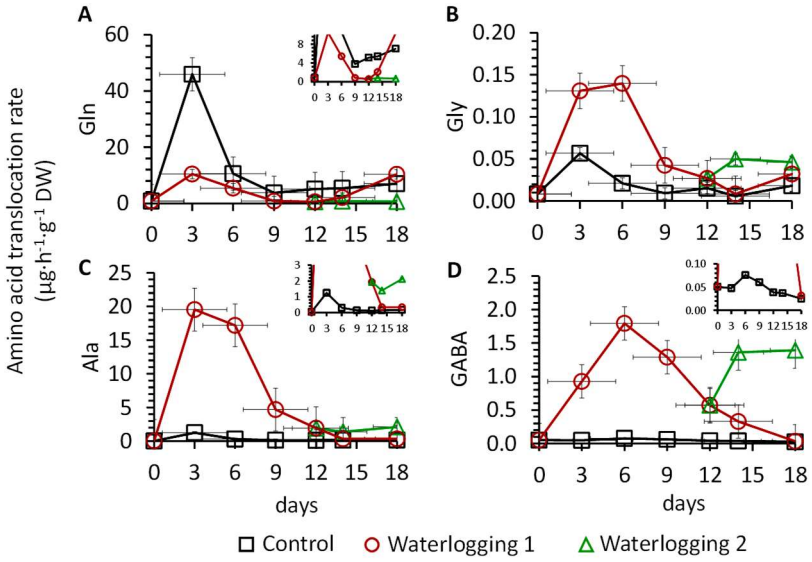

Figure 17. Influence of waterlogging on translocation rates of individual amino acids in the xylem of wheat plants. Translocation rates of (A) glutamine (Gln), (B) glycine (Gly), (C) alanine (Ala), and (D) gamma-aminobutyric acid (GABA). Xylem exudates were collected at 0, 3, 6, 9 and 12 days under control conditions or waterlogging (waterlogging 1), and at days 14 and 18 during the recovery phase or continuous waterlogging (waterlogging 2). Symbols show means ± SE (n = 8).

5.3.5 Effect of waterlogging at the tillering stage on yield-related parameters in wheat plants

At ripening (Z61-69), the plants of all treatments did not differ significantly in height and number of spikes produced individually (Figure 18A, B). However, the shoot biomass and the number of tillers recorded at the final growth stage (Figure 18C, D) showed that the group of plants for which the stress was removed on day 12 (waterlogging 1) reached similar values to those of the control. However, the set of plants that remained under waterlogging until day 24 (waterlogging 2) showed a decline in these parameters, demonstrating the strong negative impact of prolonged waterlogging on plant development and productivity. The same held true for the total weight of spikes and total weight of grains (Figure 18E, F). However, the total number of grains decreased significantly with the length of the waterlogging period and appeared thus being the most sensitive trait. Plants waterlogged for 12 days produced 20% less grains than the control plants, whereas plants waterlogged for 24 days produced two times fewer grains (Figure 18G).

In addition, seeds were recovered from control and waterlogged plants for 12 days (waterlogging 1), whereas seeds from plants waterlogged for 24 days (waterlogging 2) exhibited a much lower recovery compared to the other treatments. Then, germination rates of the recovered seeds were evaluated 7 and 14 days after sowing to examine the quality of the grains (Figure 18H). Seven-days after sowing, 87% of the seeds from control plants had germinated, whereas the germination rate of seeds from plants waterlogged for 12 days or 24 days exhibited 96% and 40% respectively. Surprisingly, 14 days after sowing, 96% and 100% of the seeds from control and waterlogging 1 plants respectively had germinated, in contrast to only 60% of the seeds from waterlogging 2 plants.

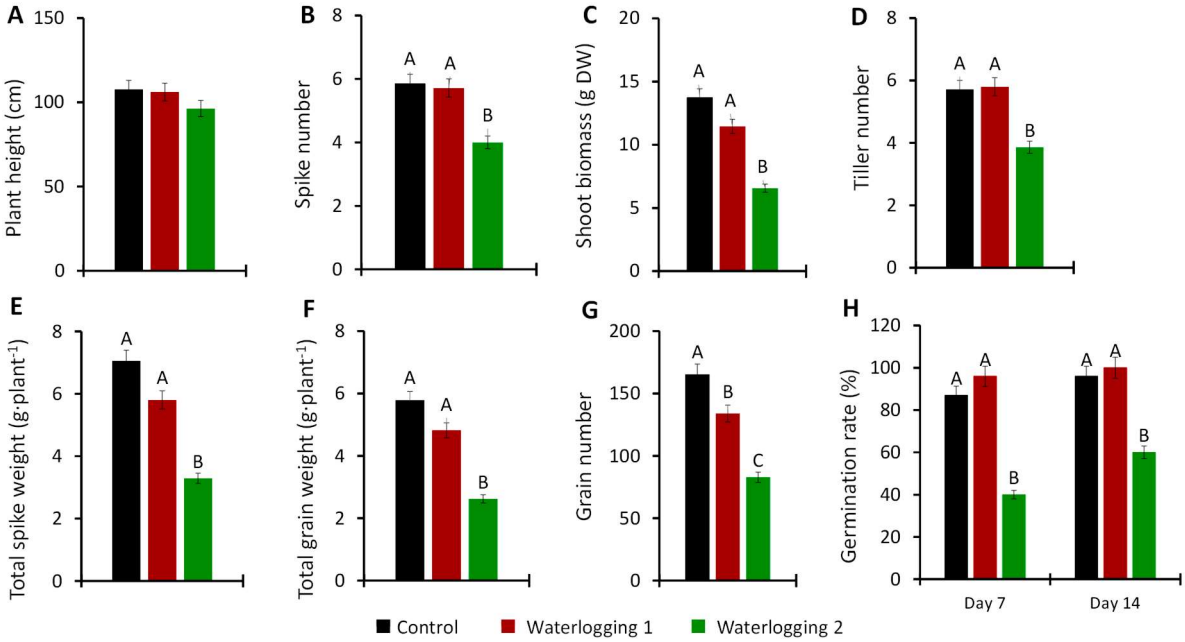

Figure 18. Yield-related parameters in wheat plants after waterlogging during tillering for either 12 or 24 days. (A) Plant height, (B) number of spikes, (C) shoot biomass, (D) number of tillers, (E) total weight of spikes, (F) total weight of grains, (G) number of grains, and (H) germination rate of recovered seeds. 12 or 24 days after the onset of waterlogging, excess water was removed. Plants being well-drained (control), waterlogged for 12 days (waterlogging 1) or waterlogged for 24 days (waterlogging 2) were allowed to continue growing until ripening (Z, 61-69) under adequate water supply and drainage. Bars show means ± SE. One-way ANOVA analysis determined the differences between groups. Different letters in (B) indicate significant differences according to Tukey's HSD or Dunn's test, $P \leq 0.05$, n = 8.

These phenotypic changes and yield-related traits show that growth depression was still mild when plants were recovered from a shorter exposition to waterlogging for 12 days, whereas growth and productivity were severely suppressed after waterlogging for 24 days. Together with the profound changes in the sugar and amino acid profiles it was concluded that metabolic adjustments must have occurred in plants during the stress and subsequent recovery at day 12 that accounted for differential plant performance to ensure plant reproductivity.

Chapter 2: Transcriptional response of wheat plants to waterlogging and drought

5.4 Effect of waterlogging on changes in gene expression in leaves and roots of wheat plants

To evaluate the effect of waterlogging on global changes in gene expression in wheat, fully expanded leaves and roots from control and waterlogged plants were collected and subjected to RNA extraction. For the transcriptome analysis, only time point 12 from the central experiment was considered, which represented plants that were adequately watered or waterlogged for 12 days.

5.4.1 Identification of common de-regulated genes expressed in leaves and roots of waterlogged plants

Analysis of global changes in gene expression in leaves and roots of waterlogged plants were compared to the corresponding controls, revealing that at the tillering stage 1915 and 6545

transcripts were counted in leaves and roots, respectively. At the booting stage, the corresponding number of transcripts increased to 4287 and 21,272, respectively. In order to compare the type of differentially expressed genes between above- and below-ground organs, unique and common transcripts were distinguished in leaves and roots at each developmental stage. In leaves, the number of up-regulated transcripts with a $\log_2$ fold-change ≥ |2| at $P_{adj} < 0.05$ was larger than those down-regulated at either stage (Figure 19 A, C). By contrast, in roots of the same plants most of the transcripts were down-regulated (Figure 19 B, D). At tillering stage, the number of commonly up-regulated (88) or down-regulated (81) transcripts in both plant organs was similar (Figure 19A, B). However, at booting stage a larger number (492) was up-regulated than down-regulated (146) (Figure 19B, C).

To distinguish the expression patterns of commonly de-regulated genes in leaves and roots of the same plants, a heatmap of their expression levels was created (Figure 19E, F). In general, up-regulated genes were found to have higher expression levels in leaves than in roots of stressed plants, irrespective of the DS (Figure 19E, F, upper panel). However, an opposite effect was registered in the down-regulated genes as higher expression levels were found in the roots (Figure 19E, F, lower panel). This effect was even stronger at booting stage, when a larger number of differentially expressed genes was counted. Considering the average of the $\log_2$ fold-change registered in leaves and roots, the five most up-regulated genes at tillering encoded a purple acid phosphatase 23 (*PAP23*), SPX domain-containing protein 3 (*SPX3*), AP2/ERF and B3 domain-containing protein (Os01g0141000), MLO-like protein 1 (*MLO1*), and a probably receptor-like protein kinase (At2g21480) (Appendix 8A, upper panel). These genes were related mainly to phosphate homeostasis, modulation of plant immunity, and the regulation of signaling pathways in response to stress. Furthermore, the five most down-regulated genes in the same plant organs and DS were encoding a dehydrin DHN3 (*DHN3*), two transcripts related to the *homeobox leucine zipper protein HOX24* (*HOX24*), *homeobox-leucine zipper protein HOX22* (*HOX22*), and *cytochrome P450-72A14* (*CYP72A14)* (Appendix 8A, lower panel), indicating suppression of important protecting plant mechanisms from cellular damage caused by abiotic stress, and inhibition of specific processes related mainly to hormone biosynthesis and root development. Furthermore, the five most up-regulated genes in either tissue at booting (Appendix 8B, upper panel) consisted of one gene encoding a protein of unknown function (DUF1262), a cell number regulator 10 (*CNR10*), phospholipase A1-II 7, the auxin-responsive protein SAUR71 (*SAUR71*), and an E3 ubiquitin-protein ligase ATL9 (*ATL9*). In general, these genes were related to plant detoxification processes, cell regulation, lipid metabolism, and regulation of plant growth and development. Finally, four transcripts related to *sucrose: sucrose 1-fructosyltransferase* (*1-SST*), which is related to the synthesis of storage forms of carbohydrates, and an *aquaporin NIP3-1* (*NIP3-1*) involved in the

regulation of water transport to maintain water balance were most strongly down-regulated in either tissue (Appendix 8B, lower panel).

In general, waterlogging stress had distinct effects on gene expression in different parts of the plant, with roots showing inhibition, while leaves showed promotion of the same genes. This effect was observed at both tillering and booting stage. However, commonly de-regulated genes in roots and leaves differed between these stages, shedding light on phosphate homestasis, stress response, hormone biosynthesis, and root development at the time of tillering, whereas plant detoxification processes, carbohydrate metabolism and water regulation were most predominat at booting.

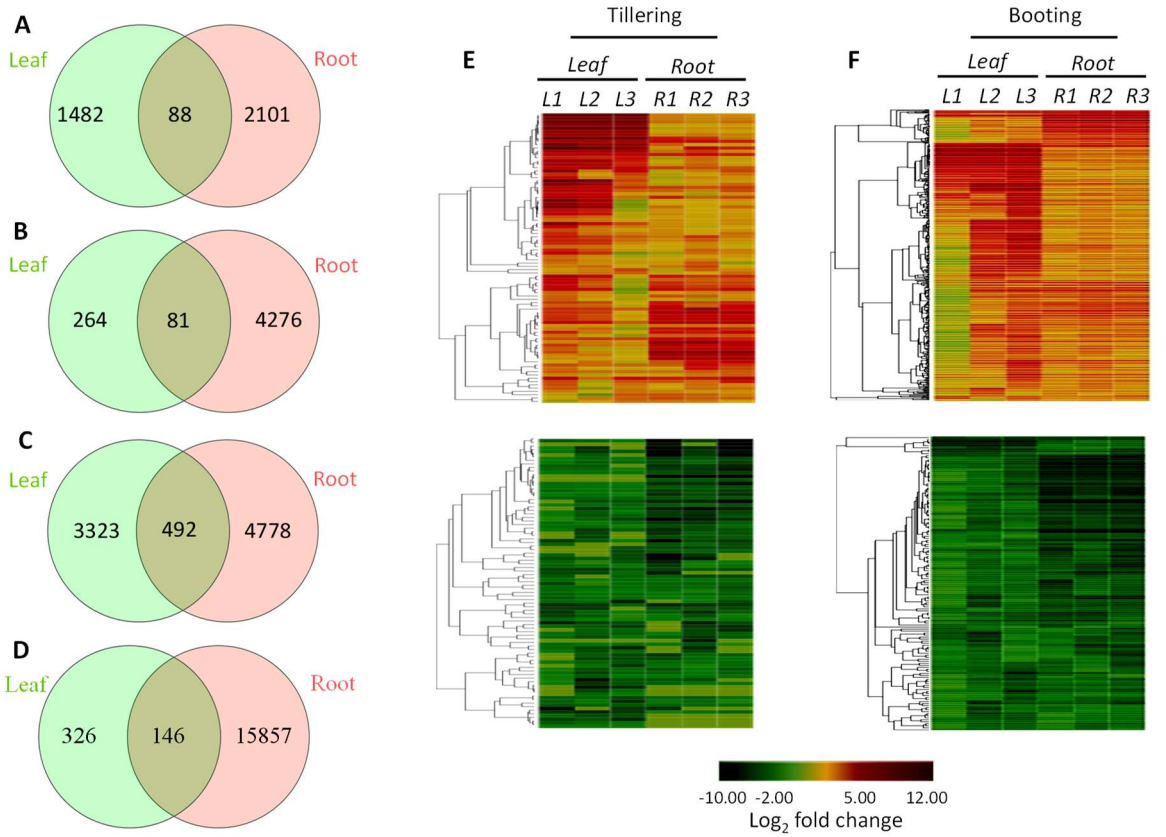

Figure 19. Commonly expressed genes in leaves and roots of waterlogged plants at two stages of development. (A-D) Venn diagrams show the number of up-regulated (A, C) and down-regulated (B, D) transcripts in leaves and roots at tillering (A, B) or booting (C, D) stage. (E-F) Heatmaps showing commonly up-regulated (upper panel) and down-regulated (lower panel) transcripts in leaves and roots of waterlogged plants at tillering (E) or at booting (F). In all cases, waterlogged plants were compared with control and genes were grouped according to their transcript abundance at day 12 after the onset of the stress. The transcripts were selected according to $\log_2$ fold-change ≥ |2| at $P_{adj} < 0.05$.

5.4.2 Identification of unique de-regulated genes in leaves and roots of waterlogged plants

Focusing on genes that were expressed only in leaves or roots of waterlogged plants compared to their respective controls revealed that waterlogging induced higher expression levels of uniquely expressed genes in roots than in leaves (Figure 20). At tillering stage, the most up-regulated genes in leaves were *glycerophosphodiester phosphodiesterase* (*GDPD1*), *SPX domain-containing protein 6* (*SPX6*), and *inorganic pyrophosphatase 2* (Figure 20A), while in roots the corresponding up-

regulated genes belonged to the central hypoxia response category, including *1-aminocyclopropane-1-carboxylate oxidase 1* (*ACO1*), *plant systeine oxidase 1* (*PCO1*), and *alcohol dehydrogenase 3* (*ADH3*) (Figure 20B). Notably, genes related to phosphomannomutase/ phosphoglucomutase (PMM) and glucan endo-1,3-beta-glucosidase GIIID were down-regulated only in leaves, while genes encoding a probably auxin efflux carrier component 9, asparagine synthetase [glutamine-hydrolyzing] 1, (2S)-flavan-3-ol-forming anthocyanidin reductase, and high-affinity nitrate transporter 2.1 were down-regulated only in roots (Figure 20A, B).

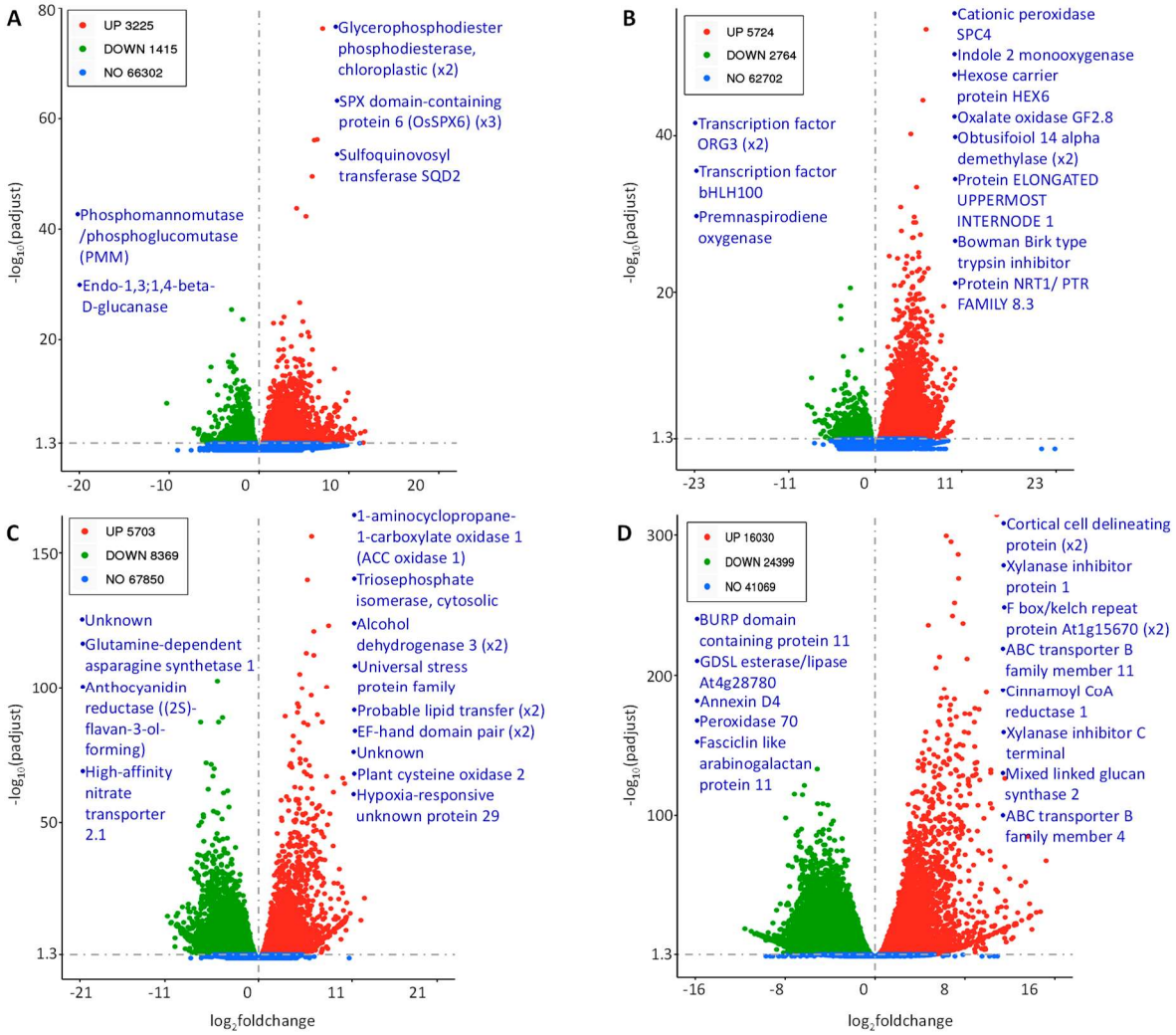

Figure 20. Uniquely expressed genes in leaves or roots of waterlogged plants at two stages of development. (A-D) De-regulated genes in leaves (A, B) or roots (C, D) of waterlogged plants compared to control at tillering (A, C) or booting (B, D) stage. In all cases, genes were grouped according to their transcript abundance on day 12 after the onset of waterlogging. All genes that are shown have a $\log_2$ fold-change ≥ |2| at $P_{adj} < 0.05$.

Interestingly, in leaves or roots of waterlogged plants at the booting stage, no hypoxia-related genes with significant de-regulation were found. Instead, genes encoding a cationic peroxidase SPC4, indole-2-monooxygenase (*CYP71C4*) , hexose carrier protein HEX6 (*HEX6*), oxalate oxidase GF-2.8, and two genes encoding the obtusifoliol 14-alpha demetylase were the five most up-regulated in leaves only (Figure 20C), while genes related to cortical cell delineating protein, xylanase inhibitor

protein 1 (*XIPI*), F-box/kelch repeat protein At1g15670, ABC transporter B family member 11 (*ABCB11*), and cinnamoyl-CoA reductase 1 (*CCR1*) were most over-represented in roots only (Figure 20D). Down-regulated genes detected in leaves were related with the transcription factor ORG3 (*ORG3*), transcription factor bHLH100 (*BHLH100*), and premnaspirodiene oxygenase (*CYP71D55*), while the down-regulated genes in roots were related with BURP-domain containing protein 11 (*BURP11*), GDSL esterase/lipase At4g28780, annexin D4 (*ANN4*), peroxidase 70 (*PER70*), and fasciclin-like arabinogalactan protein 11 (*FLA11*) (Figure 20D). In general, waterlogging affected gene expression in both leaves and roots at both developmental stages. However, de-regulated genes in leaves differed from those ones found in roots, and hypoxia-responsive genes were only significantly up-regulated in the roots of wheat plants at the time of tillering.

5.4.3 Expression analysis of nutrient-transport genes in response to waterlogging

The analysis of the nutritional status of plants under waterlogging stress revealed a significant imbalance in the concentrations of important nutrients, such as N, P, and K. This imbalance was particularly pronounced in the leaves of plants at tillering, and in the roots of plants at booting stage, where a sharp decline in nutrient levels was observed on day 12 of waterlogging (Figure 4, 5). Additionally, GO enrichment analysis in leaves and roots of waterlogged plants (Appendix 9) showed that indeed, functional categories related to nutrient transport were highly representative in both tissues at either stage, as a significative number of de-regulated genes was found under waterlogging. Altogether, indicated that perturbations in nutrient accumulation also displayed at the level of gene expression. Therefore, a focus was placed on the de-regulation of nutrient transport-related genes in both tissues of waterlogged plants at either stage. In the transcriptome study, it was found DEGs annotated for nitrogen, phosphate, iron or potassium transport functions. The same were filtered out from the global transcriptome data using a $\log_2$ fold-change ≥ |2| at P_{adj} < 0.05 as threshold.

To determine the effects of waterlogging on the total number of de-regulated genes related to nutrient transport at tillering or booting, the unique and common transcripts found in leaves and roots of stressed plants at either stage were displayed in a Venn diagram. For genes related to nitrogen transport, a larger number of DEGs was counted at booting than at tillering stage, and more de-regulated genes were counted in the roots than in leaves of the same plant (Figure 21A). About 75 % of the transcripts counted in the roots at tillering stage were also counted in the same tissue at booting stage. Notably, in the leaves of plants at tillering, only four transcripts were counted, and these were also present in the same tissue at booting. Similarly, the largest number of transcripts related to phosphate transport was counted in the roots at either stage, with more transcripts counted at booting (Figure 21B). For this, 10 transcripts out of 17 counted in roots at

tillering were also found at booting, and five out of nine transcripts counted in leaves were common to both stages.

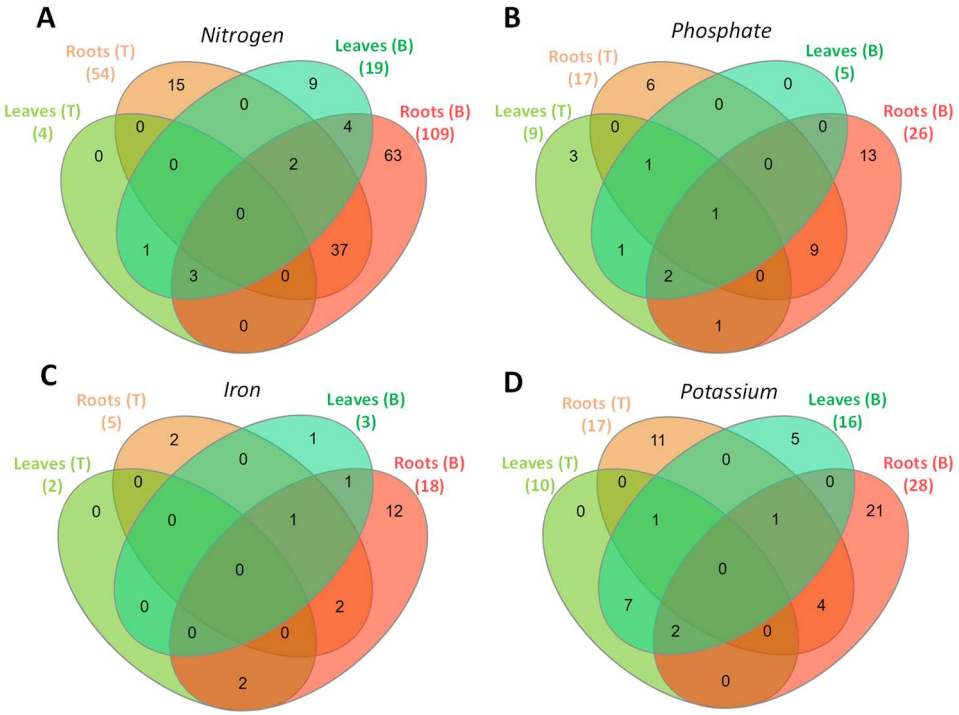

Figure 21. Influence of waterlogging on the total number of expressed genes related to nutrient transport in wheat plants at tillering or booting stages. (A-D) Venn diagrams showing the number of unique and common expressed genes related to (A) nitrogen, (B) phosphate, (C) iron and (D) potassium in leaves or roots of wheat plants at tillering (T) or booting (B) stages. In all cases, waterlogged plants were compared with control, and genes were grouped according to their transcript abundance in leaves and roots on day 12 after the onset of the stress. The genes were selected according to $\log_2$ fold-change ≥ |2| at $P_{adj} < 0.05$.

Notably, a significantly lower number of iron transport-related transcripts was counted (Figure 21C). At tillering stage, only two and five transcripts were counted in the leaves and roots respectively, whereas three and 18 transcripts were counted for the same tissues at booting stage. The second largest group of transcripts related to nutrient transport was formed by those ones related to potassium transport (Figure 21D). Again, a lower number of genes was found at tillering compared to booting, and the largest number was found in the roots at either stage. In general, waterlogging appeared to have a stronger effect on the expression of nutrient transport-related genes at the booting stage than at tillering. However, the de-regulation of genes was more evident in the roots than in the leaves regardless the stage of development.

To identify the function of the de-regulated genes and distinguish their expression patterns in leaves and roots at both stages, the number of genes in each plant tissue and developmental stage was registered according to the $\log_2$ fold-change in expression of each gene. A total of 12 different functions related to nitrogen transport were registered in the leaves and roots of wheat plants. Overall, the genes counted in the leaves were up-regulated, regardless of the developmental stage, while the genes in the roots were down-regulated (Figure 22A). For instance, genes related to

ammonium transporter 3 (*AMT3*), high-affinity nitrate transporter-activating protein 2.1 (*NAR2.1*), and NRT1/PTR family protein 2.3-2.11 (*NPF2*) or 4.4 (*NPF4*) were over-represented in leaves, with the largest number of trasncripts counted at the booting stage. Conversely, no down-regulated transcripts were identified, except for three transcripts at booting stage annotated for *NPF6.2*. The roots of plants at either stage, however, displayed an opposite effect, with the largest number of transcripts being down-regulated. Out of the 19 registered transcripts, only one related to *NRT2.1* was up-regulated by approx. fivefold in the roots of stressed plants at tillering, in addition to four transcripts related to *NPF6.2*. The most down-regulated transcripts in the roots were those related with the *NRT2.1* , which were on average threefold lower than in the control, regardless of the developmental stage. Moreover, genes annotated as *NPF2*, *NPF4*, and *NPF6* were also significantly down-regulated in the roots.

The expression pattern of genes related to phosphate transport showed transcripts related to a *putative inorganic phosphate transporter 1-8* (*PHT1-8*) highly up-regulated in leaves, with seven transcripts increasing on average by fourfold at tillering and four transcripts increasing by threefold at booting (Figure 22B). Notably, no down-regulated transcripts related to phosphate transport were found in the leaves of waterlogged plants at any developmental stage. On the other hand, in the roots of waterlogged plants, the largest number of up-regulated transcripts was counted for *inorganic phosphate transporter 1-2* (*PTH1-2*), regardless of developmental stage. The most down-regulated genes in the roots at tillering were encoding the mitochondrial phosphate carrier protein 3 (*MPT3*) and inorganic phosphate transporter 1-11 (*PHT1-11*). At booting stage, genes encoding the phosphate transporter 1-3 (*PHO1-3*), inorganic phosphate transporter 1-11 (*PHT1-11*) and a probable inorganic phosphate transporter 1-8 (*PHT1-8*) were the most down-regulated in the roots (Figure 22B).

Iron transport- related genes in leaves of waterlogged plants at either stage (Figure 22C) included mainly up-regulated trascripts related to the *vacuolar iron transporter 1.2* (*VIT1.2*) and the *vacuolar iron transporter homologue 2* (*VIT*-family). Additionally, *VIT1.1* was down-regulated in the same tissue at booting. In the roots of waterlogged plants, the most up-regulated transcripts were related to *Fe (II) transport protein 2* (*IRT1*), which was expressed at either stage. At tillering stage, down-regulated transcripts were related to *VIT1.2* and the *vacuolar iron transporter homologue 1* or 5, whereas at the booting stage, down-regulated transcripts were counted in the roots as related to *IRT1, VIT1.1, VIT1.2* and *VIT*-family (Figure 22C).

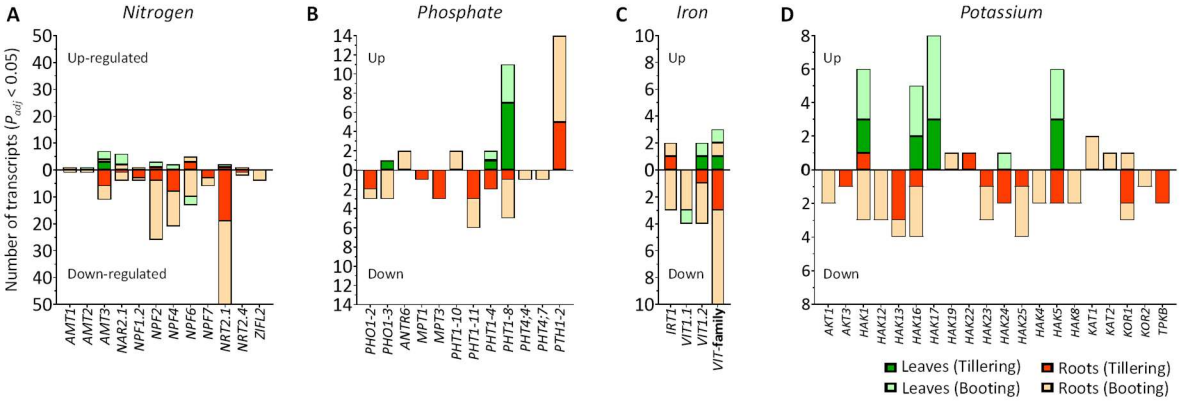

Figure 22. Influence of waterlogging on the expression of genes related to nutrient uptake and transport in leaves or roots of wheat plants at different developmental stages. (A) Number of transcripts related to nitrogen, (B) phosphate, (C) iron or (D) potassium uptake and transport. In all cases, leaves or roots form waterlogged plants were compared with their respective controls, and genes were grouped according to their transcript abundance on day 12 after the onset of the stress. The bars represent the number of specific transripts found in leaves or roots at tillering or booting stages. The transcripts were selected according to $\log_2$ fold-change ≥ |2|at P_{adj} < 0.05. AMT: ammonium transporter; NAR: high-affinity nitrate transporter-activating protein; NRT: nitrate transporter; ZIFL: putative peptide/nitrate transporter; PHO: phosphate transporter; ANTR6: putative anion transporter 6, chloroplastic; MPT: mitochondrial phosphate carrier protein; PHT: putative inorganic phosphate transporter; PTH: inorganic phosphate transporter; IRT: Fe(II) transport protein; VIT: vacuolar iron transporter; AKT: potassium channel; HAK: potassium transporter; KAT: potassium channel; KOR: potassium outward-rectifying channel; TPK: two-pore potassium channel b.

In relation to potassium transport, 20 different transcripts were identified as up-regulated in the leaves and down-regulated in the roots (Figure 22D). For example, the most up-regulated transcripts in leaves were related to *HAK-type potassium transporters 1, 5, 16,* and *17* (*HAK1, 5, 16, 17*), regardless of the DS. Only one transcript related to the *two-pore potassium channel b* (*TPKB*) was down-regulated at booting stage. However, a larger number of genes was found in the roots, of which the up-regulated ones were annotated as *HAK-type potassium channels* (*HAK1, 19, 22*), *KAT-type potassium channels* (*KAT1, 2*), and *KOR1*. At both developmental stages, the down-regulated transcripts in the roots belonged mostly to the *high-affinity potassium transporters HAK* family and *KOR1* (Figure 22D).

In general, waterlogging inhibited the expression of many genes related to the uptake and transport of nitrogen, phosphate, and potassium in roots, with the decline being greatest at the booting stage, especially those genes annotated as *NRTs, PHTs,* and *HAKs*. However, the up-regulation of nutrient transport-related genes, such as *AMTs, PHTs,* and *HAKs* in the leaves of the stressed plants suggested that under waterlogging the nutrient status of below- and above-ground organs was strongly imbalanced and related to the deficiency of N, P and K in the shoots.

5.5 Annotation enrichment analysis of differentially expressed genes in response to waterlogging using Gene Ontology

Gene Ontology (GO) analysis was performed to categorize the molecular and biochemical functions as well as cellular compartmentation of all annotated DEGs. GO analysis showed that the DEGs were

involved in a diverse range of molecular functions and biological processes. Specifically, the molecular functions with the highest significance in leaves of waterlogged plants at tillering stage were related to polysaccharide binding, pattern binding, phosphoric ester hydrolase activity, acid phosphatase activity, and phosphatase activity (Figure 23A). Furthermore, the most significant categories related to biological processes included sulphate transport, sulphur compound transport, metal ion transport, and cell recognition. However, no significant categories were identified for cellular components in same plant tissue. A different observation was made for the roots at the same stage (Figure 23B). GO analysis showed that the most significant categories for biological processes in the roots were response to acid chemical, response to oxygen-containing compound, response to water, response to inorganic substances, and response to abiotic stimuli. Moreover, the most significant molecular functions were associated with peptidase inhibitors and regulator activity. In terms of cellular components, the most represented categories included the cell wall, external encapsulation structure, extracellular region apoplast and phosphopyruvate hydratase complex.

During the booting stage, leaves from waterlogged plants exhibited a unique set of observations (Figure 23C). GO analysis showed an over-representation of biological processes belonging to drug catabolism, aminoglycan catabolism, chitin catabolism, amino sugar metabolism and cell wall macromolecule catabolism. In the category of molecular functions, chitinase and antioxidant activities were the most significant, followed by chitin binding and pyridoxal phosphate binding. Notably, the cellular components annotated were the thylakoid membrane, photosystem II oxygen evolving complex, oxidoreductase complex, and photosystem II extrinsic component of the membrane. Furthermore, the analysis of the roots at the same stage (Figure 23D) revealed several major molecular functions, including microtubule motor activity, microtubule and tubulin binding, cytoskeleton protein binding, and glucosyltransferase activity. Moreover, over-represented terms among the biological processes included cell or subcellular component movement, microtubule-based movement, cellular carbohydrate metabolism, metabolism of pyridine-containing compounds, and coenzyme biosynthesis. The analysis also identified significant changes in cellular components related to organelles, as well as the inner membrane and envelope of mitochondria.

Altogether, the results highlighted the complex molecular mechanisms that plants employ to cope with the stress caused by waterlogging. DEGs involved in the response to waterlogging were associated with diverse biological processes, molecular functions, and cellular components, which varied between plant tissues and growth stages. At the tillering stage, waterlogged plants exhibited imbalances in phosphate and sulfur metabolism, regulation of metal ion transport, impaired water and oxygen uptake and transport, and other related processes. On the other hand, at the booting

stage, changes were observed mostly in amino sugar and carbohydrate metabolism, nitrogen-containing compounds, cellular redox regulation, and photosynthesis.

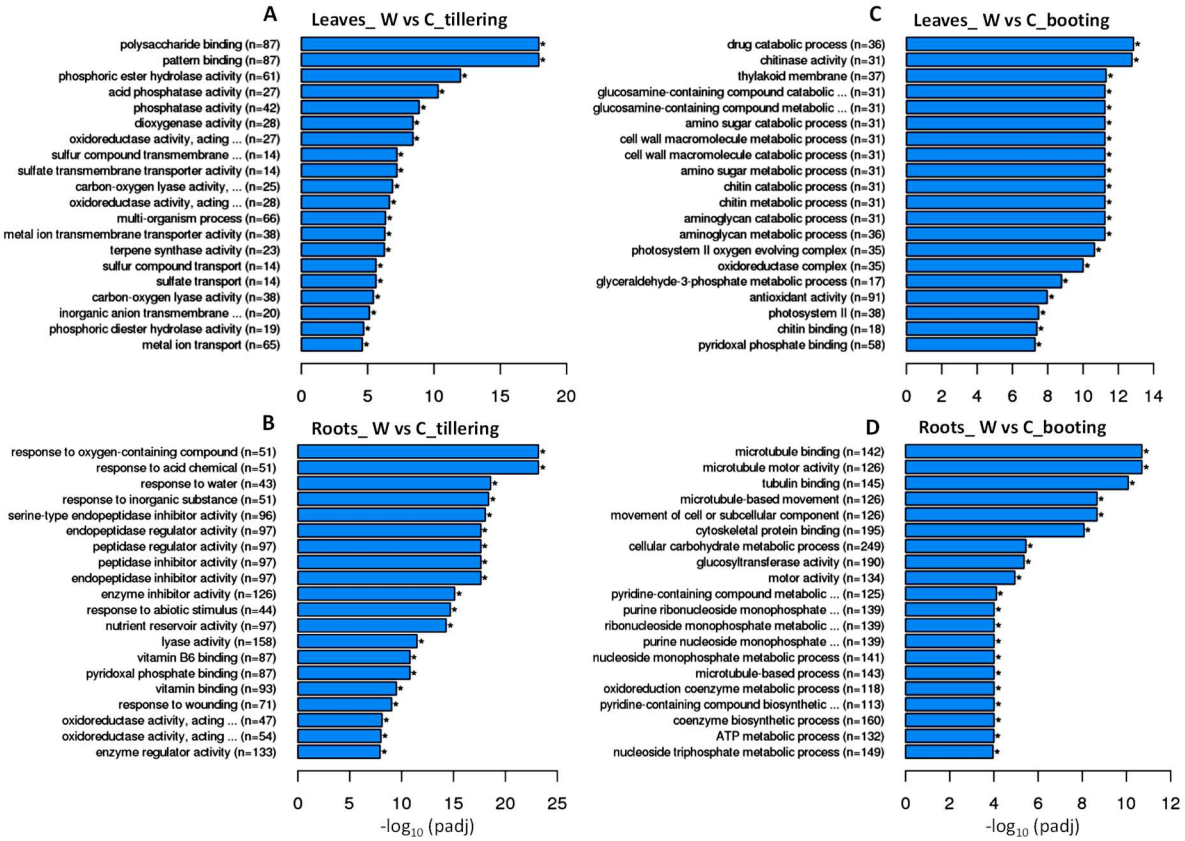

Figure 23. Gene Ontology enrichment analysis of differentially expressed genes in response to 12 days of waterlogging. (A-D) Annotated GO terms in (A, C) leaves and (B, D) roots of waterlogged plants at tillering stage (A, B) or at booting stage (C, D). In all cases, GO analysis was performed for biological processes, molecular functions and cellular components. Only transcripts showing a $\log_2$ fold-change ≥ |2| at the indicated *P* values were considered.

5.6 Identification of functional categories associated with metabolic responses under waterlogging at two developmental stages.

To identify metabolic pathways associated with leaf and/or root responses to waterlogging, the Kyoto Encyclopedia of Genes and Genomes (KEGG) enrichment analysis was performed (Figure 23). At the tillering stage, genes belonging to the functional categories' linoleic acid and amino sugar and nucleotide sugar metabolism were significantly de-regulated only in leaves (Figure 24A), with the highest number of down- and up-regulated genes counted, respectively. Specifically, three out of five significantly de-regulated genes belonging to the linoleic acid category encoded putative lipoxygenases (8-, 5-, 2.1-lipoxygenases), while the amino sugar and nucleotide sugar metabolism category was over-represented by three out of 12 genes related to pathogenesis-related (PR)3 chitinases (two chitinases 4, and chitinase 8), as well as two UDP-arabinopyranose mutase 1, and one UDP-glucose-6-dehydrogenase 4, involved in the biosynthesis of cell wall polysaccharides.

Furthermore, the common metabolic pathways between leaves and roots of waterlogged plants included alpha-linolenic acid, carbon metabolism, carotenoids and phenylpropanoid biosynthesis (Figure 24B). The highest number of genes in these categories were up-regulated in leaves, and down-regulated in the roots, specifically for carbon metabolism and phenylpropanoid biosynthesis.

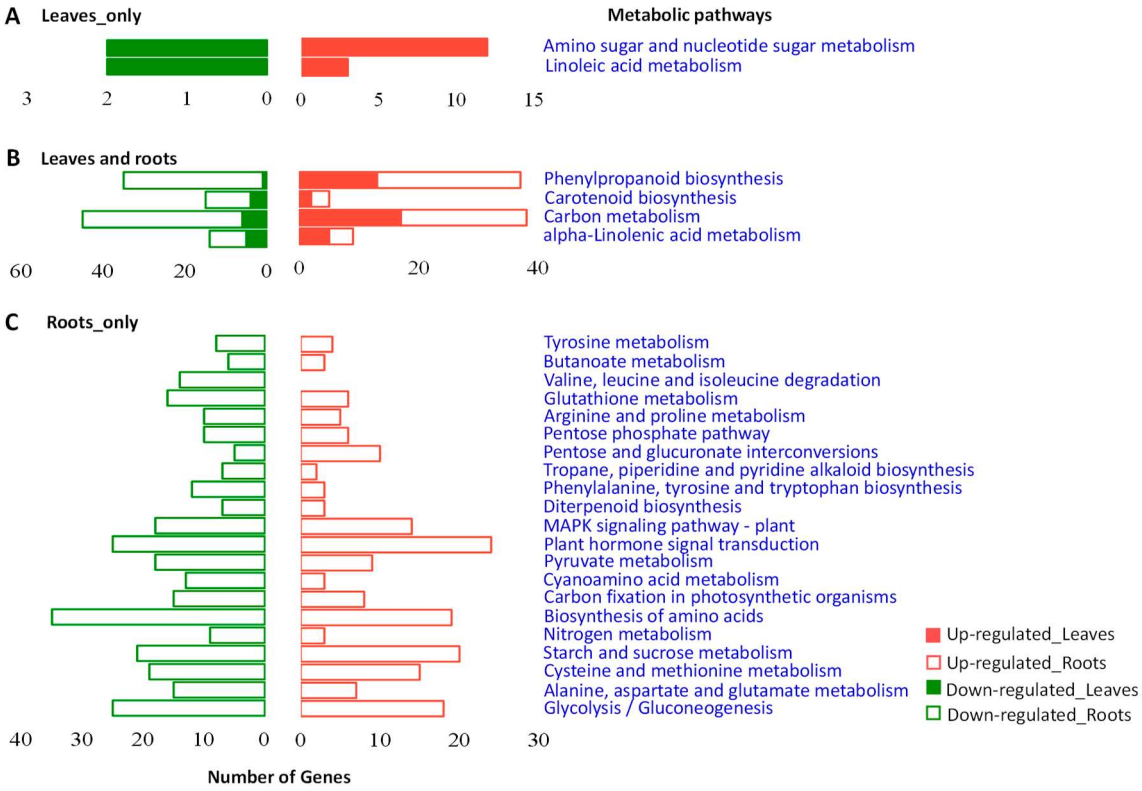

Figure 24. Over-represented functional categories associated with metabolic pathways in waterlogged plants at tillering stage. (A-C) Number of genes in metabolic pathways found only in (A) fully expanded leaves, (B) in both leaves and roots and (C) in roots only. Each class summarizes the number of genes belonging to certain metabolic pathways. Genes were assembled by KEGG classification considering a $\log_2$ fold-change ≥ |2| in expression at $P_{adj} < 0.05$.

The roots of the same plants showed a wider range of altered metabolic processes, with the majority of the counted genes being down-regulated (Figure 24C). The top five functional categories affected in the roots were glycolysis/gluconeogenesis, alanine, aspartate and glutamate metabolism, cysteine and methionine metabolism, starch and sucrose metabolism, and nitrogen metabolism. Additionally, other functional categories such as biosynthesis of amino acids and plant hormone signal transduction displayed a large number of de-regulated genes. Notably, from the indicated categories, alanine, aspartate and glutamate metabolism, nitrogen metabolism, and biosynthesis of amino acids were mostly down-regulated, while the rest were mostly up-regulated genes.

In contrast to the tillering stage, a distinct shift in the significantly enriched metabolic pathways was observed at booting stage. While the roots dominated in terms of enriched metabolic pathways during tillering, the leaves showed the most significant enrichment during the booting stage (Figure

25A). The top five metabolic pathways in the leaves during this stage were glyoxylate and dicarboxylate metabolism, alanine, aspartate and glutamate metabolism, glutathione metabolism, peroxisome, and phenylalanine metabolism. Notably, the genes counted in these functional categories were mostly up-regulated, indicating an active metabolic state in the leaves during the booting stage.

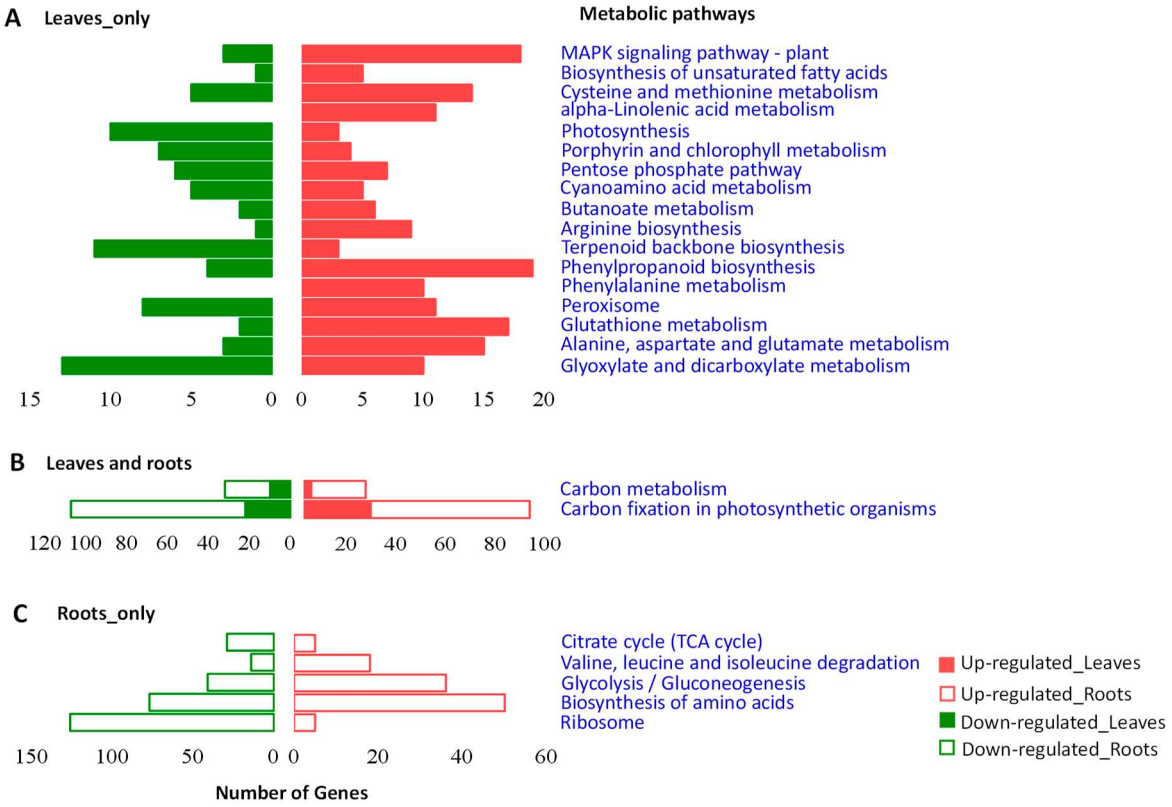

Figure 25. Over-represented functional categories associated with metabolic pathways in waterlogged plants at booting stage. (A-C) Number of genes in metabolic pathways found only in (A) fully expanded leaves, (B) in both leaves and roots and (C) in roots only. Each class summarizes the number of genes belonging to certain metabolic pathways. Genes were assembled by KEGG classification considering a $\log_2$ fold-change ≥ |2| in expression at $P_{adj} < 0.05$.

The functional categories commonly found in leaves and roots were related to carbon fixation in photosynthetic organisms and carbon metabolism (Figure 25B). Interestingly, a similar number of up- and down-regulated genes were counted in both categories, but the roots had the highest number of genes. Furthermore, the metabolic responses found only in the roots were represented by ribosome, amino acid biosynthesis, glycolysis/gluconeogenesis, valine, leucine and isoleucine degradation, and citrate cycle (Figure 25C). Notably, only ribosome- and citrate cycle-related metabolism were dominated by down-regulated genes, while most of the genes counted in the remaining categories were up-regulated.

Taken together, the different functional categories associated with metabolic responses under waterlogging depended on the type of tissue and plant DS. At the tillering stage, a larger number of functional categories was noted in the roots than in the leaves of the same plants. Moreover,

most of the genes counted within such categories were down-regulated. However, the opposite effect occurred at booting stage. The largest number of functional categories were identified in the leaves, and most of the genes counted were up-regulated. Notably, only a few functional categories were common to both leaves and roots, and carbon metabolism was the only category common to both plant tissues and developmental stages. Furthermore, the genes counted for such categories were mostly up-regulated, with the largest number observed in the roots at both stages.

5.7 Comparative transcriptome analysis between waterlogging and drought in relation to differentially expressed genes in wheat

In a final step, the extent of changes in the leaf and root transcriptome was compared between waterlogging and drought stress. For this purpose, all significantly de-regulated genes under both stresses and at both developmental stages were taken together and separately considered for leaves and roots. In general, a larger number of stress-de-regulated genes was observed in roots than in leaves (Figure 26A, B). Additionally, a higher number of DEGs was identified in waterlogged plants compared to drought-stressed plants when considering a $\log_2$ fold-change of 2. This trend was observed in both plant tissues and developmental stages. Interestingly, in the leaves of both waterlogged and drought-stressed plants, most of the genes were up-regulated except for a set of genes exclusively found in the leaves of drought-stressed plants during the booting stage (Figure 26A). Conversely, in the roots of stressed plants, most of the genes were down-regulated at either stage (Figure 26B).

Next, particular interest was placed on the genes that were co-expressed in drought-stressed and waterlogged plants to identify both, common and unique expression patterns. Surprisingly, only 35 genes were co-expressed in the leaves of both waterlogged and drought-stressed plants at tillering stage (Figure 26A). Interestingly most of these co-expressed genes were up-regulated in either water-stress and only few genes showed an opposite de-regulation. At the booting stage, a larger number of commonly de-regulated genes (621) were found in the leaves of plants under drought and waterlogging (Figure 26A). Of these, 288 were up-regulated and 110 were down-regulated in both stress treatments. Additionally, 17 genes exhibited opposite regulation, with more down-regulated genes observed in drought-stressed compared to waterlogged plants, and more up-regulated genes found in response to waterlogging.

In roots of waterlogged or drought-stressed plants, 258 genes were found to be commonly de-regulated at the tillering stage. Among them, 194 genes were down-regulated, 6 genes were up-regulated, and 8 genes showed an opposite regulation. At booting stage, a larger number of commonly de-regulated genes (3831) was identified in the same treatments (Figure 26B).

Consistent with the findings at the tillering stage, the majority of these genes was down-regulated (3014), while 205 were up-regulated, and 211 had an opposite expression pattern.

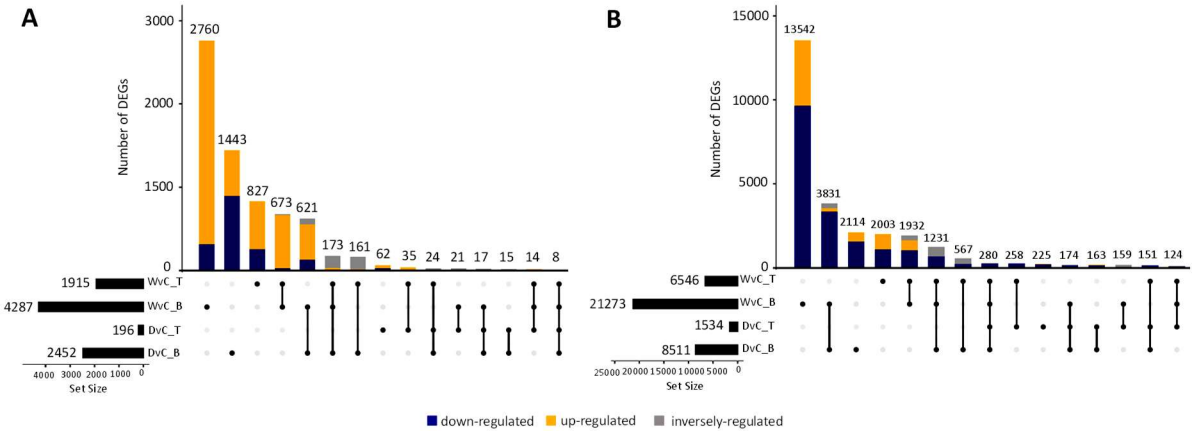

Figure 26. Comparison of the number of genes with altered expression under drought or waterlogging in leaves and roots. (A, B) UpSet plots showing quantitative intersections of all differentially expressed genes (DEGs; $\log_2$ fold-change ≥ |2| at $P_{adj} < 0.05$) in (A) leaves and (B) roots of wheat plants 12 days after onset of waterlogging or drought stress. The black bars indicate the total number of identified DEGs in each comparison (D, drought; W, waterlogging; C, control) at either tillering (T) or booting (B) stage. The vertical bars indicate the total number of DEGs unique to each comparison or shared between different comparisons as represented by single and connected black dots.

Overall, leaves and roots of stressed plants showed some commonly de-regulated genes in response to waterlogging and drought stress. However, there were also unique expression patterns in response to each stress condition. At the tillering stage, a relatively small number of genes was found to be co-expressed in both stress conditions, with most of them being up-regulated. However, at the booting stage, a larger number of commonly regulated genes was identified, with most of them being down-regulated. Some other genes showed opposite expression patterns between the two stress conditions, indicating the complexity of plant responses to waterlogging and drought stress.

5.8 Identification of common functional categories associated with metabolic responses under waterlogging and drought stress

To identify functional categories of de-regulated genes under waterlogging or drought, the genes were first clustered according to their expression pattern and displayed in a heatmap (Figure 27A, B). Generally, most of the genes commonly de-regulated in the leaves of waterlogged or drought-stressed plants were up-regulated compared to control plants (Figure 27A, upper panel). However, under waterlogging, they showed a higher $\log_2$ fold-change than under drought, indicating a higher extent of up-regulation of the same genes in the leaves when plants were under waterlogging than under drought. Notably, most of the genes commonly de-regulated in the roots of the same plant treatments exhibited an opposite pattern. Most of them were down-regulated under either stress, and the highest down-regulated ones were found under drought (Figure 27A, lower panel).

Furthermore, the de-regulation patterns of genes commonly expressed in both treatments were independent of the developmental stage of the plants.

At the tillering stage, KEGG enrichment analysis of DEGs in leaves showed a larger number of functional categories under waterlogging than under drought (Appendix 10A). Among them, the five most significant categories, at $P_{adj} < 0.05$, included alpha-linolenic acid and linolenic acid metabolism, phenylpropanoid biosynthesis, amino sugar and nucleotide sugar metabolism, and carbon metabolism. In all cases, a larger number of genes were up-regulated, with carbon metabolism having the largest number of up-regulated genes. Notably, in the leaves of drought-stressed plants, only down-regulation of genes related to the ribosome-related pathway were detected. In below-ground organs of the same developmental stage, a larger number of genes was again found under waterlogging than under drought (Appendix 10B). The top five most significant KEGG pathways for this group included glycolysis/gluconeogenesis, cysteine and methionine metabolism, nitrogen metabolism, carotenoid biosynthesis, and carbon metabolism. In all cases, most of the genes were down-regulated, and again carbon metabolism had the largest number of down-regulated genes. Furthermore, in the roots of drought-stressed plants, the most significant category was the terpenoid backbone biosynthesis pathway, whereas amino sugar and nucleotide sugar metabolism exhibited the largest number of down-regulated genes.

In contrast, at booting stage the leaves of drought-stressed plants showed a stronger metabolic response than those subjected to waterlogging (Appendix 10C). In leaves of waterlogged plants, the top five metabolic pathways included alanine, aspartate and glutamate metabolism, the peroxisome-related pathway, phenylalanine metabolism, phenylpropanoid biosynthesis, and terpenoid backbone biosynthesis, with a larger number of genes being upregulated. Furthermore, in the leaves of drought-stressed plants, the top five most significant functional categories were valine, leucine and isoleucine degradation, beta-alanine metabolism, fatty acid degradation, galactose metabolism, and photosynthetic antenna proteins. With the exception of the latter, up-regulated genes were over-represented in all metabolic functions. Interestingly, the roots of waterlogged plants exhibited more functional categories than of drought-stressed plants (Appendix 10D). Among them, the ribosome-related pathway, carbon metabolism, amino acids biosynthesis, glycolysis/gluconeogenesis, and valine, leucine and isoleucine degradation were the most significant functional categories with the majority of genes counted as down-regulated. However, in drought-exposed roots, only glutathione metabolism, phenylpropanoid biosynthesis were represented, and most of the gene were down-regulated. Phenylpropanoid biosynthesis was the functional category with the largest number of down-regulated genes.

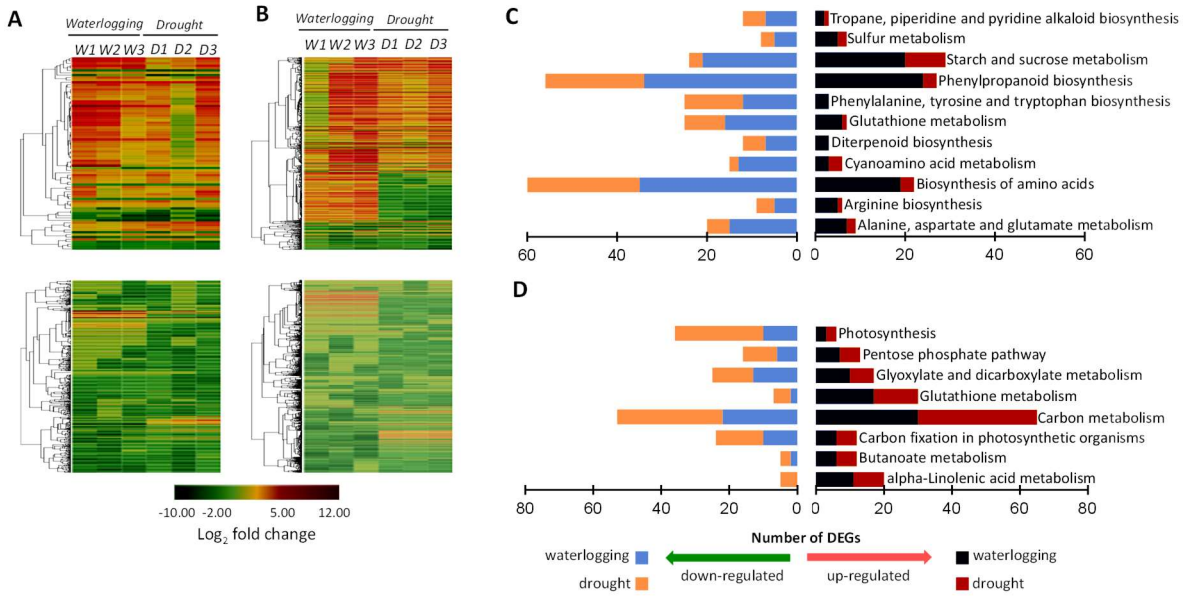

Figure 27. Genome-wide analysis of differentially expressed genes (DEGs) in leaves (upper panel) and roots (lower panel) in response to waterlogging or drought. (A-B) Heatmap representation of hierarchically clustered genes commonly up- or down-regulated under waterlogging or drought at (A) tillering or (B) booting stage. (C-D) Kyoto Encyclopedia of Genes and Genomes (KEGG) enrichment analysis of commonly functional categories and de-regulated genes in fully expanded leaves or roots of plants under drought and waterlogging at tillering (C) or (D) booting stage. Transcript abundance was determined on day 12 after the onset of waterlogging or drought and considered significant if $\log_2$ fold-change ≥ |2| at $P_{adj} < 0.05$.

Interestingly, in leaves of stressed plants at tillering stage, no commonly functional categories and de-regulated genes were found. However, in roots of the same plants, the most significant categories included alanine, aspartate and glutamate metabolism, arginine biosynthesis, amino acid biosynthesis, cyanoamino acid metabolism, and diterpenoid biosynthesis (Figure 27C). Among them, amino acids biosynthesis exhibited the largest number of genes commonly de-regulated in waterlogged and drought-exposed plants. In both water treatments, most of these genes were down-regulated, and a larger number was noticed in roots under waterlogging than under drought. Yet in the same functional category, waterlogged roots also exhibited a larger number of up-regulated genes than drought-exposed roots. Notably, in roots of stressed plants at booting stage, no commonly functional categories were noticed as in leaves of the same plants at tillering. However, in the leaves of stressed plants at booting, commonly functional categories included alpha-linolenic acid, butanoate metabolism, carbon fixation in photosynthetic organisms, carbon metabolism, and glutathione metabolism (Figure 27D). Among them, carbon metabolism exhibited the largest number of genes, and the majority of them were up-regulated under both water treatments. However, drought-stressed plants showed a larger number of de-regulated genes than waterlogged plants.

In general, waterlogging and drought stresses triggered metabolic responses and de-regulation of genes in wheat plants depending on plant tissues and plant growth stages. At tillering stage, more

functional categories were listed in waterlogged than in drought-stressed plants, especially in the roots. Among these categories, carbon metabolism showed the largest number of genes, being up-regulated in leaves and down-regulated in roots. However, at booting stage, more functional categories were listed in drought-exposed than in waterlogged plants, especially in the leaves. Yet, waterlogging triggered strong down-regulation of genes annotated for carbon metabolism in the roots. Common functional categories during tillering, seemed to be related mostly to down-regulation of genes annotated for amino acid biosynthesis in roots, where waterlogging showed the strongest effect. However, at booting stage, carbon metabolism seemed to be the most significant functional category commonly to both water stresses, especially in the leaves, where more up-regulated genes were expressed under drought than under waterlogging.

6. DISCUSSION

6.1. Differential responses of roots and leaves to waterlogging at tillering and booting

Current studies on crops under waterlogging have mainly described changes in the roots, which are the immediate organs exposed to excess water (Hwang *et al.,* 2011). However, there was less emphasis on whether and to what extent the metabolic and transcriptomic changes are linked throughout the whole plant as part of a coordinated response to waterlogging. Therefore, the focus of the existing thesis was to investigate the physiological changes, metabolic and transcriptomic responses in roots and shoots of wheat plants under waterlogging, and to verify whether these responses are linked and whether they point to a possible systemic regulation.

Exposure of wheat to waterlogging for 12 days at the tillering or booting stage resulted in changes in soil physico-chemical properties, imbalances in nutrient uptake capacity, and assimilation in the plant. At both stages, waterlogging decreased or tended to decrease N levels in roots and leaves (Figure 4A). This effect may be due to lower N uptake, reduced root system development (Figure 3D), inactivation of *NRT*s (Figure 22A), and reduced soil N availability probably as a result of denitrification under waterlogging (Kaur *et al.,* 2020; Kemmann *et al.,* 2023; Schulze *et al.,* 2019). In waterlogged oat plants, N losses have been linked to N leakage from damaged roots and leaves, and the eventual decay of these tissues (Arduini *et al.,* 2019a). On the other hand, more C accumulated only in the roots of the plants at the tillering stage, probably as a result of impaired respiration (Figure 4B), and maybe also of higher translocation of carbon sources, i.e. sucrose, as energy carriers to meet the energy demand in the roots (Kreuzwieser *et al.*, 2009; Voesenek, and Bailey-Serres, 2013).

The lower P concentration in the leaves of waterlogged plants at tillering stage (Figure 5A), was accompanied by a lower rate of P translocation in the xylem (Figure 15A). Notably, in the roots of the same plants at tillering, P concentration remained unchanged, whereas it decreased significantly at booting (Figure 5A). Furthermore, genes encoding inorganic phosphate transporters were highly up-regulated (Figure 22B) at either stages, and PDL concentration in the waterlogged

soil increased significantly compared to the well-drained soil (Appendix 2). These results suggest that P availability increased during waterlogging and P uptake was not affected, rather the P translocation rates from the roots to the shoots, especially at tillering stage, when functional categories related to phosphate metabolism were highly representative (Figure 23A). The increased P availability in waterlogged soils has been related to the soil characteristics involved in reduction processes, especially reduction of Fe (III) to Fe (II) where the P bound to Fe oxides is released (Maranguit *et al.,* 2017). Additionally, other studies have pointed out that the P released (desorbed) and adsorbed under waterlogging is mainly influenced by large amounts of poorly crystalline oxalate-extractable Fe oxides. Additionally, the reduction of Mn oxide-associated phosphate can be a significant source of P for plants (Shahandeh *et al.,* 2003; Lambers *et al.,* 2015). The highly reductive conditions of waterlogged soils are leading to increased availability of Mn and Fe (Shahandeh *et al.,* 1994). Notably, leaves of waterlogged plants exhibited higher concentrations of Mn than of Fe (Figure 5B), most likely due to the lower redox potential of Mn (IV) compared to that of Fe (III) (Marschner, 2011; Schulze *et al.,* 2019). The leaves of stressed plants at tillering showed a sharp decrease in K concentration (Figure 5A), in correspondence with a strong reduction in the K translocation rates in the xylem of the same plants (Figure 15A). Additionally, the K concentration in the roots remained unchanged (Figure 5A). These results indicated that, although waterlogging may have restricted oxygen availability in the roots, K uptake from the soil was not severely affected. Instead, impaired translocation due to waterlogging impeded the movement of K to the shoots, where its concentration decreased drastically. Interestingly, there is a controversy about the effect of waterlogging on K concentration in the roots, especially because it seems to depend on the duration of the stress and the plant species (Shabala and Pottosin, 2014).

Furthermore, at the gene expression level, several K transport-related genes were up-regulated in the leaves, whereas most of them were down-regulated in roots, except for two transcripts of the *Shaker-like* K^+ channels *KAT1*, and *KAT2,* and one transcript related to the *Potassium channel* KOR1 (Figure 22D). These results indicated that probably a re-translocation of K from the shoots to roots

as a signaling mechanism for the demand of higher nutrient uptake and translocation increased under waterlogging (Dreyer *et al.,* 2017). In the presence of K^+ the activation of *HYDRAULIC CONDUCTIVITY OF ROOT 1* (*HCR1)* in the roots would promote the plant acclimation to flooded soils, and provide optimal growth capacity in the recovery phase (Maurel and Nacry, 2020). Interestingly, K^+ could also serve as a decentralised energy storage that can be used under energy limitations (Gajdanowicz *et al.,* 2011). Notably, at booting stage a higher translocation rates may have increased K concentration in the shoots to maintain active growth and grain development (Figure 5A). This was in correspondence with the decreased K concentration in the roots (Figure 5A), which was probably a result of decreased respiration rates and the main reason for the cessation of root growth (Smethurst *et al.,* 2005; Board 2008).

The structure of rhizosphere and root microbiota is greatly influenced by soil hydrodynamics, root architecture, and soil and root nutrient concentration, as highlighted by various studies (Fitzpatrick *et al.,* 2018; Schöps *et al.,* 2018; Francioli *et al.,* 2021). When soil is waterlogged, there is a significant shift in the composition of both, the rhizosphere and root microbiota towards anaerobic bacteria, and a decrease in beneficial plant taxa (Appendix 11B, C). In addition, waterlogging results in dramatic changes in the mycobiota, with increased abundance of fungal pathogens and a decline in mutualistic fungi (Appendix 12). Reduced oxygen availability during waterlogging impairs root growth, being the main drivers of below-ground microbiota changes (Schulze *et al.,* 2019) and eventually, with consequences also for the microbiota community assembly in the leaves (Appendix 11A, 12). Notably, the composition of the plant-microbiota exhibited a strong association with changes in soil and plant characteristics, especially with plant growth stages and root nutrient concentration during waterlogging and more pronounced at tillering stage (Francioli *et al.,* 2021; Francioli *et al.,* 2022a, Francioli *et al.,* 2022b).

In addition to nutrient availability and microbiota composition, plant hormones play an important role in the regulatory mechanisms of plant growth and response to environmental factors. At tillering stage, waterlogged plants exhibited reduced xylem translocation rates (Appendix 4),

probably due to lower root hydraulic conductivity and thus lower water uptake (Maurel and Nacry 2020), leading to reduced translocation rates of some hormones including GA, ABA, IAA, and SA along the whole evaluation period (Figure 13, 14, Appendix 5). Under waterlogging plants often produce and accumulate high levels of ethylene due to reduced gas exchange under water. This hormone plays a key role in the complex interaction among hormones to regulate plant growth and development in response to waterlogging (Zhang *et al.,* 2021). For example, ethylene controls the interaction between ABA and GA in the contrasting strategies i.e. quiescence or escape via the regulation of differential gene expression through ERF-type transcription factors (Hsu *et al.,* 2011; Schulze *et al.,* 2019). While ethylene was not directly measured here, the roots of waterlogged plant exhibited significant up-regulation of genes encoding ACC oxidase (*ACO1*) (Figure 20C), involved in the synthesis of ethylene. Either leaves or roots of the same plants also showed strong up-regulation of differentially expressed the ERF TFs AP2/ERF and B3 domain containing protein (Appendix 8A, upper panel). Notably, root-derived hormones transported into the xylem have long been associated with hypoxia in roots. Under waterlogging, roots can rapidly produce higher levels of hormones, which move towards the shoots to induce responses including stomatal closure and changes in plant growth and development (Najeeb *et al.,* 2015). Among them, ABA has been reported as the major root-borne hormone transported through the xylem to regulate stomatal closure and decrease transpiration rates in leaves (Else *et al.,* 2009; Kreuzwieser and Rennenberg, 2014; Najeeb *et al.,* 2015). Although previous studies have shown the dominant role of ABA as a signal under waterlogging, in this study waterlogged plants exhibited a sharp decrease in the translocation rates of most hormones, including ABA (Figures 13, 14). One possible reason may be the inhibition of hormone synthesis in the roots due to low oxygen availability, leading to decreased levels of hormone translocation in the xylem. Interestingly, other studies found that ABA translocation in the xylem of flooded tomato is strongly reduced rather than increased, rejecting the possibility that early stomata closure is a response to increased ABA from roots (Else *et al.,* 2009). Furthermore, signaling molecules have also been described as "negative messages" when

exported to shoots in lower amounts (Jackson 1997, Else *et al.,* 2009), suggesting that in this study, the hormone response and signaling in waterlogged wheat may have been associated to lower translocation rates rather than increased delivery from the roots to the shoots.

Altogether, these changes were reflected in reduced root biomass and root length of the stressed plants mostly at the tillering stage, indicating a rapid decline in energy metabolism in the organs directly exposed. However, photosynthetic products accumulated in the leaves of the stressed plants at both DS, as reflected by higher sugar levels (Figure 6). At tillering stage, glucose, fructose and starch were significantly higher in the leaves and roots of waterlogged plants. Interestingly, sucrose accumulated only in the roots, probably as an energy saving strategy of the plants during energy limitation to ensure sufficient energy for the recovery phase (Voesenek and Bailey-Serres, 2013; Schulze *et al.,* 2019). Furthermore, the same sugars accumulated in the leaves but decreased significantly in the roots of waterlogged plants at booting stage, maybe due to a decreasing sink activity of roots relative to the rapidly developing shoot. Considering the nutritional needs of plants at either stage, sucrose may play a central role for the continued functioning of N and C metabolism, especially at tillering stage. Increased sucrose in the roots could serve as energy source to sustain root metabolism, and as a regulator to modulate nutrient transport and re-mobilization of N in the leaves.

The formation of AR (Figure 11C) at later time points during tillering stage indicated the need of the plant to reach oxygen from above-ground after several days under waterlogging to ensure survival. In addition, AR may also help to overcome the limitations in the nutrient uptake and facilitate the formation of tillers during waterlogging. However, AR may be rather inhibited during booting as the resources and energy may shift to reproductive structures rather than root development. Several plant species such as wheat (Malik *et al.,* 2002; Herzog *et al.,* 2016), maize, willow, Forsythia and *Rumex palustris* (Bailey-Serres *et al.,* 2012) have evolved the formation of AR as an adaptive mechanism to circumvent oxygen limitations and ensure plant growth. However, these effects vary within different wheat genotypes and the period of exposition to the stress (Setter and Waters

2003; Herzog *et al.,* 2016). Interestingly, the formation of AR has been related to increased sucrose concentration in the roots under waterlogging, as sugars may act as energy sources and molecular signals mediated by auxins to induce AR emergence (Qi *et al.,* 2020).

Notably, chlorophyll concentrations decreased sharply under waterlogging (Figure 2C,D), indicating a reduction in the photosynthetic capacity of stressed plants, as waterlogging can cause reduction in photosynthetic parameters such as carbon exchange rate, intracellular CO_2 concentration, transpiration rates, and stomatal conductance (Bansal and Srivastava 2015). However, the Chl *a/b* ratio did not change in response to the stress (Figure 2E). This adjustment of the Chl a/b ratio has been suggested as an integral feature of plant acclimation, especially when there is a low N status in the leaves (Kitajima and Hogan 2003). Other important parameters to assess plant health, such as the root-to-shoot ratio (Agathokleous *et al.,* 2019), remained also unchanged in the stressed plants (Figure 3G).

Altogether, these results indicate that wheat plants responded to waterlogging through a complex process that involves various physiological and molecular changes to help them cope with the stress. The lack of oxygen during waterlogging lead to nutrient imbalance and metabolic changes in the roots, which triggered a re-orchestration of the metabolism in the leaves. The higher energy demand for root metabolism was supported by higher accumulation of sugars in this tissue, and probably more transport of the same from the shoots. This was accompanied by specific changes in gene expression, such as up-regulation of fermentation-related genes in the roots and up-regulation of specific nutrient transport-related genes, which may be associated with specific mechanisms that plants undergo to facilitate higher nutrient uptake and transport, remobilization of nitrogen compounds, AR formation, tiller development and the subsequent grain formation.

6.2. Carbon and amino acid metabolisms mediate the systemic response of wheat plants to waterlogging at tillering stage

Gene expression analysis and metabolite profiling in wheat allowed to discriminate some major metabolic processes by which wheat plants responded to waterlogging. Initially, it was found that

wheat responded differently at tillering than at booting, with some of the known adaptive traits, such as induction of hypoxia-responsive mechanisms (Herzog *et al.,* 2016; Malik *et al.,* 2002; Pan *et al.,* 2021) found at tillering only. Therefore, the metabolic and transcriptomic changes that plants may undergo during waterlogging are discussed here at the tillering stage only. At first, fermentation processes occurred only in the roots, when genes encoding LDH, ADH and PDC were highly up-regulated under waterlogging (Figure 20C). Inhibited respiration, with the concomitant accumulation of sucrose in the roots, led to up-regulation of specific genes in the shoots, including those annotated for ion transport (Appendix 9), and carbon and amino acid metabolism (Figures 24A, B). Interestingly, in the roots of waterlogged plants non-structural carbohydrates and in particular sucrose accumulated (Figure 6), while in the leaves of the same plants, two transcripts related to a sugar exporter of the SWEET family (*SWEET14,* Appendix 13) were highly up-regulated. In fact, *SWEET14* belongs to the Clade III of the SWEETs that show preferential transport activity for sucrose over glucose, as found in rice plants (Chen *et al.,* 2012). Therefore, it was hypothesised here that under waterlogging more sucrose transported to the roots may meet the energy demand of anaerobic metabolism and ensure replenishment of energy sources for a faster recovery once the stress has ceased. As summarised in Voesenek and Baley-Serres, (2013), phloem loading and transport of soluble sugars mainly sucrose, may increase under waterlogging to sustain energy metabolism in roots. In addition to the inhibited breakdown of carbohydrate, this resulted in a strong accumulation of sucrose in the roots. Notably, studies of the carbohydrate composition in leaves, roots, and phloem sap of tolerant and non-tolerant species under waterlogging, showed increased sugar concentration in the phloem in several plant species (Kreuzwieser *et al.,* 2009). However, the non-tolerant species showed a negative effect on phloem unloading as sugar concentrations in the roots remained lowered compared with well drained-plants. It can be then suggested that roots of waterlogged plants may exhibit accumulation of sucrose associated with increased sucrose transport in the phloem in response to waterlogging. Computational-based studies showed that under ATP shortage, sucrose loading into the phloem and transport to sink

organs can be increased by the continued movement of K^+ through the outward-rectified K^+ channel AKT2/AKT3, balancing the membrane potential and supporting the H^+-coupled transporter SUT1 during phloem loading (Gajdanowicz *et al.,* 2011; Dreyer *et al.,* 2017). The same studies confirmed that following this mechanism, K could also be transported back to the roots to serve as a signal for the K channels to load the xylem according to nutritional needs. Although in this study AKT2/AKT3-related genes were down-regulated in the roots, the increased K and sucrose concentrations, and the strong up-regulation of genes encoding KATs and KOR channels in the roots, may constitute good indicators to assume that sucrose transport was mediated by such mechanism.

Transcriptome analysis in waterlogged Arabidopsis plants revealed re-programming of carbohydrate metabolism in leaves, indicative for root-derived signals triggering a systemic response (Hsu *et al.,* 2011). Since a part of the shoot transcriptome changes got lost in ethylene- and ABA-signaling mutants, these two hormones have been proposed as potential signals coordinating the systemic plant response. Further evidence for the involvement of phytohormone signaling in the systemic regulation of shoot responses to waterlogged roots came from enhanced transcript levels of an APETALA2/ERF-type transcription factor in leaves (Appendix 8A, upper panel). This transcription factor was also up-regulated in the root tissue and is known to be involved in the regulation of the gene expression to enhance tolerance to waterlogging. Notably, the transcriptional activation of this TF also integrates ethylene and jasmonic acid signals in plant defense (Lorenzo *et al.,* 2003; Zhang *et al.,* 2004; Pré *et al.,* 2008). In particular, ethylene plays an important role under O_2 deficiency as most of the morphological modifications such as adventitious roots are controlled by this hormone (Schulze *et al.,* 2019). In tomato and *Rumex* spp., the export of the ethylene precursor ACC from waterlogged roots to the shoots constituted evidence for the role of ethylene in the root-to-shoot signaling under oxygen deficiency (Voesenek and Baley-Serres 2013). Although it was not possible to directly measure ethylene formation in the present experiments, the above-mentioned changes in the transcriptome indicate that ethylene was also a relevant systemic rot-to-shoot signal here.

The readjustment of leaf and root metabolism became apparent by the differentially expressed genes associated with carbon and amino acid metabolism (Figure 24B), in particular *LDH, ADH, PDC* and *ALAT2*. Under certain conditions also amino acids can serve as an alternative source of carbons skeletons for glucose biosynthesis and on top serve as a source of nitrogen (Eastmond *et al.,* 2015). Partial de-amination of amino acids for energy provision may contribute not only to the production of substrates, like organic acids from the TCA cycle, for mitochondrial respiration (Heinemann and Hildebrandt 2021), but also of substrates, such as pyruvate to undergo gluconeogenesis and synthesise glucose *de novo*. In this regard, transcriptome studies in waterlogged maize seedlings provided evidence for a crosstalk between carbon and amino acid metabolism, in which the latter may take over a role as energy source through breakdown of carbon skeletons (Zou *et al.,* 2010). Furthermore, fermentation requires an increased throughput of energy carriers due to the much lower energy yield gained via glycolysis compared to that gained via oxidative phosphorylation (Schulze *et al.,* 2019). In this context, glucose plays a central role as energy carrier, and in order to produce more glucose, reserve substances including starch, and breakdown of structural components, such as proteins, are used to produce more glucose. Notably, starch strongly accumulated in the roots of waterlogged plants (Figure 6D), whereas molecular functions related to the regulation or inhibition of protein breakdown, i.e. endo-/peptidase regulators and inhibitors were mostly down-regulated (Figure 23B). This suggests that starch breakdown was not the primary source of glucose, rather intermediates of protein degradation, such as amino acids. This was supported by the KEGG analysis, in which carbon and amino acid metabolism turned out to constitute the most significant categories in the leaves and roots of waterlogged plants (Figure 24), as well as by the strong accumulation of some glycolysis-derived amino acids in roots (Figure 8). Therefore, it is proposed here that some amino acids accumulating in the roots due to local anaerobiosis- or fermentation-related processes are translocated to the shoots, triggering then a systemic response. This, may enable the transport of nitrogen to the shoots to support essential metabolic processes and the synthesis of other nitrogen-containing compounds. Additionally, these

amino acids could also undergo gluconeogenesis and serve as carbon skeletons for *de novo* glucose synthesis, without compromising high sucrose degradation or mechanisms by which ATP is highly consumed.

6.3. Alanine is the major root-to-shoot translocated amino acid and a putative dual-function metabolite for the systemic response under waterlogging

Analysis of the major primary metabolites showed that Ala was most abundant in the roots and xylem exudates of plants under waterlogging (Figures 8, 16, 17). At the same time, Ala decreased in the leaves of the same plants (Figure 8). The accumulation of Ala in waterlogged organs has been linked to the conversion of pyruvate to prevent carbon losses during ethanol fermentation and ethanol diffusion out of cells (Ricoult *et al.,* 2006; Miyashita and Good 2008; Schulze *et al.,* 2019). This process is catalysed by ALAT, which is responsible for the conversion of Ala and oxoglutarate to pyruvate and glutamate in many plant species (Watson *et al.,* 1992; Puiatti and Sodek 1999; Rocha, *et al.,* 2010; Diab and Limami 2016; Bashar *et al.,* 2020). Since ALAT shares the same substrate with ADH and PDC, Ala production may be linked to the regulatory mechanism in the activation or support the fermentation process in a controlled manner. One such mechanism relies on Ala accumulation to regulate the levels of pyruvate, which can otherwise interfere with the respiration rates when oxygen availability is low (Rocha *et al.,* 2010), preventing in that way, the losses of C skeleton due to ethanol production.

In addition, Ala accumulation may also serve as a transient storage molecule for nitrogen, allowing plants to recycle the nitrogen during waterlogging. In addition to *ADH* and *PDC*, a strong up-regulation of *ALAT2* mRNA was found in waterlogged roots, whereas no transcripts associated with this enzyme were found in leaves (Appendix 15A). The importance of ALAT2 in the context of Ala production to regulate pyruvate levels has been questioned, since NAD^+ is not regenerated during Ala production (De Sousa and Sodek 2003; Rocha *et al.,* 2010). Other studies on *Lotus japonicus* and on mutants unable to fix N_2 via symbiotic interaction with rhizobia showed that Ala accumulation is independent of the N status of the plant (Rocha *et al.,* 2010). These results suggest that Ala

metabolism may be a response to prevent pyruvate accumulation and allow the continued operation of glycolysis during waterlogging. Following ALAT2, a higher abundance of transcripts encoding *AGT2* was recorded in leaves of stressed plants (Appendix 15B). The corresponding enzyme is known as one of the two structurally distinct types of AGTs, which catalyse the transfer of an amino group from alanine to glyoxylate. To date, the function of AGT2 in plants has not been well elucidated, whereas in animals AGT2 has been described as a "promiscuous" aminotransferase involved in multiple transamination reactions (Rodionov *et al.,* 2014) and the regulation of endogenous inhibitors of NO synthases (Rodionov *et al.,* 2010). Although AGT2 is localized exclusively in the mitochondria of mammalian cells, in Arabidopsis plants AGT2 homologs appeared to have also peroxisomal localization, suggesting that this enzyme may have a role in the transamination reactions that occur during photorespiration (Liepman and Olsen 2003).

In contrast to Ala, Gln was the most abundant amino acid found in the xylem sap of well-drained plants, accounting for about 60% of all amino acids identified (Figure 16B). This confirms that Gln is one of the most abundant free amino acids in plants. In addition to protein and nucleotide biosynthesis, it is a major amino donor for the synthesis of other amino acids and nitrogen-containing compounds in plants (Forde and Lea 2007). It plays an important role in the remobilisation of nitrogen and the assimilation of ammonium (Okumoto and Pilot 2011). In addition, it may play a role in N nutrition on organic growth substrates, and it is supposed to act as a signaling molecule to regulate the expression of genes involved in N uptake and N-related stress responses (Kan *et al.,* 2015). Interestingly, the translocation of Gln in the xylem of waterlogged plants was largely replaced by Ala (Figure 16B). Since Ala was the major source of amino-nitrogen transported to shoots, where the nitrogen concentration decreased below the critical deficiency level, Ala may also serve to meet the N demand in the shoot. Thus, it is hypothesised that Ala is a metabolite with a dual function as an amino-nitrogen and carbon carrier during waterlogging, originating from the switch to oxygen-restricted nitrogen assimilation in the roots. Once transported to above-ground plant organs, Ala can be used as a source of energy through its

transamination and conversion to pyruvate. Two questions arise at this point: 1) What is the function of Ala translocation in a system with a negative nitrogen balance and energy limitation? 2) Is the conversion of Ala to pyruvate in leaves mediated by AGT2? In humans, the function of Ala as a "shuttle" that undergoes transamination for pyruvate synthesis and the subsequent provision of energy to muscles in the form of glucose as a result of gluconeogenesis is well documented (Petersen *et al.,* 2019). However, it remains to be shown in plants whether Ala serves as a carbon and nitrogen source in above-ground organs to replenish glucose via *de novo* glucose synthesis and/or nitrogen-containing compounds.

Based on the observations in the current study, a working model is proposed that shows how local metabolic adaptations to waterlogging in roots alter metabolic pathways in leaves, thereby causing a systemic metabolic response. As shown in Figure 28, waterlogging-induced limitation of O_2 in roots leads to partial conversion of pyruvate to Ala via ALAT2 to prevent excessive carbon loss from fermentation. Ala accumulates strongly in the roots as a local response to O_2 depletion and is translocated to the shoots via the xylem to compensate for lacking Gln and for the low N status there. In the leaves, Ala is not only used as an amino-nitrogen source, but it is also converted to pyruvate and Gly via AGT2. In leaves, there are two possible alternatives: pyruvate is recycled and incorporated into the TCA cycle to contribute to higher net ATP production, or pyruvate is incorporated into the gluconeogenesis pathway for *de novo* glucose biosynthesis. Glucose can be used immediately in glycolysis bypassing the energy-demanding sucrose degradation. Instead, sucrose could be used to reinforce the higher demand of energy carriers in the roots for the fermentation process as indicated previously by Schulze *et al.* (2019).

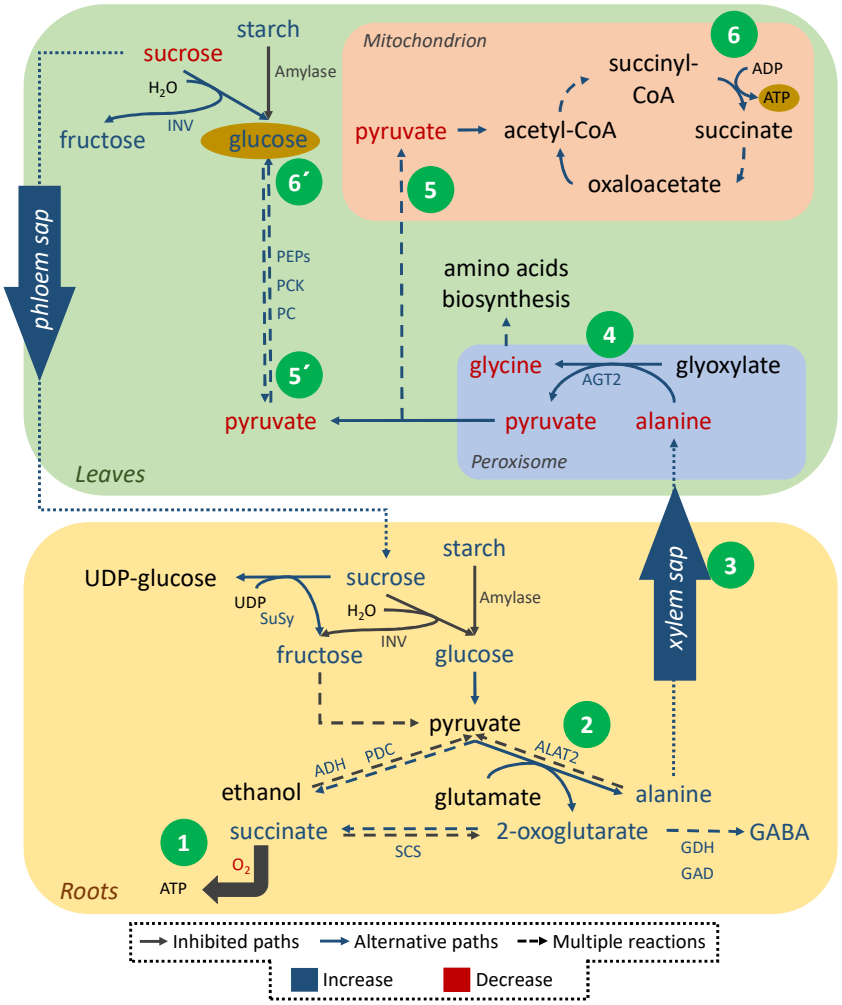

Figure 28. Working model for the metabolic adaptation of leaves and roots of wheat plants to cope with waterlogging stress. Under waterlogging, O_2 concentration decreases and fermentation takes place in the roots (1). To prevent the carbon losses in the form of ethanol, pyruvate is converted to Ala using alanine aminotransferase 2 (ALAT2) (2). Ala is translocated to the shoots via the xylem (3). In shoots, Ala and glyoxylate are converted to pyruvate and Gly by alanine glyoxylate aminotransferase 2 (AGT2) (4). The produced pyruvate can either be recycled and directed to the TCA cycle (5) or it is used to synthesize glucose *de novo* via gluconeogenesis (5', 6'). INV: invertases; PEPs: phosphoenolpyruvate synthase; PCK: phosphoenolpyruvate carboxykinase; PC: pyruvate carboxylase; AGT2: alanine glyoxylate aminotransferase 2; SuSy: sucrose synthase; ADH: alcohol dehydrogenase; PDC: pyruvate decarboxylase; ALAT2: alanine aminotransferase 2; SCS: succinyl CoA ligase; GDH: glutamate dehydrogenase; GAD: glutamic acid decarboxylase.

6.4. Waterlogging and drought stress lead to similar adaptive response mechanisms in wheat

Extreme changes in soil water availability due to the irregular precipitation patterns lead to severe drought in some areas and re-occurring flooding events in others. The effects on plants of waterlogging and drought as individual abiotic stressors occurring at opposite ends of soil water content are well documented. Waterlogging leads to oxygen deficiency (Irfan *et al.,* 2010; Elzenga and Veen, 2010; Kreuzwieser and Rennenberg, 2014), while drought limits water availability (Gilbert and Medina, 2016; Huang *et al.,* 2020). Therefore, different morphological and physiological

responses to these stress factors are to be expected. While waterlogged plants acclimate to oxygen deficiency by developing shorter root systems with enhanced formation of aerenchyma and adventitious roots (Schulze *et al.,* 2019, Pedersen *et al.,* 2021) to provide oxygen to the root tips, drought-stressed plants develop deeper and extensive root systems to increase water accessibility and nutrient uptake (Franco *et al.,* 2011, Polania *et al.,* 2017, Plett *et al.,* 2020). Although these changes in the morphology and architecture of the roots differ completely between the two stresses, the common denominator relies on the ability of roots to acclimate to the changes in soil water regimes and to maintain root functionality. This, otherwise may result in reduced nutrient uptake and thus in similar symptoms, such as yellowing of leaves, stunted growth and lower dry matter production. However, it remains yet poorly understood how the contrasting effect of each of the stresses that cause different morphological responses in the root can lead to similar symptoms in the shoot. It has been proposed that a plant species or genotype tolerant to one stress type may also be tolerant to another whenever the plant response provides protection against multiple stresses evolving common adaptive traits or activation of common sets of genes or metabolic pathways (Vashisth *et al.,* 2018). Another study has shown that adaptive plasticity in traits may be an important mechanism allowing plants to tolerate a wide range of hydrological gradients (Zhang *et al.,* 2016).

In this study, differential phenotypic, metabolic and transcriptomic responses were recorded under drought or waterlogging stress. Especially in stress-susceptible species such as wheat, it is of great importance to focus on plant responses to drought and waterlogging at the same time in order to develop crop improvement strategies to achieve the best possible adaptation to either stress situation. Notably, the effects of drought or waterlogging on plant functions depend on the duration, intensity and timing of the stress, the plant species and its stage of development (Pearson *et al.,* 2013). To evaluate the effects of these two contrasting types of stress on wheat growth and metabolism, well-irrigated plants were compared with plants subjected to drought or waterlogging, either at tillering or booting stage. Both stress conditions led to distinct effects on plant growth and

metabolism of the wheat plants. Compared to control, plants under either stress produced less biomass and had a lower chlorophyll concentration. However, this effect was more pronounced under waterlogging than under drought (Appendix 16). The effect of drought stress on stomata closure, which reduces net photosynthesis, carbon dioxide assimilation and thus plant growth, is well documented (Tombesi *et al.,* 2015). Furthermore, the negative effect of waterlogging on photosynthetic activity has been associated with soil oxygen depletion and impaired root hydraulic conductivity. Interestingly, the same effect has also been related to drought stress causing lower stomatal aperture and photosynthetic activity (Atkinson *et al.,* 2008; Kreuzwieser and Rennenberg, 2014; Toral-Juárez *et al.,* 2021).

In this study, waterlogging had a greater effect on plant metabolism (Figure 10) than drought, especially in the roots as the first plant organ to cope with either stress. Of course, this comparison needs to be taken with care, because stress intensities of drought and waterlogging were probably not the same. Soluble sugars strongly accumulated in either stress situation, especially in the roots of plants at tillering stage (Figure 6, Appendix 17). This effect has been observed in various plant species as an adaptive mechanism under these stressors (Mostajeran and Rahimi-Eichi, 2009; Redillas *et al.,* 2012; Hossain and Uddin, 2019; Barickman *et al.,* 2019). The accumulation of sugars during drought is considered an osmoprotective mechanism to stabilise proteins and membranes (Sánchez *et al.,* 1998), while under waterlogging sugar accumulation results from anaerobic metabolism and higher throughput of energy carrier to meet the energy demand (Schulze *et al.,* 2019). However, the convergence of both stresses in the accumulation of sugars may rely on reduced water potential and photosynthesis. As a result, plants may switch to anaerobic respiration leading to higher sugar translocation and thus accumulation in the roots. Although in drought-stressed plants anaerobic respiration-related responses were not found, such as induction of fermentation-related metabolites or changes in gene expression, there is evidence that mild drought stress may induce similar changes in root metabolism as under low oxygen, in particular the expression of the anaerobically-induced enzymes, such as alcohol dehydrogenase and malate

dehydrogenase (Irigoyen *et al.,* 1992). Another possibility consists that plants under either stress may operate in an energy-saving mode to ensure sufficient energy reserves for the recovery phase. In the particular case of waterlogging, this hypothesis is confirmed by the "quiescence" strategy already described in several studies (Manzur *et al.,* 2009; Bailey-Serres *et al.,* 2011; Schulze *et al.,* 2019). Furthermore, the immediate conservation of energy, has been suggested as an "appropriate response" to drought to ensure survival in the long run (Verelst, Skirycz, and Inzé, 2010).

Notably, the major amino acid found in the leaves and roots of drought-stressed plants was proline, which may be related to cellular osmoprotective adjustments (Adamipour *et al.,* 2020) and maintenance of the hydration status to protect the structural integrity of proteins (Rajendrakumar *et al.,* 1994). Notably, the major metabolite found in response to waterlogging was Ala, whose putative metabolic function has been described above. Although the apparent reason for the accumulation of theses amino acids under drought or waterlogging seems to be related to different strategies of plant acclimation, a common feature that relates Pro and Ala relies on protecting the cell environment from the damaging effects and disrupting cell homeostasis caused by either stress (Jogawat, 2019).

As reported here, the developmental stage defined whether waterlogging and drought lead to common or contrasting effects in wheat. At tillering stage, common metabolic responses to either stress were present only in the roots. In general, amino acid metabolism and diterpenoid biosynthesis were the most significant categories being altered in the transcriptome under both stressors at tillering stage, when most genes were down-regulated. An opposite effect was observed at the booting stage. Common biological categories were only found in the leaves. At this stage, alpha-linolenic acid metabolism, butanoate metabolism, carbon fixation in photosynthetic organisms and carbon metabolism were the most important categories, as most genes were up-regulated under waterlogging but down-regulated under drought. These results indicated that similar response mechanisms of wheat plants to either stress may also be linked to the physiological and metabolic needs of plants at specific growth stage. At tillering stage, roots are most responsive

to waterlogging or drought due to the higher demand for nutrients transport to shoots than at booting, when plants may invest more resources in restructuring the leaf metabolism for grain development. Additionally, metabolic adaptations may be more prominent and evident in the roots at tillering stage than at booting, due to an increased sugar transport to roots during tillering as observed in this study.

In general, the regulatory systems that allow plants to respond to either stress are complex. However, this study showed that environmental constraints disrupt and re-direct metabolic pathways leading to common metabolic disorders, due to the shared underlying physiological and molecular mechanisms, e.g. lower photosynthesis in leaves and sugar accumulation in roots.

7. REFERENCES

1. Adamipour, N., Khosh-Khui, M., Salehi, H., Razi, H., Karami, A., & Moghadam, A. (2020). Metabolic and genes expression analyses involved in proline metabolism of two rose species under drought stress. *Plant Physiology and Biochemistry*, 155, 105-113.

2. Agathokleous, E., Belz, R. G., Kitao, M., Koike, T., & Calabrese, E. J. (2019). Does the root to shoot ratio show a hormetic response to stress? An ecological and environmental perspective. *Journal of Forestry Research*, 30(5), 1569-1580.

3. Aguirre, A. (2020). Quantification of the impact of enhanced urea uptake in cereal grain crops on growth, nitrogen metabolism, yield formation and grain quality. Martin-Luther-Universität Halle-Wittenberg, Sachsen-Anhalt, Germany doi: http://dx.doi.org/10.25673/37297.

4. Arbona, V., & Gómez-Cadenas, A. (2008). Hormonal modulation of citrus responses to flooding. *Journal of Plant Growth Regulation*, 27(3), 241-250.

5. Arduini, I., Baldanzi, M., & Pampana, S. (2019a). Reduced growth and nitrogen uptake during waterlogging at tillering permanently affect yield components in late sown oats. *Frontiers in plant science*, 10, 1087.

6. Arduini, I., Kokubun, M., & Licausi, F. (2019b). Crop Response to Waterlogging. *Frontiers Media SA* In, 10, 1578).

7. Atkinson, C. J., Harrison-Murray, R., & Taylor, J. (2008). Rapid flood-induced stomatal closure accompanies xylem sap transportation of root-derived acetaldehyde and ethanol in Forsythia. *Environmental and Experimental Botany*, 64(2), 196-205.

8. Bailey-Serres, J., Fukao, T., Gibbs, D. J., Holdsworth, M. J., Lee, S. C., Licausi, F., Perata, P., Voesenek, L. A. C. J., & van Dongen, J. T. (2012). Making sense of low oxygen sensing. *Trends in Plant Science*, 17(3), 129-138.

9. Bailey-Serres, J., Lee, S., & Brinton, E. (2012). Waterproofing crops: effective flooding survival strategies. *Plant Physiology*, 160(4), 1698-1709.

10. Bailey-Serres, J., & Voesenek, L. (2008). Flooding stress: acclimations and genetic diversity. *Annual Review of Plant Biology*, 59, 313.

11. Bansal, R., & Srivastava, J. (2015). Effect of waterlogging on photosynthetic and biochemical parameters in pigeonpea. *Russian Journal of Plant Physiology*, 62(3), 322-327.

12. Barickman, T. C., Simpson, C. R., & Sams, C. E. (2019). Waterlogging causes early modification in the physiological performance, carotenoids, chlorophylls, proline, and soluble sugars of cucumber plants. *Plants*, 8(6), 160.

13. Bashar, K. K., Tareq, M. Z., & Islam, M. S. (2020). Unlocking the mystery of plants' survival capability under waterlogging stress. *Plant Science Today*, 7(2), 142-153.

14. Beier, S., Marella, N. C., Yvin, J.-C., Hosseini, S. A., & von Wirén, N. (2022). Silicon mitigates potassium deficiency by enhanced remobilization and modulated potassium transporter regulation. *Environmental and Experimental Botany*, 198, 104849.

15. Blom, C. (1999). Adaptations to flooding stress: from plant community to molecule. *Plant Biology*, 1(03), 261-273.

16. Blöschl, G., Hall, J., Parajka, J., Perdigão, R. A. P., Merz, B., Arheimer, B., . . . Živković, N. (2017). Changing climate shifts timing of European floods. *Science*, 357(6351), 588-590. doi:10.1126/science.aan2506.

17. Board, J. (2008). Waterlogging effects on plant nutrient concentrations in soybean. *Journal of Plant Nutrition*, 31(5), 828-838.

18. Bradford, K. J., Hsiao, T. C., & Yang, S. F. (1982). Inhibition of ethylene synthesis in tomato plants subjected to anaerobic root stress. *Plant Physiology*, 70(5), 1503-1507.

19. Bramley, H., Turner, N. C., Turner, D. W., & Tyerman, S. D. (2010). The contrasting influence of short-term hypoxia on the hydraulic properties of cells and roots of wheat and lupin. *Functional Plant Biology*, 37(3), 183-193.

20. Chen, L.-Q., Qu, X.-Q., Hou, B.-H., Sosso, D., Osorio, S., Fernie, A. R., & Frommer, W. B. (2012). Sucrose efflux mediated by SWEET proteins as a key step for phloem transport. *Science*, 335(6065), 207-211.

21. Colmer, T. D., & Greenway, H. (2011). Ion transport in seminal and adventitious roots of cereals during O2 deficiency. *Journal of Experimental Botany*, 62(1), 39-57.

22. CRED. 2022 Disasters in numbers. Brussels: CRED; 2023. This document is available at: https://cred.be/sites/default/files/2022_EMDAT_report.pdf.

23. Cui, J., Davanture, M., Zivy, M., Lamade, E., & Tcherkez, G. (2019). Metabolic responses to potassium availability and waterlogging reshape respiration and carbon use efficiency in oil palm. *New Phytologist*, 223(1), 310-322.

24. D'Odorico, P., Bhattachan, A., Davis, K. F., Ravi, S., & Runyan, C. W. (2013). Global desertification: Drivers and feedbacks. *Advances in Water Resources*, 51, 326-344.

25. De Sousa, C., & Sodek, L. (2003). Alanine metabolism and alanine aminotransferase activity in soybean (Glycine max) during hypoxia of the root system and subsequent return to normoxia. *Environmental and Experimental Botany*, 50(1), 1-8.

26. den Besten, N., Steele-Dunne, S., de Jeu, R., & van der Zaag, P. (2021). Towards monitoring waterlogging with remote sensing for sustainable irrigated agriculture. *Remote Sensing*, 13(15), 2929.

27. Diab, H., & Limami, A. M. (2016). Reconfiguration of N metabolism upon hypoxia stress and recovery: roles of alanine aminotransferase (AlaAT) and glutamate dehydrogenase (GDH). *Plants*, 5(2), 25.

28. Dreyer, I., Gomez-Porras, J. L., & Riedelsberger, J. (2017). The potassium battery: a mobile energy source for transport processes in plant vascular tissues. *New Phytologist*, 216(4), 1049-1053.

29. Eastmond, P. J., Astley, H. M., Parsley, K., Aubry, S., Williams, B. P., Menard, G. N., Craddock, C. P., Nunes-Nesi, A., Fernie, A. R., Hibberd, J. M. (2015). Arabidopsis uses two gluconeogenic gateways for organic acids to fuel seedling establishment. *Nature Communications*, 6(1), 1-8.

30. Eggert, K., & von Wirén, N. (2017). Response of the plant hormone network to boron deficiency. *New Phytologist*, 216(3), 868-881.

31. Ellis, M. H., Dennis, E. S., & James Peacock, W. (1999). Arabidopsis roots and shoots have different mechanisms for hypoxic stress tolerance. *Plant Physiology*, 119(1), 57-64.

32. Else, M. A., Janowiak, F., Atkinson, C. J., & Jackson, M. B. (2009). Root signals and stomatal closure in relation to photosynthesis, chlorophyll a fluorescence and adventitious rooting of flooded tomato plants. *Annals of Botany*, 103(2), 313-323.

33. Elzenga, J. T. M., & Veen, H. v. (2010). Waterlogging and plant nutrient uptake. In *Waterlogging signalling and tolerance in plants* (pp. 23-35): Springer.

34. Evans, D. E. (2004). Aerenchyma formation. *New Phytologist*, 161(1), 35-49. doi: https://doi.org/10.1046/j.1469-8137.2003.00907.

35. FAO. 2022. Crop Prospects and Food Situation-Quarterly Global Report No. 3, September (2022). Rome. https://doi.org/10.4060/cc2300en.

36. FAO. (2021). The impact of disasters and crises on agriculture and food security: 2021. Rome. https://doi.org/10.4060/cb3673en.

37. Fitzpatrick, C. R., Copeland, J., Wang, P. W., Guttman, D. S., Kotanen, P. M., & Johnson, M. T. (2018). Assembly and ecological function of the root microbiome across angiosperm plant species. *Proceedings of the National Academy of Sciences*, 115(6), E1157-E1165.

38. Forde, B. G., & Lea, P. J. (2007). Glutamate in plants: metabolism, regulation, and signalling. *Journal of Experimental Botany*, 58(9), 2339-2358.

39. Francioli, D., Cid, G., Hajirezaei, M.-R., & Kolb, S. (2022a). Leaf bacterial microbiota response to flooding is controlled by plant phenology in wheat (Triticum aestivum L.). *Scientific Reports*, 12(1), 1-13.

40. Francioli, D., Cid, G., Hajirezaei, M.-R., & Kolb, S. (2022b). Response of the wheat mycobiota to flooding revealed substantial shifts towards plant pathogens. *Frontiers in Plant Science*, 3:1028153. doi: 10.3389/fpls.2022.1028153.

41. Francioli, D., Cid, G., Kanukollu, S., Ulrich, A., Hajirezaei, M.-R., & Kolb, S. (2021). Flooding Causes Dramatic Compositional Shifts and Depletion of Putative Beneficial Bacteria on the Spring Wheat Microbiota. *Frontiers in Microbiology*, 2:773116. doi: 10.3389/fmicb.2021.773116.

42. Franco, J., Bañón, S., Vicente, M., Miralles, J., & Martínez-Sánchez, J. (2011). Root development in horticultural plants grown under abiotic stress conditions–a review. *The Journal of Horticultural Science and Biotechnology*, 86(6), 543-556.

43. Fukao, T., & Bailey-Serres, J. (2004). Plant responses to hypoxia–is survival a balancing act? *Trends in Plant Science*, 9(9), 449-456.

44. Fukao, T., Barrera-Figueroa, B. E., Juntawong, P., & Peña-Castro, J. M. (2019). Submergence and waterlogging stress in plants: a review highlighting research opportunities and understudied aspects. *Frontiers in Plant Science*, 10, 340.

45. Gajdanowicz, P., Michard, E., Sandmann, M., Rocha, M., Corrêa, L. G. G., Ramírez-Aguilar, S. J., Gomez-Porras, J. L., González, W., Thibaud, J.-B., & van Dongen, J. T. (2011). Potassium (K+) gradients serve as a mobile energy source in plant vascular tissues. *Proceedings of the National Academy of Sciences*, 108(2), 864-869.

46. Ghaffari, M. R., Shahinnia, F., Usadel, B., Junker, B., Schreiber, F., Sreenivasulu, N., & Hajirezaei, M. R. (2016). The metabolic signature of biomass formation in barley. *Plant and Cell Physiology*, 57(9), 1943-1960.

47. Gibbs, D. J., Lee, S. C., Md Isa, N., Gramuglia, S., Fukao, T., Bassel, G. W., Correia, C. S., Corbineau, F., Theodoulou, F. L., & Bailey-Serres, J. (2011). Homeostatic response to hypoxia is regulated by the N-end rule pathway in plants. *Nature*, 479(7373), 415-418.

48. Gibbs, J., & Greenway, H. (2003). Mechanisms of anoxia tolerance in plants. I. Growth, survival and anaerobic catabolism. *Functional Plant Biology*, 30(1), 1-47.

49. Gilbert, M. E., & Medina, V. (2016). Drought adaptation mechanisms should guide experimental design. *Trends in Plant Science*, 21(8), 639-647.

50. Guan, B., Lin, Z., Liu, D., Li, C., Zhou, Z., Mei, F., Li, J., & Deng, X. (2019). Effect of waterlogging-induced autophagy on programmed cell death in Arabidopsis roots. *Frontiers in Plant Science*, 10, 468.

51. Heberle, H., Meirelles, G. V., da Silva, F. R., Telles, G. P., & Minghim, R. (2015). InteractiVenn: a web-based tool for the analysis of sets through Venn diagrams. *BMC Bioinformatics*, 16:169.

52. Heinemann, B., & Hildebrandt, T. M. (2021). The role of amino acid metabolism in signaling and metabolic adaptation to stress-induced energy deficiency in plants. *Journal of Experimental Botany*, 72(13), 4634-4645.

53. Herzog, M., Striker, G. G., Colmer, T. D., & Pedersen, O. (2016). Mechanisms of waterlogging tolerance in wheat–a review of root and shoot physiology. *Plant, Cell & Environment*, 39(5), 1068-1086.

54. Hossain, M. A., & Uddin, S. N. (2011). Mechanisms of waterlogging tolerance in wheat: Morphological and metabolic adaptations under hypoxia or anoxia. *Australian Journal of Crop Science*, 5(9), 1094-1101.

55. Hsu, F.-C., Chou, M.-Y., Peng, H.-P., Chou, S.-J., & Shih, M.-C. (2011). Insights into hypoxic systemic responses based on analyses of transcriptional regulation in Arabidopsis. *PLoS One*, 6(12), e28888.

56. Huang, Z., Liu, Y., Tian, F.-P., & Wu, G.-L. (2020). Soil water availability threshold indicator was determined by using plant physiological responses under drought conditions. *Ecological Indicators*, 118, 106740.

57. Huber, B., Luster, J., Bernasconi, S. M., Shrestha, J., & Graf Pannatier, E. (2012). Nitrate leaching from short-hydroperiod floodplain soils. *Biogeosciences*, 9(11), 4385-4397.

58. Hwang, J. H., Lee, M. O., Choy, Y.-H., Ha-Lee, Y.-M., Hong, C. B., & Lee, D.-H. (2011). Expression profile analysis of hypoxia responses in Arabidopsis roots and shoots. *Journal of Plant Biology*, 54(6), 373-383.

59. Institute for Economics & Peace. Ecological Threat Report (2022): Analysing Ecological Threats, Resilience & Peace, Sydney, October 2022. Available from: http://visionofhumanity.org/resources (last access on 12.05.2023).

60. Irfan, M., Hayat, S., Hayat, Q., Afroz, S., & Ahmad, A. (2010). Physiological and biochemical changes in plants under waterlogging. *Protoplasma*, 241(1), 3-17.

61. Irigoyen, J. J., Sanchez-Diaz, M., & Emerich, D. W. (1992). Transient increase of anaerobically-induced enzymes during short-term drought of alfalfa root nodules. *Journal of Plant Physiology*, 139(4), 397-402.

62. Jackson, M. (1997). Hormones from roots as signals for the shoots of stressed plants. *Trends in Plant Science*, 2(1), 22-28.

63. Jogawat, A. (2019). Osmolytes and their role in abiotic stress tolerance in plants. *Molecular Plant Abiotic Stress: Biology and Biotechnology*, 91-104.

64. Kan, C.-C., Chung, T.-Y., Juo, Y.-A., & Hsieh, M.-H. (2015). Glutamine rapidly induces the expression of key transcription factor genes involved in nitrogen and stress responses in rice roots. *BMC Genomics*, 16(1), 1-15.

65. Kaur, G., Singh, G., Motavalli, P. P., Nelson, K. A., Orlowski, J. M., & Golden, B. R. (2020). Impacts and management strategies for crop production in waterlogged or flooded soils: A review. *Agronomy Journal*, 112(3), 1475-1501. doi: https://doi.org/10.1002/agj2.20093

66. Kemmann, B., Ruf, T., Matson, A., & Well, R. (2023). Waterlogging effects on N. *Biology and Fertility of Soils*, 59, 53-71.

67. Kitajima, K., & Hogan, K. P. (2003). Increases of chlorophyll a/b ratios during acclimation of tropical woody seedlings to nitrogen limitation and high light. *Plant, Cell & Environment*, 26(6), 857-865.

68. Kogo, B. K., Kumar, L., & Koech, R. (2021). Climate change and variability in Kenya: a review of impacts on agriculture and food security. *Environment, Development and Sustainability*, 23(1), 23-43. doi:10.1007/s10668-020-00589-1

69. Kreuzwieser, J., Hauberg, J., Howell, K. A., Carroll, A., Rennenberg, H., Millar, A. H., & Whelan, J. (2009). Differential response of gray poplar leaves and roots underpins stress adaptation during hypoxia. *Plant Physiology*, 149(1), 461-473.

70. Kreuzwieser, J., & Rennenberg, H. (2014). Molecular and physiological responses of trees to waterlogging stress. *Plant, Cell & Environment*, 37(10), 2245-2259.

71. Kruczkiewicz, A., Cian, F., Monasterolo, I., Di Baldassarre, G., Caldas, A., Royz, M., Glasscoe, M., Ranger, N., & van Aalst, M. (2022). Multiform flood risk in a rapidly changing world: what we do not do, what we should and why it matters. *Environmental Research Letters*, 17(8), 081001.

72. Lambers, H., Hayes, P. E., Laliberte, E., Oliveira, R. S., & Turner, B. L. (2015). Leaf manganese accumulation and phosphorus-acquisition efficiency. *Trends in Plant Science*, 20(2), 83-90.

73. Lee, S. C., Mustroph, A., Sasidharan, R., Vashisht, D., Pedersen, O., Oosumi, T., Voesenek, L. A. C. J., & Bailey-Serres, J. (2011). Molecular characterization of the submergence response of the Arabidopsis thaliana ecotype Columbia. *New Phytologist*, 190(2), 457-471.

74. Licausi, F., Kosmacz, M., Weits, D. A., Giuntoli, B., Giorgi, F. M., Voesenek, L. A., Perata, P., & van Dongen, J. T. (2011). Oxygen sensing in plants is mediated by an N-end rule pathway for protein destabilization. *Nature*, 479(7373), 419-422.

75. Liepman, A. H., & Olsen, L. J. (2003). Alanine aminotransferase homologs catalyze the glutamate: glyoxylate aminotransferase reaction in peroxisomes of Arabidopsis. *Plant Physiology*, 131(1), 215-227.

76. Liu, K., Harrison, M. T., Ibrahim, A., Manik, S. N., Johnson, P., Tian, X., Meinke, H., & Zhou, M. (2020). Genetic factors increasing barley grain yields under soil waterlogging. *Food and Energy Security*, 9(4), e238.

77. Lorenzo, O., Piqueras, R., Sánchez-Serrano, J. J., & Solano, R. (2003). ETHYLENE RESPONSE FACTOR1 integrates signals from ethylene and jasmonate pathways in plant defense. *The Plant Cell*, 15(1), 165-178.

78. Loreti, E., & Perata, P. (2020). The Many Facets of Hypoxia in Plants. *Plants*, 9(6), 745. doi: https://www.mdpi.com/2223-7747/9/6/745.

79. Lothier, J., Diab, H., Cukier, C., Limami, A. M., & Tcherkez, G. (2020). Metabolic responses to waterlogging differ between roots and shoots and reflect phloem transport alteration in *Medicago truncatula*. *Plants*, 9(10), 1373.

80. Mäkinen, H., Kaseva, J., Trnka, M., Balek, J., Kersebaum, K., Nendel, C., Gobin, A., Olesen, J. E., Bindi, M., & Ferrise, R. (2018). Sensitivity of European wheat to extreme weather. *Field Crops Research*, 222, 209-217.

81. Malik, A. I., Colmer, T. D., Lambers, H., Setter, T. L., & Schortemeyer, M. (2002). Short-term waterlogging has long‐term effects on the growth and physiology of wheat. *New Phytologist*, 153(2), 225-236.

82. Mancuso, S., & Shabala, S. (2010). *Waterlogging signalling and tolerance in plants:* Springer.

83. Manzur, M., Grimoldi, A., Insausti, P., & Striker, G. (2009). Escape from water or remain quiescent? Lotus tenuis changes its strategy depending on depth of submergence. *Annals of Botany*, 104(6), 1163-1169.

84. Maranguit, D., Guillaume, T., & Kuzyakov, Y. (2017). Effects of flooding on phosphorus and iron mobilization in highly weathered soils under different land-use types: Short-term effects and mechanisms. *Catena*, 158, 161-170.

85. Marschner, H. (2011). *Marschner's mineral nutrition of higher plants*: Academic press.

86. Marti, J., Savin, R., & Slafer, G. (2015). Wheat yield as affected by length of exposure to waterlogging during stem elongation. *Journal of Agronomy and Crop Science*, 201(6), 473-486.

87. Maurel, C., & Nacry, P. (2020). Root architecture and hydraulics converge for acclimation to changing water availability. *Nature Plants*, 6(7), 744-749.

88. McDermott, T. K. (2022). Global exposure to flood risk and poverty. *Nature Communications*, 13(1), 1-3.

89. Men, S., Chen, H., Chen, S., Zheng, S., Shen, X., Wang, C., Yang, Z., & Liu, D. (2020). Effects of supplemental nitrogen application on physiological characteristics, dry matter and nitrogen accumulation of winter rapeseed (*Brassica napus* L.) under waterlogging stress. *Scientific Reports,* 10(1), 1-10.

90. Mignolli, F., Barone, J. O., & Vidoz, M. L. (2021). Root submergence enhances respiration and sugar accumulation in the stem of flooded tomato plants. *Plant, Cell & Environment*, 44(11), 3643-3654.

91. Miyashita, Y., & Good, A. G. (2008). Contribution of the GABA shunt to hypoxia-induced alanine accumulation in roots of *Arabidopsis thaliana*. *Plant and Cell Physiology*, 49(1), 92-102.

92. Mostajeran, A., & Rahimi-Eichi, V. (2009). Effects of drought stress on growth and yield of rice (*Oryza sativa* L.) cultivars and accumulation of proline and soluble sugars in sheath and blades of their different ages leaves. *American-Euroasian Journal of Agricultural and Environmental Sciences*, 5(2), 264-272.

93. Mousavi, M. E., Irish, J. L., Frey, A. E., Olivera, F., & Edge, B. L. (2011). Global warming and hurricanes: the potential impact of hurricane intensification and sea level rise on coastal flooding. *Climatic Change*, 104(3), 575-597. doi:10.1007/s10584-009-9790-0.

94. Mugnai, S., Azzarello, E., Baluška, F., & Mancuso, S. (2012). Local root apex hypoxia induces NO-mediated hypoxic acclimation of the entire root. *Plant and Cell Physiology*, 53(5), 912-920.

95. Mugnai, S., Marras, A. M., & Mancuso, S. (2011). Effect of hypoxic acclimation on anoxia tolerance in Vitis roots: response of metabolic activity and K+ fluxes. *Plant and Cell Physiology*, 52(6), 1107-1116.

96. Murphy, J., and Riley, J. P. (1962). A modified single solution method for the determination of phosphate in natural waters. *Analytica Chimica Acta* 27, 31–36. doi: 10.1016/S0003-2670(00)88444-5.

97. Mustroph, A., Barding Jr, G. A., Kaiser, K. A., Larive, C. K., & Bailey-Serres, J. (2014). Characterization of distinct root and shoot responses to low‐oxygen stress in Arabidopsis with a focus on primary C-and N-metabolism. *Plant, Cell & Environment*, 37(10), 2366-2380.

98. Najeeb, U., Bange, M. P., Tan, D. K., & Atwell, B. J. (2015). Consequences of waterlogging in cotton and opportunities for mitigation of yield losses. *AoB Plants*, 7.

99. Nishiuchi, S., Yamauchi, T., Takahashi, H., Kotula, L., & Nakazono, M. (2012). Mechanisms for coping with submergence and waterlogging in rice. *Rice*, 5(1), 2. doi:10.1186/1939-8433-5-2.

100. Okumoto, S., & Pilot, G. (2011). Amino acid export in plants: a missing link in nitrogen cycling. *Molecular Plant*, 4(3), 453-463.

101. Oliveira, H. C., Freschi, L., & Sodek, L. (2013). Nitrogen metabolism and translocation in soybean plants subjected to root oxygen deficiency. *Plant Physiology and Biochemistry*, 66, 141-149.

102. Orzechowski, S., Socha-Hanc, J., & Paszkowski, A. (1999). Alanine aminotransferase and glycine aminotransferase from maize (*Zea mays* L.) leaves. *Acta Biochimica Polonica*, 46(2), 447-457.

103. Pan, J., Sharif, R., Xu, X., & Chen, X. (2021). Mechanisms of Waterlogging Tolerance in Plants: Research Progress and Prospects. *Frontiers in Plant Science*, 11. doi:10.3389/fpls.2020.627331

104. Paprotny, D., Sebastian, A., Morales-Nápoles, O., & Jonkman, S. N. (2018). Trends in flood losses in Europe over the past 150 years. *Nature Communications*, 9(1), 1985. doi:10.1038/s41467-018-04253-1.

105. Parent, C., Capelli, N., Berger, A., Crèvecoeur, M., & Dat, J. F. (2008). An overview of plant responses to soil waterlogging. *Plant Stress*, 2(1), 20-27.

106. Parlanti, S., Kudahettige, N. P., Lombardi, L., Mensuali-Sodi, A., Alpi, A., Perata, P., & Pucciariello, C. (2011). Distinct mechanisms for aerenchyma formation in leaf sheaths of rice genotypes displaying a quiescence or escape strategy for flooding tolerance. *Annals of Botany*, 107(8), 1335-1343. doi:10.1093/aob/mcr086.

107. Paterson, D. L., Wright, H., & Harris, P. N. A. (2018). Health Risks of Flood Disasters. *Clinical Infectious Diseases*, 67(9), 1450-1454. doi:10.1093/cid/ciy227.

108. Pauwels, R., Jansa, J., Püschel, D., Müller, A., Graefe, J., Kolb, S., & Bitterlich, M. (2020). Root growth and presence of Rhizophagus irregularis distinctly alter substrate hydraulic properties in a model system with *Medicago truncatula*. *Plant and Soil*, 457(1-2), 131-151.

109. Pearson, M., Saarinen, M., Nummelin, L., Heiskanen, J., Roitto, M., Sarjala, T., & Laine, J. (2013). Tolerance of peat-grown Scots pine seedlings to waterlogging and drought: Morphological, physiological, and metabolic responses to stress. *Forest Ecology and Management*, 307.

110. Pedersen, O., Sauter, M., Colmer, T. D., & Nakazono, M. (2021). Regulation of root adaptive anatomical and morphological traits during low soil oxygen. *New Phytologist*, 229(1), 42-49.

111. Petersen, K. F., Dufour, S., Cline, G. W., & Shulman, G. I. (2019). Regulation of hepatic mitochondrial oxidation by glucose-alanine cycling during starvation in humans. *The Journal of Clinical Investigation,* 129(11), 4671-4675.

112. Plett, D. C., Ranathunge, K., Melino, V. J., Kuya, N., Uga, Y., & Kronzucker, H. J. (2020). The intersection of nitrogen nutrition and water use in plants: new paths toward improved crop productivity. *Journal of Experimental Botany*, 71(15), 4452-4468.

113. Ploschuk, R. A., Miralles, D. J., Colmer, T. D., Ploschuk, E. L., & Striker, G. G. (2018). Waterlogging of winter crops at early and late stages: impacts on leaf physiology, growth and yield. *Frontiers in Plant Science*, 9, 1863.

114. Ploschuk, R. A., Miralles, D. J., Colmer, T. D., & Striker, G. G. (2020). Waterlogging differentially affects yield and its components in wheat, barley, rapeseed and field pea depending on the timing of occurrence. *Journal of Agronomy and Crop Science*, 206(3), 363-375.

115. Polania, J., Poschenrieder, C., Rao, I., & Beebe, S. (2017). Root traits and their potential links to plant ideotypes to improve drought resistance in common bean. *Theoretical and Experimental Plant Physiology*, 29, 143-154.

116. Pré, M., Atallah, M., Champion, A., De Vos, M., Pieterse, C. M., & Memelink, J. (2008). The AP2/ERF domain transcription factor ORA59 integrates jasmonic acid and ethylene signals in plant defense. *Plant Physiology*, 147(3), 1347-1357.

117. Puiatti, M., & Sodek, L. (1999). Waterlogging affects nitrogen transport in the xylem of soybean. *Plant Physiology and Biochemistry*, 37(10), 767-773.

118. Qi, X., Li, Q., Shen, J., Qian, C., Xu, X., Xu, Q., & Chen, X. (2020). Sugar enhances waterlogging-induced adventitious root formation in cucumber by promoting auxin transport and signalling. *Plant, Cell & Environment*, 43(6), 1545-1557.

119. Qiu, F., Zheng, Y., Zhang, Z., & Xu, S. (2007). Mapping of QTL associated with waterlogging tolerance during the seedling stage in maize. *Annals of Botany*, 99(6), 1067-1081.

120. Rajendrakumar, C. S., Reddy, B. V., & Reddy, A. R. (1994). Proline-protein interactions: protection of structural and functional integrity of M4 lactate dehydrogenase. *Biochemical and Biophysical Research Communications*, 201(2), 957-963.

121. Reddy, K., Patrick, W., & Broadbent, F. (1984). Nitrogen transformations and loss in flooded soils and sediments. *Critical Reviews in Environmental Science and Technology*, 13(4), 273-309.

122. Redillas, M. C., Park, S.-H., Lee, J. W., Kim, Y. S., Jeong, J. S., Jung, H., Bang, S. W., Hahn, T.-R., & Kim, J.-K. (2012). Accumulation of trehalose increases soluble sugar contents in rice plants conferring tolerance to drought and salt stress. *Plant Biotechnology Reports*, 6(1), 89-96.

123. Reggiani, R. (1999). Amino acid metabolism under oxygen deficiency. *Phytochemistry*, 2, 171-174.

124. Reggiani, R., Nebuloni, M., Mattana, M., & Brambilla, I. (2000). Anaerobic accumulation of amino acids in rice roots: role of the glutamine synthetase/glutamate synthase cycle. *Amino acids*, 18(3), 207-217.

125. Ricoult, C., Echeverria, L. O., Cliquet, J.-B., & Limami, A. M. (2006). Characterization of alanine aminotransferase (AlaAT) multigene family and hypoxic response in young seedlings of the model legume *Medicago truncatula*. *Journal of Experimental Botany*, 57(12), 3079-3089.

126. Riehm, H. (1943). Bestimmung der laktatlöslichen phosphorsäure in karbonathaltigen *Böden. Phosphorsäure* 1, 167–178. doi: 10.1002/jpln. 19420260107.

127. Roca, M., Chen, K., & Pérez-Gálvez, A. (2016). Chlorophylls. In *Handbook on Natural Pigments in Food and Beverages* (pp. 125-158): Elsevier.

128. Rocha, M., Licausi, F., Araújo, W. L., Nunes-Nesi, A., Sodek, L., Fernie, A. R., & Van Dongen, J. T. (2010a) b. Glycolysis and the tricarboxylic acid cycle are linked by alanine aminotransferase during hypoxia induced by waterlogging of *Lotus japonicus. Plant Physiology*, 152(3), 1501-1513.

129. Rocha, M., Sodek, L., Licausi, F., Hameed, M. W., Dornelas, M. C., & Van Dongen, J. (2010b). Analysis of alanine aminotransferase in various organs of soybean (Glycine max) and in dependence of different nitrogen fertilisers during hypoxic stress. *Amino acids*, 39(4), 1043-1053.

130. Rodionov, R. N., Jarzebska, N., Weiss, N., & Lentz, S. R. (2014). AGXT2: a promiscuous aminotransferase. *Trends in Pharmacological Sciences*, 35(11), 575-582.

131. Rodionov, R. N., Murry, D. J., Vaulman, S. F., Stevens, J. W., & Lentz, S. R. (2010). Human alanine-glyoxylate aminotransferase 2 lowers asymmetric dimethylarginine and protects from inhibition of nitric oxide production. *Journal of Biological Chemistry*, 285(8), 5385-5391.

132. Rosenzweig, C., Tubiello, F. N., Goldberg, R., Mills, E., & Bloomfield, J. (2002). Increased crop damage in the US from excess precipitation under climate change. *Global Environmental Change*, 12(3), 197-202.

133. Sachdev, S., Ansari, S. A., Ansari, M. I., Fujita, M., & Hasanuzzaman, M. (2021). Abiotic Stress and Reactive Oxygen Species: Generation, Signaling, and Defense Mechanisms. *Antioxidants*, 10(2), 277. doi: https://www.mdpi.com/2076-3921/10/2/277.

134. Safavi-Rizi, V., Herde, M., & Stöhr, C. (2020). RNA-Seq reveals novel genes and pathways associated with hypoxia duration and tolerance in tomato root. *Scientific Reports*, 10(1), 1692. doi:10.1038/s41598-020-57884-0.

135. Sánchez, F. J., Manzanares, M. a., de Andres, E. F., Tenorio, J. L., & Ayerbe, L. (1998). Turgor maintenance, osmotic adjustment and soluble sugar and proline accumulation in 49 pea cultivars in response to water stress. *Field Crops Research*, 59(3), 225-235.

136. Santaniello, A., Loreti, E., Gonzali, S., Novi, G., & Perata, P. (2014). A reassessment of the role of sucrose synthase in the hypoxic sucrose-ethanol transition in Arabidopsis. *Plant, Cell & Environment*, 37(10), 2294-2302.

137. Schmitt J, Offermann F, Söder M, Frühauf C, & R, F. (2022). Extreme weather events cause significant crop yield losses at the farm level in German agriculture. *Food Policy*, 112.

138. Schöps, R., Goldmann, K., Herz, K., Lentendu, G., Schöning, I., Bruelheide, H., Wubet, T., & Buscot, F. (2018). Land-use intensity rather than plant functional identity shapes bacterial and fungal rhizosphere communities. *Frontiers in Microbiology*, 2711.

139. Schulze, E.-D., Beck, E., Buchmann, N., Clemens, S., Müller-Hohenstein, K., & Scherer-Lorenzen, M. (2019). Oxygen deficiency. In *Plant Ecology* (pp. 143-164): Springer.

140. Setter, T., & Waters, I. (2003). Review of prospects for germplasm improvement for waterlogging tolerance in wheat, barley and oats. *Plant and Soil*, 253(1), 1-34.

141. Shabala, S., & Pottosin, I. (2014). Regulation of potassium transport in plants under hostile conditions: implications for abiotic and biotic stress tolerance. *Physiologia Plantarum*, 151(3), 257-279.

142. Shahandeh, H., Hossner, L., & Turner, F. (1994). Phosphorus relationships in flooded rice soils with low extractable phosphorus. *Soil Science Society of America Journal*, 58(4), 1184-1189.

143. Shahandeh, H., Hossner, L., & Turner, F. (2003). Phosphorus relationships to manganese and iron in rice soils. *Soil Science*, 168(7), 489-500.

144. Shirzaei, M., Khoshmanesh, M., Ojha, C., Werth, S., Kerner, H., Carlson, G., Sherpa, S. F., Zhai, G., & Lee, J.-C. (2021). Persistent impact of spring floods on crop loss in US Midwest. *Weather and Climate Extremes*, 34, 100392.

145. Smethurst, C. F., Garnett, T., & Shabala, S. (2005). Nutritional and chlorophyll fluorescence responses of lucerne (*Medicago sativa*) to waterlogging and subsequent recovery. *Plant and Soil*, 270(1), 31-45.

146. Steffens, D., Hutsch, B., Eschholz, T., Losak, T., & Schubert, S. (2005). Water logging may inhibit plant growth primarily by nutrient deficiency rather than nutrient toxicity. *Plant Soil and Environment*, 51(12), 545.

147. Stoimenova, M., Igamberdiev, A. U., Gupta, K. J., & Hill, R. D. (2007). Nitrite-driven anaerobic ATP synthesis in barley and rice root mitochondria. *Planta*, 226, 465-474.

148. Tognetti, V. B., Zurbriggen, M. D., Morandi, E. N., Fillat, M. F., Valle, E. M., Hajirezaei, M.-R., & Carrillo, N. (2007). Enhanced plant tolerance to iron starvation by functional substitution of chloroplast ferredoxin with a bacterial flavodoxin. *Proceedings of the National Academy of Sciences*, 104(27), 11495-11500.

149. Tombesi, S., Nardini, A., Frioni, T., Soccolini, M., Zadra, C., Farinelli, D., Poni, S., & Palliotti, A. (2015). Stomatal closure is induced by hydraulic signals and maintained by ABA in drought-stressed grapevine. *Scientific Reports*, 5(1), 1-12.

150. Tong, C., Hill, C. B., Zhou, G., Zhang, X.-Q., Jia, Y., & Li, C. (2021). Opportunities for improving waterlogging tolerance in cereal crops-physiological traits and genetic mechanisms. *Plants*, 10(8), 1560.

151. Toral-Juárez, M. A., Avila, R. T., Cardoso, A. A., Brito, F. A., Machado, K. L., Almeida, W. L., Souza, R. P. B., Martins, S. C. V., & DaMatta, F. M. (2021). Drought-tolerant coffee plants display increased tolerance to waterlogging and post-waterlogging reoxygenation. *Environmental and Experimental Botany*, 182, 104311.

152. Tula, S., Shahinnia, F., Melzer, M., Rutten, T., Gómez, R., Lodeyro, A. F., von Wirén, N., Carrillo, N., & Hajirezaei, M. R. (2020). Providing an additional electron sink by the introduction of cyanobacterial flavodiirons enhances growth of *A. thaliana* under various light intensities. *Frontiers in Plant Science*, 11, 902.

153. Vashisth, D., Kumar, R., Rastogi, S., Patel, V. K., Kalra, A., Gupta, M. M., Gupta, A. K., & Shasany, A. K. (2018). Transcriptome changes induced by abiotic stresses in *Artemisia annua*. *Scientific Reports*, 8(1), 1-14.

154. Verelst, W., Skirycz, A., & Inzé, D. (2010). Abscisic acid, ethylene and gibberellic acid act at different developmental stages to instruct the adaptation of young leaves to stress. *Plant Signaling & Behavior*, 5(4), 473-475.

155. Voesenek, L., & Bailey-Serres, J. (2013). Flooding tolerance: O2 sensing and survival strategies. *Current Opinion in Plant Biology*, 16(5), 647-653.

156. Voesenek, L., & Sasidharan, R. (2013). Ethylene–and oxygen signalling-drive plant survival during flooding. *Plant Biology*, 15(3), 426-435.

157. Waters, I., Morrell, S., Greenway, H., & Colmer, T. (1991). Effects of anoxia on wheat seedlings: II. Influence of O2 supply prior to anoxia on tolerance to anoxia, alcoholic fermentation, and sugar levels. *Journal of Experimental Botany*, 42(11), 1437-1447.

158. Watson, N. R., Peschke, V. M., Russell, D. A., & Sachs, M. M. (1992). Analysis of L-alanine: 2-oxoglutarate aminotransferase isozymes in maize. *Biochemical Genetics*, 30(7), 371-383.

159. Wei, X., Xu, H., Rong, W., Ye, X., & Zhang, Z. (2019). Constitutive expression of a stabilized transcription factor group VII ethylene response factor enhances waterlogging tolerance in wheat without penalizing grain yield. *Plant, Cell & Environment*, 42(5), 1471-1485.

160. Wongs-Aree, C., & Noichinda, S. (2018). Glycolysis fermentative by-products and secondary metabolites involved in plant adaptation under hypoxia during pre-and postharvest. *Hypoxia and Anoxia*, 59-72.

161. Zaman, M. S. U., Malik, A. I., Erskine, W., & Kaur, P. (2019). Changes in gene expression during germination reveal pea genotypes with either "quiescence" or "escape" mechanisms of waterlogging tolerance. *Plant, Cell & Environment*, 42(1), 245-258. doi: https://doi.org/10.1111/pce.13338.

162. Zhang, H., Huang, Z., Xie, B., Chen, Q., Tian, X., Zhang, X., Zhang, H., Lu, X., Huang, D., & Huang, R. (2004). The ethylene-, jasmonate-, abscisic acid-and NaCl-responsive tomato transcription factor JERF1 modulates expression of GCC box-containing genes and salt tolerance in tobacco. *Planta*, 220(2), 262-270.

163. Zhang, Q., Peters, J. L., Visser, E. J., de Kroon, H., & Huber, H. (2016). Hydrologically contrasting environments induce genetic but not phenotypic differentiation in *Solanum dulcamara*. *Journal of Ecology*, 104(6), 1649-1661.

164. Zhang, Y., Liu, G., Dong, H., & Li, C. (2021). Waterlogging stress in cotton: Damage, adaptability, alleviation strategies, and mechanisms. *The Crop Journal*, 9(2), 257-270.

165. Zou, X., Jiang, Y., Liu, L., Zhang, Z., & Zheng, Y. (2010). Identification of transcriptome induced in roots of maize seedlings at the late stage of waterlogging. *BMC Plant Biology*, 10(1), 1-16.

166. Zurweller, B. A., Motavalli, P. P., Nelson, K. A., & Dudenhoeffer, C. J. (2015). Short-term soil nitrous oxide emissions as affected by enhanced efficiency nitrogen fertilizers and temporarily waterlogged conditions. *Journal of Agricultural Science*, 7(12), 1.

8. APPENDIX

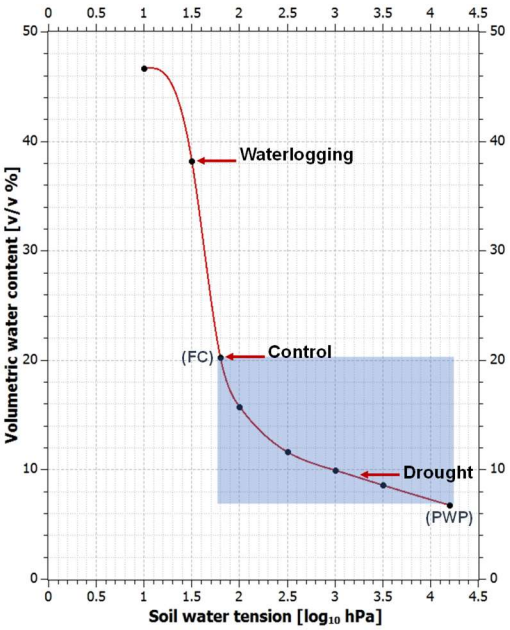

Appendix 1. Assessment of the water retention in the soil used in this study. Soil samples were water saturated for 24 h and subjected to the HYPROP™ system (Meter group, Munich, Germany). Two tensiometers were introduced into the soil at different depths (z = 1.25 cm and 3.75 cm) and the tension was recorded every ten minutes. The soil was weighed two times a day to calculate gravimetric water loss. The method returns the volumetric water content (Θ) as a function of tension (h, hPa) assuming that the geometric mean of h of both tensiometers equals the mean soil matric potential (Ψ) in the core soil volume (Pauwels et al. 2020).

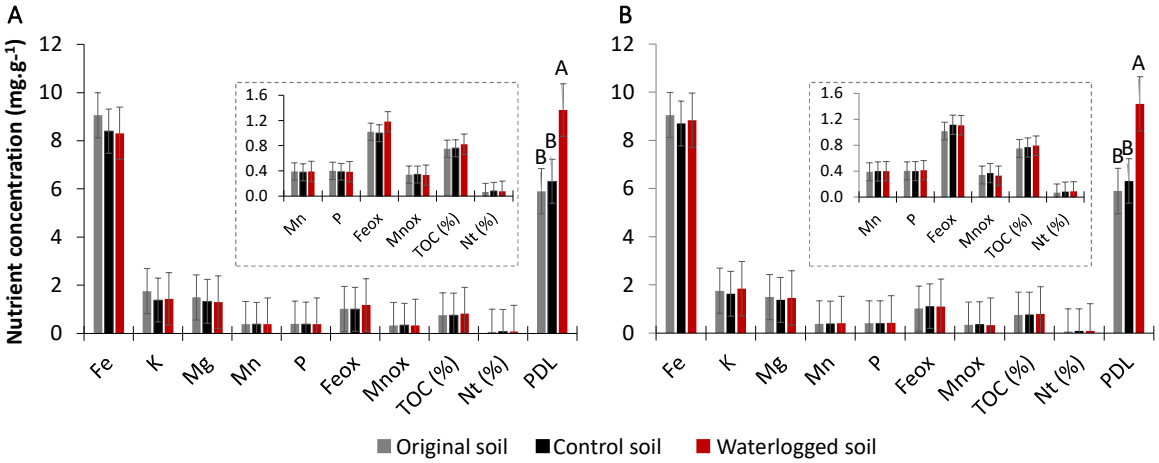

Appendix 2. Physico-chemical soil properties before and after waterlogging. (A) Nutrient concentrations in the soil at tillering and (B) booting stage. Samples from the original soil used in the experiments were collected during the onset of the treatments. After 12 days of waterlogging, soil samples from control or waterlogging treatments were collected at tillering or booting stage. The bars show the mean ± SE. One-way ANOVA analysis determined the differences between groups. Different letters in indicate significant differences according to Tukey's HSD or Dunn's test, $P \leq 0.05$, n = 8.

Appendix 3. Amino acid concentrations in fully developed leaves and roots of wheat plants exposed to 12 days of waterlogging during tillering or booting.

Amino Acid	DS	L-C	L-W	*P*-value	R-C	R-W	*P*-value
His	Tillering	6.24 ± 2.645**	3.79 ± 0.761	*< 0.01*	4.22 ± 2.24	2.65 ± 2.369	*n.s*
	Booting	17.5 ± 11.473	35.04 ± 32.847	*n.s*	16.82 ± 7.579	11.19 ± 5.949	*n.s*
Arg	Tillering	3.67 ± 1.148	3.94 ± 1.374	*n.s*	3.86 ± 4.26	7.71 ± 3.273*	*< 0.05*
	Booting	17.92 ± 9.829	62.32 ± 102.96	*n.s*	23.05 ± 9.821**	12.62 ± 3.192	*< 0.01*
Thr	Tillering	13.02 ± 5.735	9.19 ± 4.72	*n.s*	8.27 ± 1.968	10.81 ± 5.779	*n.s*
	Booting	70.61 ± 35.659	75.08 ± 30.057	*n.s*	33.17 ± 11.911	23.78 ± 6.827	*n.s*
Lys	Tillering	4.58 ± 2.273*	1.77 ± 1.014	*< 0.05*	2.21 ± 0.059	5.07 ± 3.535	*n.s*
	Booting	13.22 ± 8.979	24.58 ± 29.925	*n.s*	12.6 ± 8.238	8.9 ± 3.154	*n.s*
Ile	Tillering	2.62 ± 1.558	1.95 ± 1.195	*n.s*	3.86 ± 2.064	6 ± 2.426	*n.s*
	Booting	15.18 ± 8.142	22.76 ± 9.103	*n.s*	22.95 ± 8.676	24.39 ± 9.673	*n.s*
Leu	Tillering	2.19 ± 1.459	2.01 ± 1.18	*n.s*	2.35 ± 1.939	5.96 ± 1.957**	*< 0.01*
	Booting	18.52 ± 11.432	23.68 ± 14.202	*n.s*	26.76 ± 9.022	31.72 ± 8.564	*n.s*

Values show means ± SE of amino acid concentrations in leaves of control (L-C) or waterlogging (L-W) plants, and roots of control (R-C) or waterlogging (R-W) plants at different developmental stages (DS). Different asterisks indicate significant differences at * $P < 0.05$; ** $P < 0.01$ according to Student's *t*-test or Mann-Whitney *U*-test, $P \leq 0.05$, n =8. Not-significative differences between groups are identified as n.s.

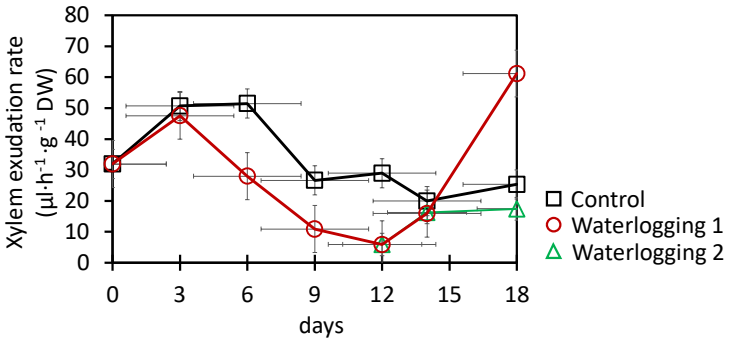

Appendix 4. Influence of waterlogging on the dynamics of xylem exudation rates in wheat plants at tillering stage. Xylem exudates were collected at days 0, 3, 6, 9 and 12 (under waterlogging), and 14 and 18 (during the recovery phase). Symbols show means ± SE, (n = 8).

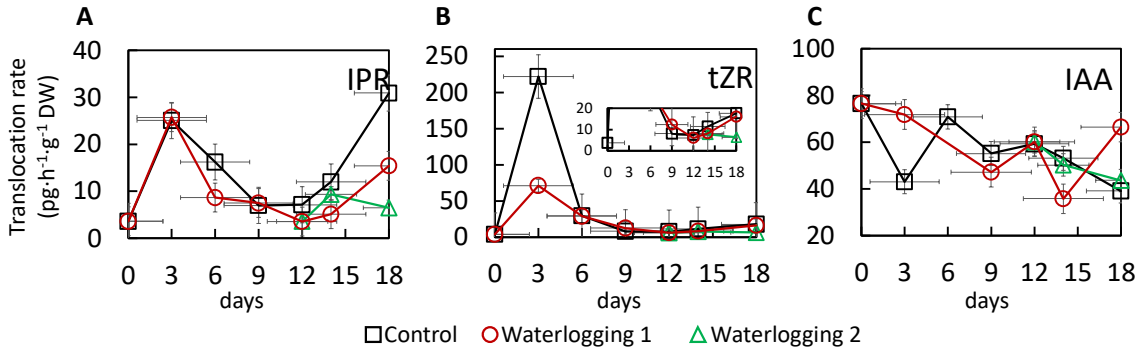

Appendix 5. Influence of waterlogging on the translocation rates of hormones in the xylem of wheat plants. (A) N6-isopentenyladenosine (IPR), (B) *trans*-zeatin riboside (tZR), and (C) indoleacetic acid (IAA). Xylem exudates were collected at 0, 3, 6, 9 and 12 days under waterlogging, and 14 and 18 days during the recovery phase. Symbols show means ± SE, (n = 8).

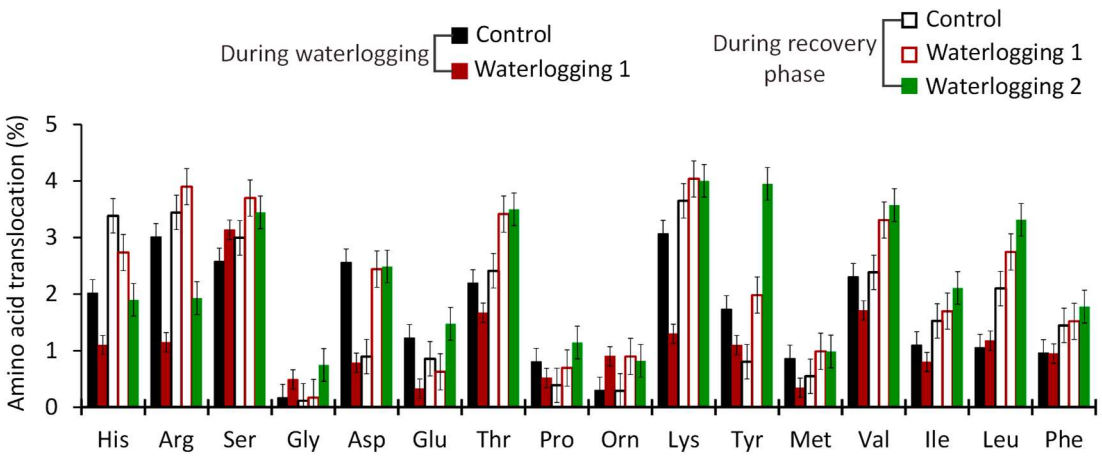

Appendix 6. Total percentage of the major amino acids in the xylem exudate determined at the end of each phase of the experiment. Xylem exudates were collected at 0, 3, 6, 9, and 12 days during waterlogging, and 14 and 18 days during the recovery phase. Bars show the mean ± SE, (n = 10) of the total percentage of each amino acid determined at the end of each phase of the experiment.

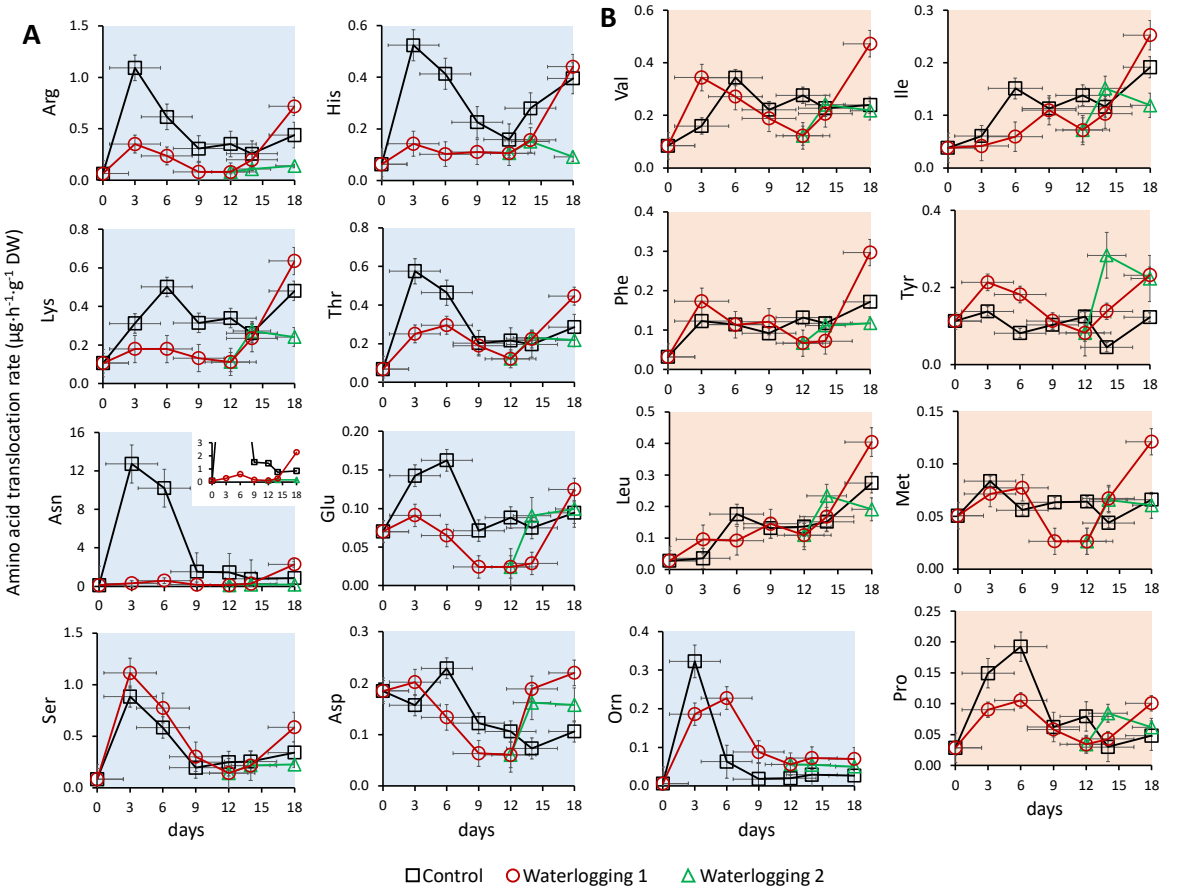

Appendix 7. Influence of waterlogging on translocation rates of individual amino acids in the xylem of wheat plants. Translocation rates of (A) hydrophilic, and (B) hydrophobic amino acids. Xylem exudates were collected at 0, 3, 6, 9 and 12 days under waterlogging, and 14 and 18 days during the recovery phase. Symbols show means ± SE, (n = 8).

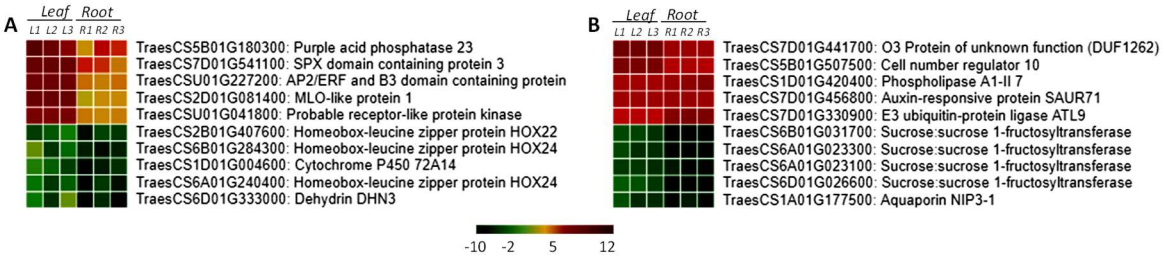

Appendix 8. Differentially expressed genes in wheat in response to waterlogging. (A) Heatmap showing the five most up-regulated (upper panel) and down-regulated (lower panel) common genes between leaves and roots of plants with waterlogging at tillering or (B) booting stage. In all cases, genes were grouped according to their transcription abundance on day 12 after the onset of the waterlogging treatment. The genes were selected considering a $\log_2$ fold-change ≥ |2| and $P_{adj} < 0.05$.

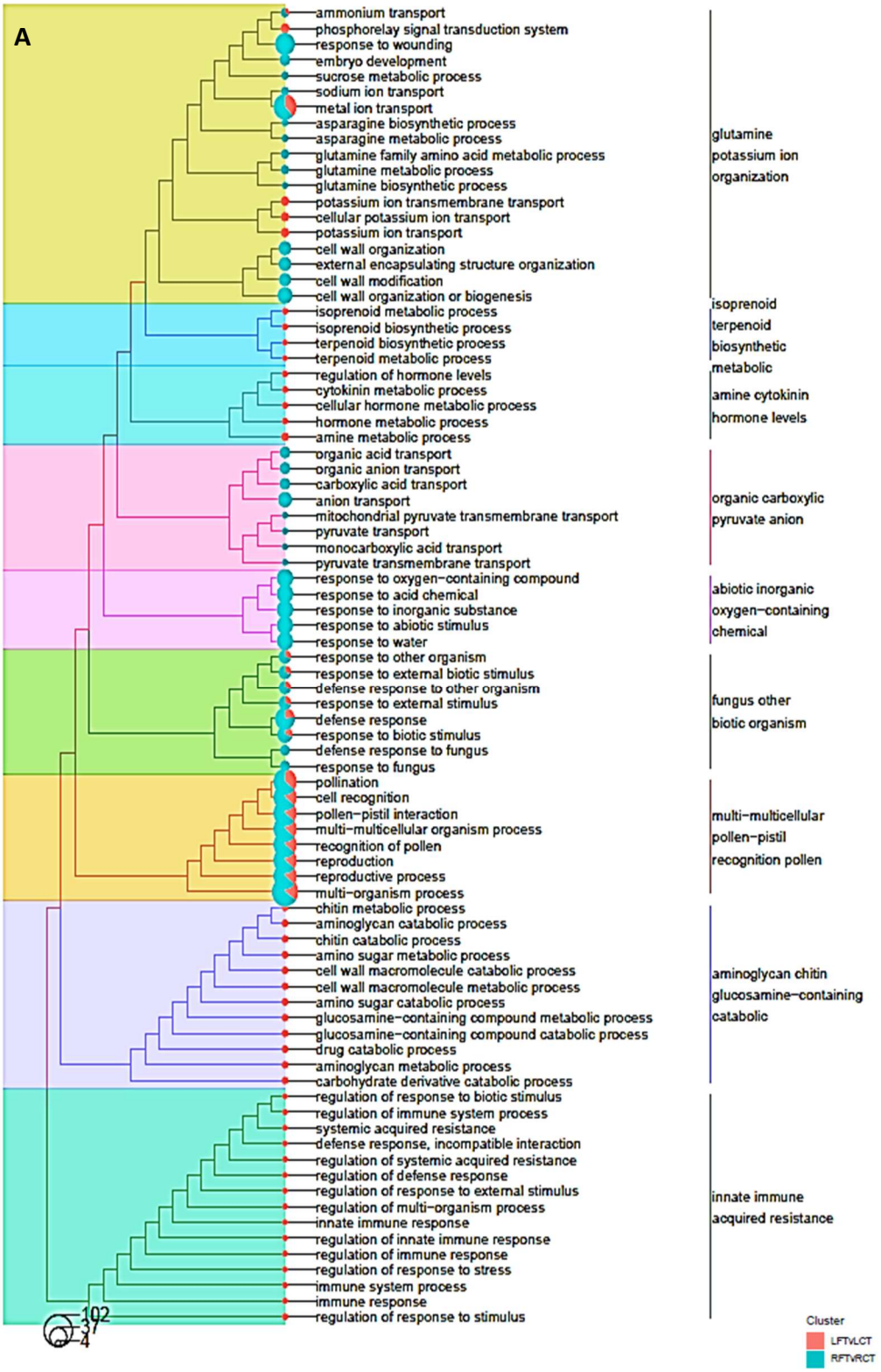
A
ammonium transport
phosphorelay signal transduction system
response to wounding
embryo development
sucrose metabolic process
sodium ion transport
metal ion transport
asparagine biosynthetic process
asparagine metabolic process
glutamine family amino acid metabolic process
glutamine metabolic process
glutamine biosynthetic process
potassium ion transmembrane transport
cellular potassium ion transport
potassium ion transport
cell wall organization
external encapsulating structure organization
cell wall modification
cell wall organization or biogenesis
isoprenoid metabolic process
isoprenoid biosynthetic process
terpenoid biosynthetic process
terpenoid metabolic process
regulation of hormone levels
cytokinin metabolic process
cellular hormone metabolic process
hormone metabolic process
amine metabolic process
organic acid transport
organic anion transport
carboxylic acid transport
anion transport
mitochondrial pyruvate transmembrane transport
pyruvate transport
monocarboxylic acid transport
pyruvate transmembrane transport
response to oxygen−containing compound
response to acid chemical
response to inorganic substance
response to abiotic stimulus
response to water
response to other organism
response to external biotic stimulus
defense response to other organism
response to external stimulus
defense response
response to biotic stimulus
defense response to fungus
response to fungus
pollination
cell recognition
pollen−pistil interaction
multi−multicellular organism process
recognition of pollen
reproduction
reproductive process
multi−organism process
chitin metabolic process
aminoglycan catabolic process
chitin catabolic process
amino sugar metabolic process
cell wall macromolecule catabolic process
cell wall macromolecule metabolic process
amino sugar catabolic process
glucosamine−containing compound metabolic process
glucosamine−containing compound catabolic process
drug catabolic process
aminoglycan metabolic process
carbohydrate derivative catabolic process
regulation of response to biotic stimulus
regulation of immune system process
systemic acquired resistance
defense response, incompatible interaction
regulation of systemic acquired resistance
regulation of defense response
regulation of response to external stimulus
regulation of multi−organism process
innate immune response
regulation of innate immune response
regulation of immune response
regulation of response to stress
immune system process
immune response
regulation of response to stimulus
102
37
4
glutamine
potassium ion
organization
isoprenoid
terpenoid
biosynthetic
metabolic
amine cytokinin
hormone levels
organic carboxylic
pyruvate anion
abiotic inorganic
oxygen−containing
chemical
fungus other
biotic organism
multi−multicellular
pollen−pistil
recognition pollen
aminoglycan chitin
glucosamine−containing
catabolic
innate immune
acquired resistance
Cluster
LFTvLCT
RFTvRCT

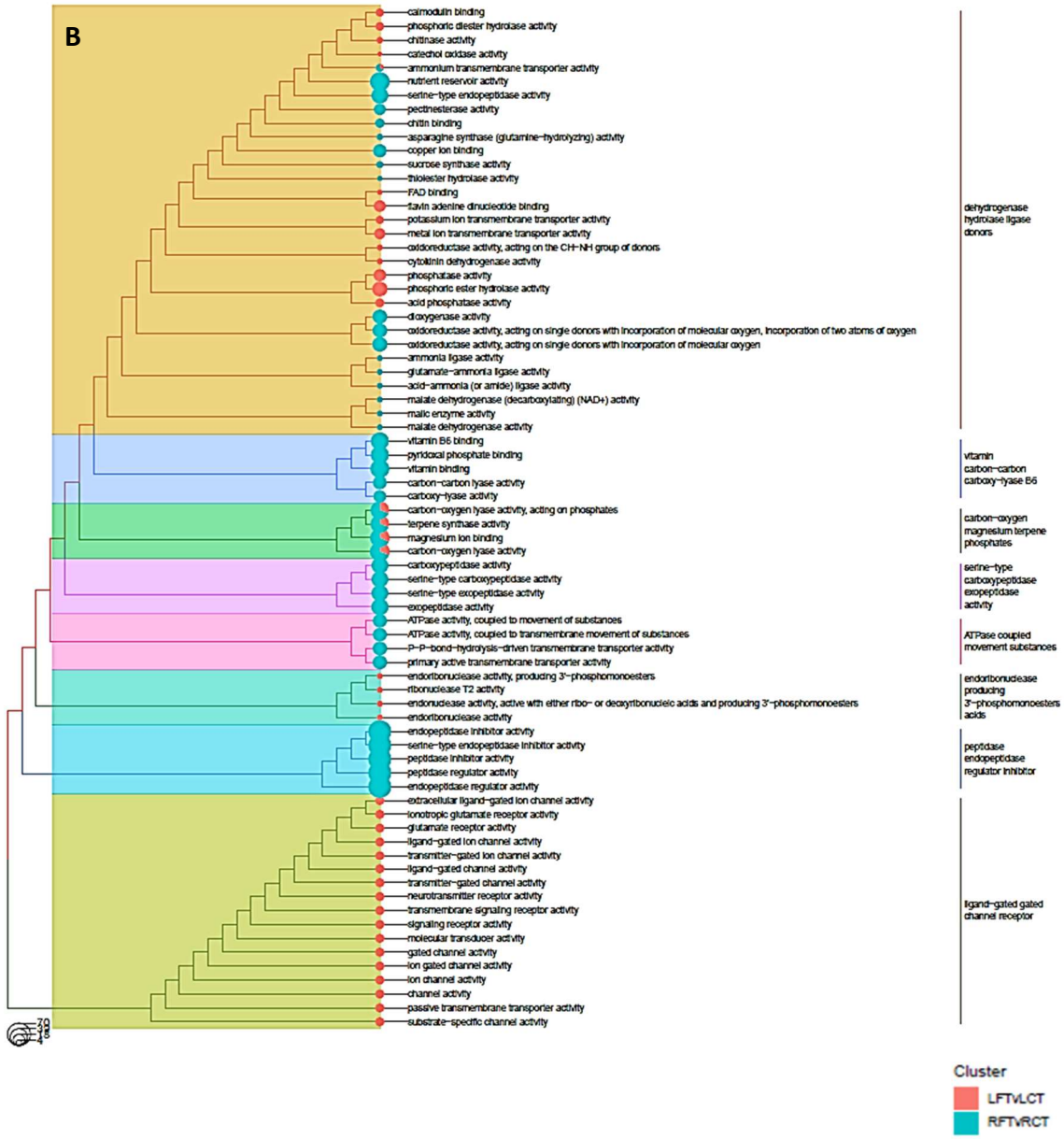
B
calmodulin binding
phosphoric diester hydrolase activity
chitinase activity
catechol oxidase activity
ammonium transmembrane transporter activity
nutrient reservoir activity
serine-type endopeptidase activity
pectinesterase activity
chitin binding
asparagine synthase (glutamine-hydrolyzing) activity
copper ion binding
sucrose synthase activity
thiolester hydrolase activity
FAD binding
flavin adenine dinucleotide binding
potassium ion transmembrane transporter activity
metal ion transmembrane transporter activity
oxidoreductase activity, acting on the CH-NH group of donors
cytokinin dehydrogenase activity
phosphatase activity
phosphoric ester hydrolase activity
acid phosphatase activity
dioxygenase activity
oxidoreductase activity, acting on single donors with incorporation of molecular oxygen, incorporation of two atoms of oxygen
oxidoreductase activity, acting on single donors with incorporation of molecular oxygen
ammonia ligase activity
glutamate-ammonia ligase activity
acid-ammonia (or amide) ligase activity
malate dehydrogenase (decarboxylating) (NAD+) activity
malic enzyme activity
malate dehydrogenase activity
vitamin B6 binding
pyridoxal phosphate binding
vitamin binding
carbon-carbon lyase activity
carboxy-lyase activity
carbon-oxygen lyase activity, acting on phosphates
terpene synthase activity
magnesium ion binding
carbon-oxygen lyase activity
carboxypeptidase activity
serine-type carboxypeptidase activity
serine-type exopeptidase activity
exopeptidase activity
ATPase activity, coupled to movement of substances
ATPase activity, coupled to transmembrane movement of substances
P-P-bond-hydrolysis-driven transmembrane transporter activity
primary active transmembrane transporter activity
endoribonuclease activity, producing 3'-phosphomonoesters
ribonuclease T2 activity
endonuclease activity, active with either ribo- or deoxyribonucleic acids and producing 3'-phosphomonoesters
endoribonuclease activity
endopeptidase inhibitor activity
serine-type endopeptidase inhibitor activity
peptidase inhibitor activity
peptidase regulator activity
endopeptidase regulator activity
extracellular ligand-gated ion channel activity
ionotropic glutamate receptor activity
glutamate receptor activity
ligand-gated ion channel activity
transmitter-gated ion channel activity
ligand-gated channel activity
transmitter-gated channel activity
neurotransmitter receptor activity
transmembrane signaling receptor activity
signaling receptor activity
molecular transducer activity
gated channel activity
ion gated channel activity
ion channel activity
channel activity
passive transmembrane transporter activity
substrate-specific channel activity
dehydrogenase hydrolase ligase donors
vitamin carbon-carbon carboxy-lyase B6
carbon-oxygen magnesium terpene phosphates
serine-type carboxypeptidase exopeptidase activity
ATPase coupled movement substances
endoribonuclease producing 3'-phosphomonoesters acids
peptidase endopeptidase regulator inhibitor
ligand-gated gated channel receptor
Cluster
LFTvLCT
RFTvRCT

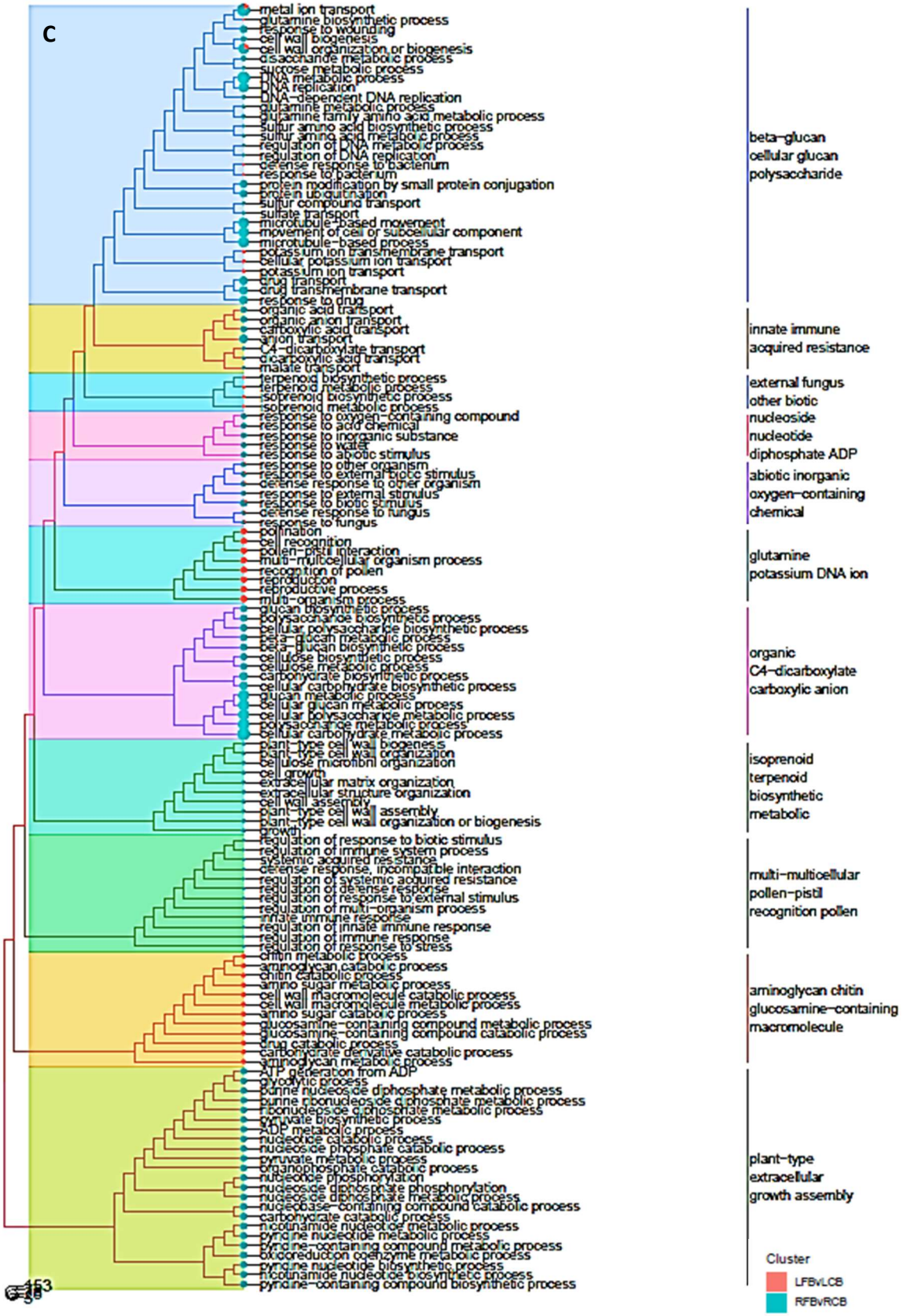
C
metal ion transport
glutamine biosynthetic process
response to wounding
cell wall biogenesis
cell wall organization or biogenesis
disaccharide metabolic process
sucrose metabolic process
DNA metabolic process
DNA replication
DNA-dependent DNA replication
glutamine metabolic process
glutamine family amino acid metabolic process
sulfur amino acid biosynthetic process
sulfur amino acid metabolic process
regulation of DNA metabolic process
regulation of DNA replication
defense response to bacterium
response to bacterium
protein modification by small protein conjugation
protein ubiquitination
sulfur compound transport
sulfate transport
microtubule-based movement
movement of cell or subcellular component
microtubule-based process
potassium ion transmembrane transport
cellular potassium ion transport
potassium ion transport
drug transport
drug transmembrane transport
response to drug
organic acid transport
organic anion transport
carboxylic acid transport
anion transport
C4-dicarboxylate transport
dicarboxylic acid transport
malate transport
terpenoid biosynthetic process
terpenoid metabolic process
isoprenoid biosynthetic process
isoprenoid metabolic process
response to oxygen-containing compound
response to acid chemical
response to inorganic substance
response to water
response to abiotic stimulus
response to other organism
response to external biotic stimulus
defense response to other organism
response to external stimulus
response to biotic stimulus
defense response to fungus
response to fungus
pollination
cell recognition
pollen-pistil interaction
multi-multicellular organism process
recognition of pollen
reproduction
reproductive process
multi-organism process
glucan biosynthetic process
polysaccharide biosynthetic process
cellular polysaccharide biosynthetic process
beta-glucan metabolic process
beta-glucan biosynthetic process
cellulose biosynthetic process
cellulose metabolic process
carbohydrate biosynthetic process
cellular carbohydrate biosynthetic process
glucan metabolic process
cellular glucan metabolic process
cellular polysaccharide metabolic process
polysaccharide metabolic process
cellular carbohydrate metabolic process
plant-type cell wall biogenesis
plant-type cell wall organization
cellulose microfibril organization
cell growth
extracellular matrix organization
extracellular structure organization
cell wall assembly
plant-type cell wall assembly
plant-type cell wall organization or biogenesis
growth
regulation of response to biotic stimulus
regulation of immune system process
systemic acquired resistance
defense response, incompatible interaction
regulation of systemic acquired resistance
regulation of defense response
regulation of response to external stimulus
regulation of multi-organism process
innate immune response
regulation of innate immune response
regulation of immune response
regulation of response to stress
chitin metabolic process
aminoglycan catabolic process
chitin catabolic process
amino sugar metabolic process
cell wall macromolecule catabolic process
cell wall macromolecule metabolic process
amino sugar catabolic process
glucosamine-containing compound metabolic process
glucosamine-containing compound catabolic process
drug catabolic process
carbohydrate derivative catabolic process
aminoglycan metabolic process
ATP generation from ADP
glycolytic process
purine nucleoside diphosphate metabolic process
purine ribonucleoside diphosphate metabolic process
ribonucleoside diphosphate metabolic process
pyruvate biosynthetic process
ADP metabolic process
nucleotide catabolic process
nucleoside phosphate catabolic process
pyruvate metabolic process
organophosphate catabolic process
nucleotide phosphorylation
nucleoside diphosphate phosphorylation
nucleoside diphosphate metabolic process
nucleobase-containing compound catabolic process
carbohydrate catabolic process
nicotinamide nucleotide metabolic process
pyridine nucleotide metabolic process
pyridine-containing compound metabolic process
oxidoreduction coenzyme metabolic process
pyridine nucleotide biosynthetic process
nicotinamide nucleotide biosynthetic process
pyridine-containing compound biosynthetic process
beta-glucan
cellular glucan
polysaccharide
innate immune
acquired resistance
external fungus
other biotic
nucleoside
nucleotide
diphosphate ADP
abiotic inorganic
oxygen-containing
chemical
glutamine
potassium DNA ion
organic
C4-dicarboxylate
carboxylic anion
isoprenoid
terpenoid
biosynthetic
metabolic
multi-multicellular
pollen-pistil
recognition pollen
aminoglycan chitin
glucosamine-containing
macromolecule
plant-type
extracellular
growth assembly
Cluster
LFBvLCB
RFBvRCB

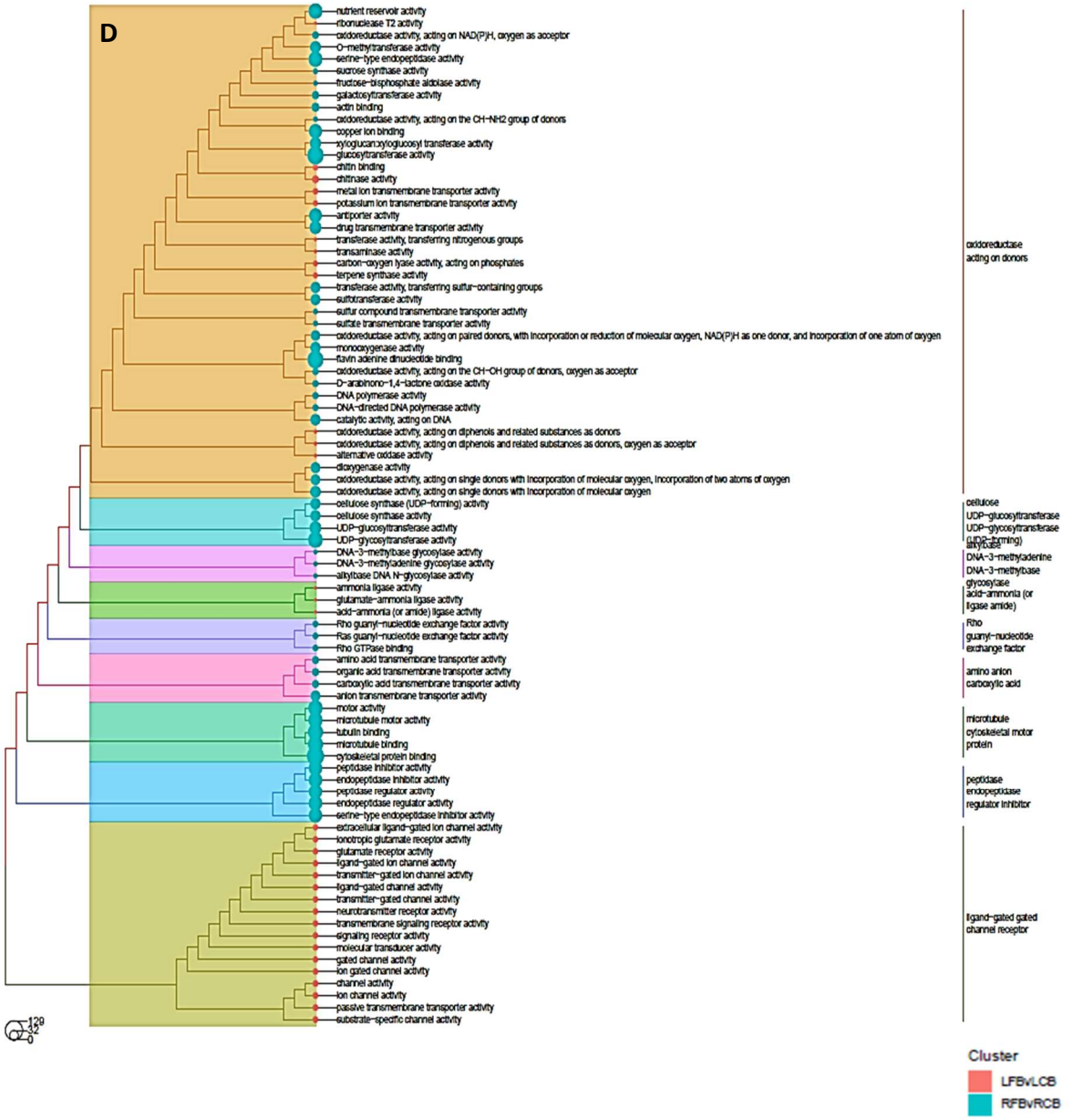

Appendix 9. Gene Ontology enrichment analysis of commonly de-regulated genes in response to 12 days of waterlogging. (A-D) Annotated GO terms in leaves (L) and roots (R) of waterlogged plants (F) compared with their respective controls (C) at (A, B) tillering (T) or (C, D) booting (B) stage. In all cases, GO analysis was performed for (A, D) biological processes and (B, C) molecular functions. Only transcripts showing a $\log_2$ fold-change ≥ |2| and P_{adj} ≤ 0.05 were considered.

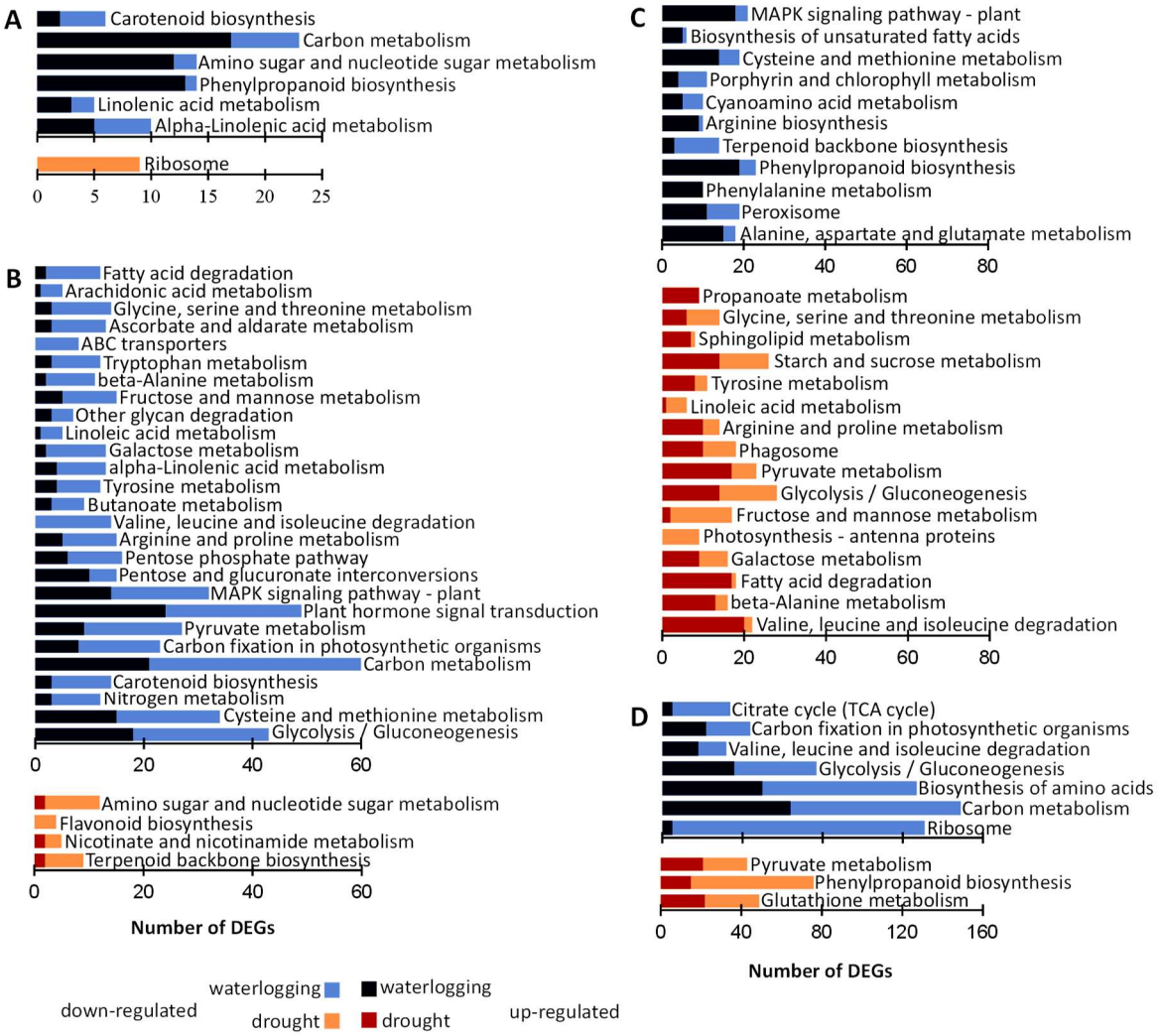

Appendix 10. Identification of functional categories associated with metabolic response mechanisms in waterlogged or drought-stressed plants. (A-D) Kyoto Encyclopedia of Genes and Genomes (KEGG) enrichment analysis of unique functional categories and de-regulated genes in (A, C) fully expanded leaves or (B, D) roots of plants under drought and waterlogging at (A, B) tillering or (C, D) booting stage. Transcript abundance was determined on day 12 after the onset of waterlogging or drought and considered significant if $\log_2$ fold-change $\geq |2|$ at $P_{adj} < 0.05$.

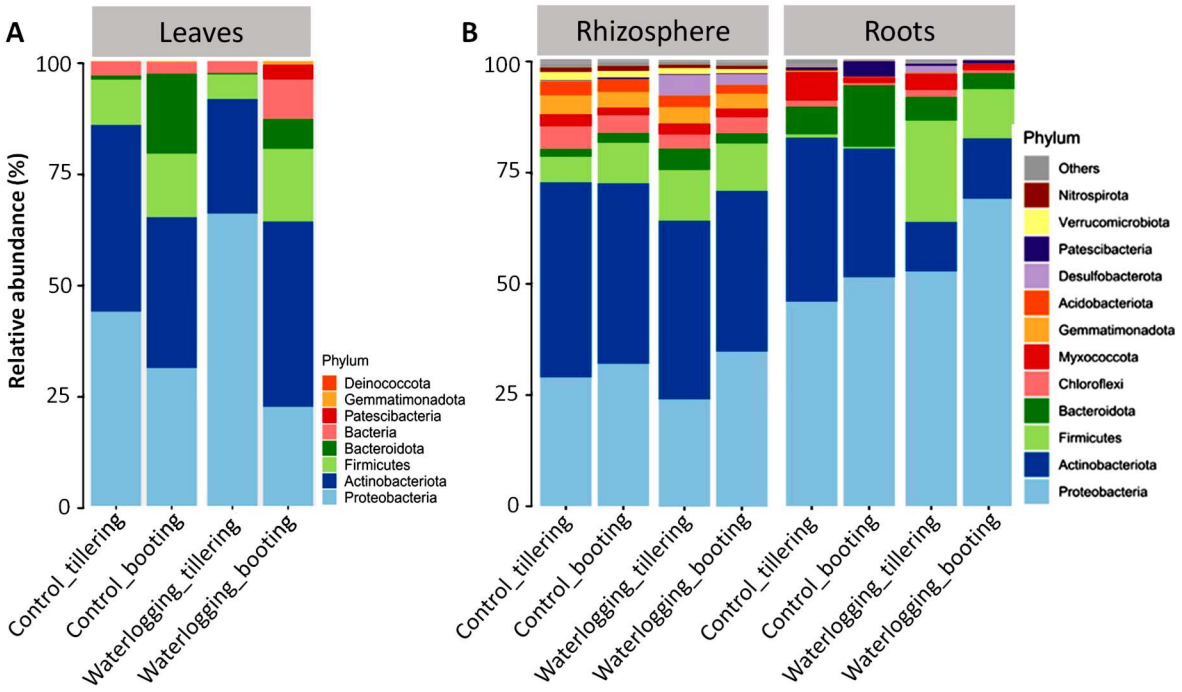

*Figure modified from Francioli *et al.* (2021), and Francioli *et al.* (2022a)

Appendix 11. Compositional shifts of the bacterial community in wheat plants in response to waterlogging at different developmental stages. (A) Relative abundance of the main bacterial phyla in the above-ground and (B) below-ground compartments. After 12 days of the onset of waterlogging, fully developed leaves, roots and rhizosphere soil were collected from control and waterlogging treatments at each developmental stage.

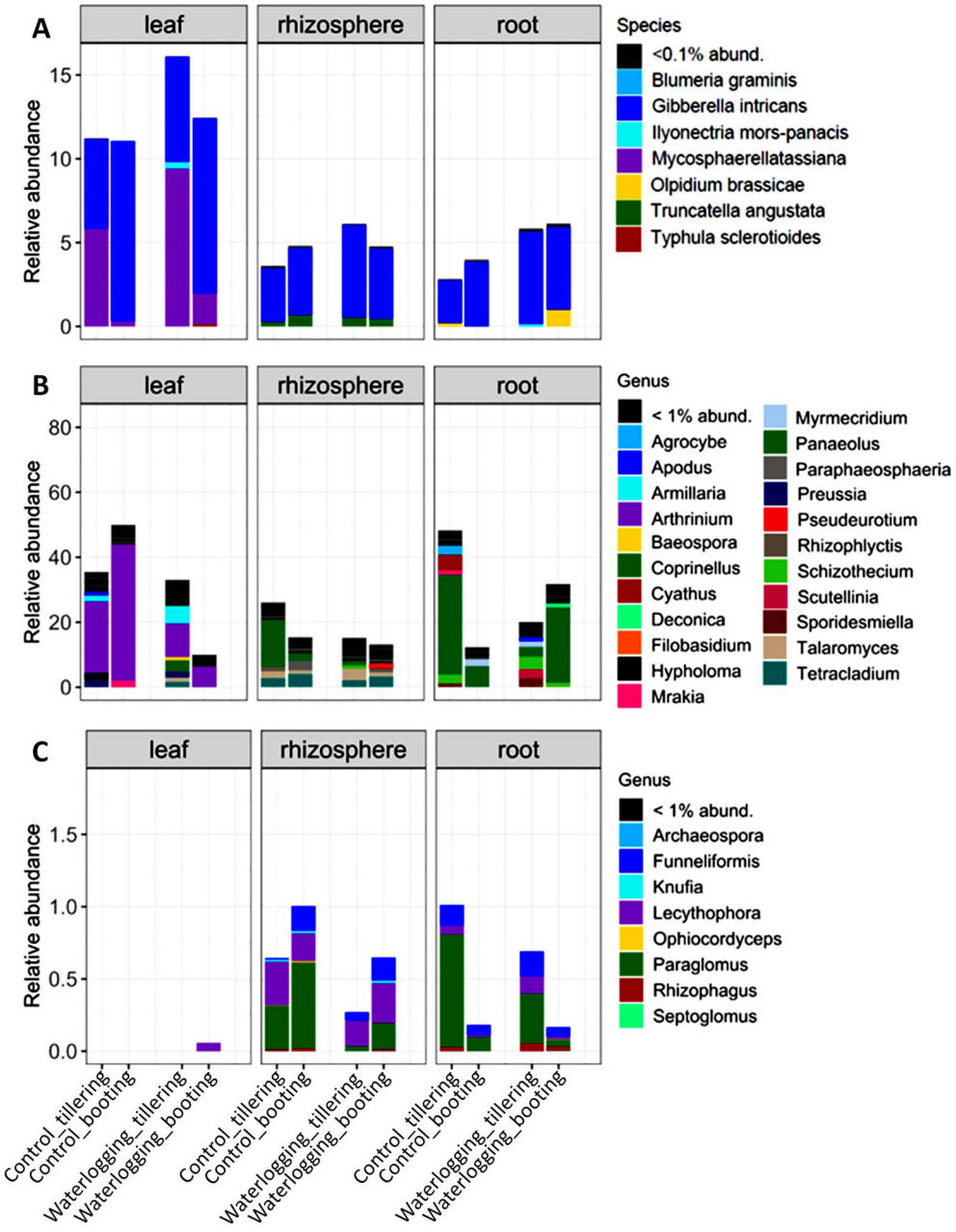

*Figure modified from Francioli *et al.* (2022b)

Appendix 12. Relative abundance of the (A) pathogenic, (B) saprotrophic and (C) mutualistic taxa detected in the leaves, roots and rhizosphere soil in response to waterlogging stress at different developmental stages. After 12 days of the onset of waterlogging, fully developed leaves, roots and rhizosphere soil were collected from control and waterlogging treatments at each developmental stage.

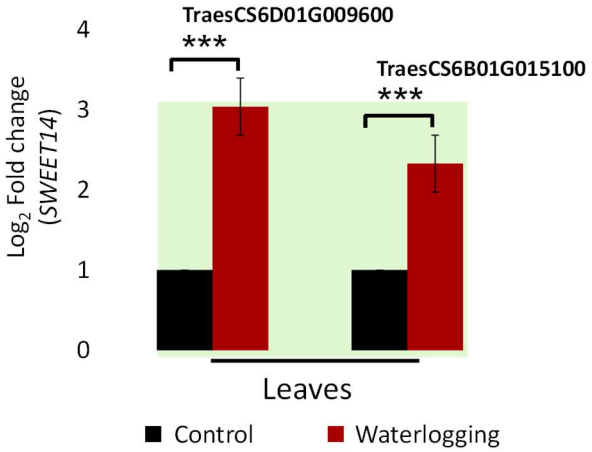

Appendix 13. Relative expression of *SWEET14* in the leaves of waterlogged plants. After 12 days of waterlogging, the fully developed leaves of the control or waterlogging treatments were collected at tillering stage. The bars show means ± SE. Different asterisks indicate significant differences at *** $P < 0.001$ according to Student's *t*-test or Mann-Whitney *U*-test, $P \leq 0.05$, n = 3.

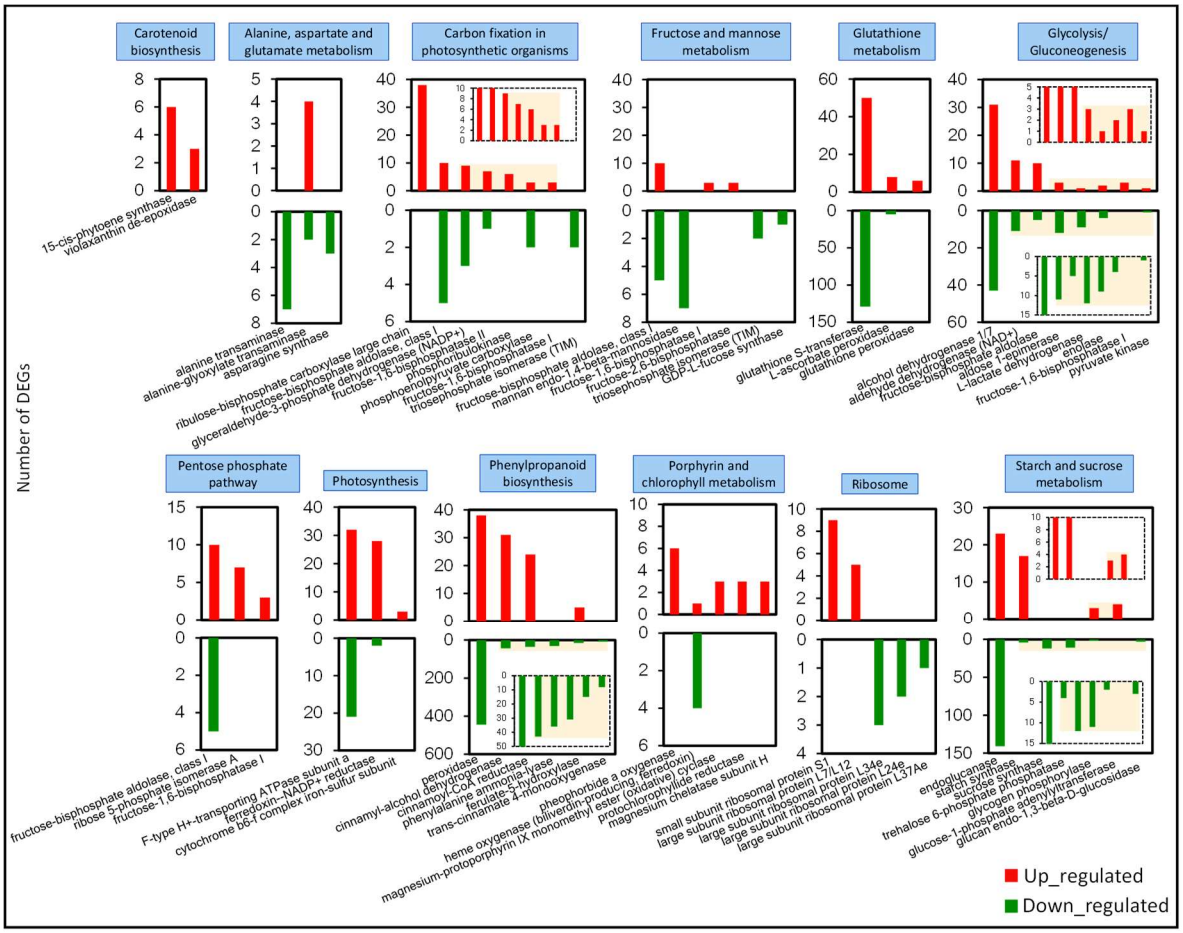

Appendix 14. Identification of functional categories associated with metabolic response mechanisms in waterlogged plants. Number of de-regulated genes present in the common metabolic pathways between leaves and roots of the same waterlogged plants at tillering stage. Green and red bars represent down- and up-regulated genes, respectively. In all cases, the genes for each metabolic pathway were considered according to their transcript abundance on day 12 after the onset of the waterlogging treatment. Genes were counted for each metabolic pathway considering $\log_2$ fold-change ≥ |2| and $P_{adj} < 0.05$.

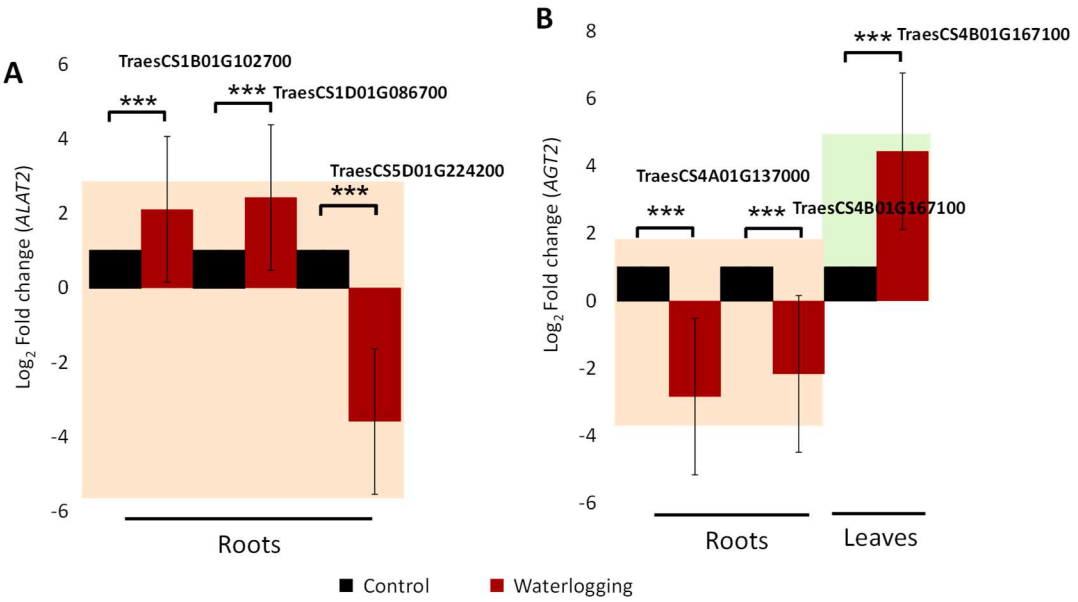

Appendix 15. Relative expression of (A) *ALAT2* in the roots and (B) *AGT2* in the leaves and roots of waterlogged plants. After 12 days of waterlogging, the fully developed leaves and roots of the control or waterlogging treatments were collected at tillering stage. The bars show the mean ± SE. Different asterisks indicate significant differences at *** $P < 0.001$ according to Student's *t*-test or Mann-Whitney *U*-test, $P \leq 0.05$, n = 3.

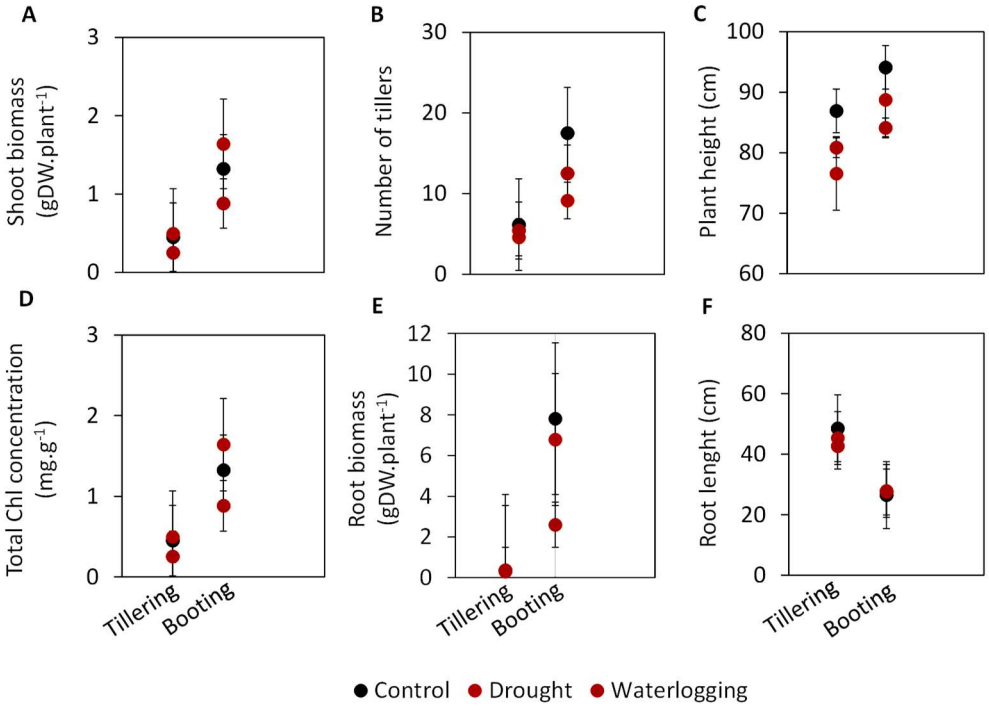

Appendix 16. Effect of drought and waterlogging on the growth of wheat plants at different stages of development. (A) Shoot biomass, (B) number of tillers, (C) plant height, (D) total chlorophyll concentration, (E) root biomass and (F) root length. After 12 days of drought or waterlogging, either at tillering or booting, the fully developed leaves and roots of the control and water treatments were collected. Each dot shows the mean ± SE (n=8).

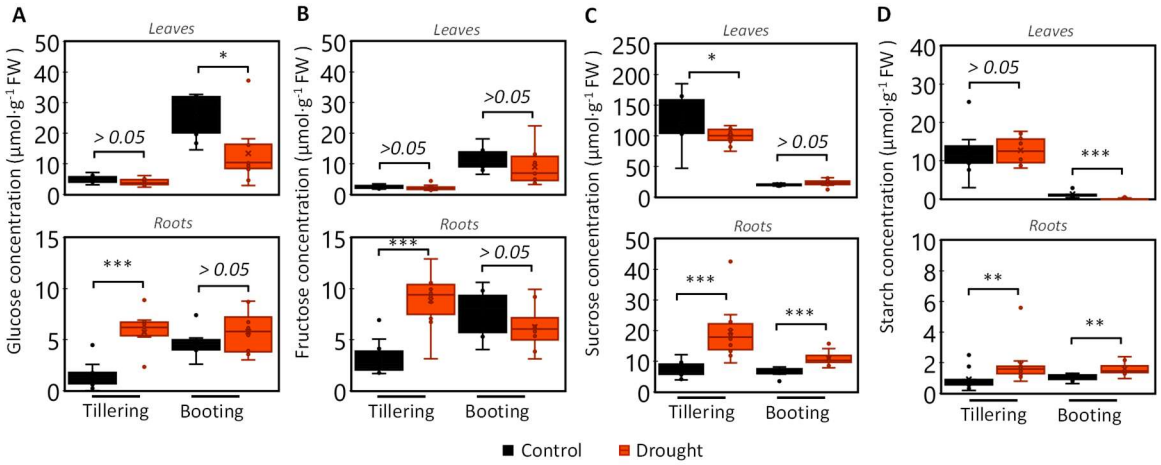

Appendix 17. Changes in non-structural carbohydrates in wheat plants exposed to drought. (A) Glucose concentration, (B) fructose concentration, (C) sucrose concentration, and (D) starch concentration in fully developed leaves and roots of drought-stressed plants. Soluble sugars were determined on the 12th day after the onset of drought in wheat plants at tillering or booting stage. Box limits indicate the 25th and 75th percentiles, horizontal lines show medians and whiskers extend to 1.5 times the interquartile range from the 25th and 75th percentiles. Different asterisks indicate significant differences at *** $P < 0.001$ according to Student's *t*-test or Mann-Whitney *U*-test, $P \leq 0.05$, n = 10 leaves, n = 9 roots.

9. ABBREVIATIONS

Abbreviation	***Name***
ABA	Abscisic acid
ACC	1-aminocyclopropane-1-carboxylic acid
ADH	Alcohol dehydrogenase
AGT	Alanine glyoxylate aminotransferase
AR	Adventitious roots
ALAT	Alanine aminotransferase
AQC	6-aminoquinolyl-N hydroxysuccinimidyl carbamate
ATP	Adenosine 5'-triphosphate
cDNA	Complementary Deoxyribonucleic Acid
CE	Collision Energy
Chl	Chlorophyll
cZR	*cis*-zeatin riboside
DEG	Differentially expressed genes
DM	Dry matter
DS	Developmental stages
Eh	Redox potential
ERF -VIIs	Ethylene response factors of the VII group
ESI	Electrospray Ionisation
ET	Ethylene
FAO	Food and Agriculture Organization of the United Nations
ENO2	Enolase 2
FM:	Fresh matter
FDR	False discovery rate
GAs	Giberellins
GABA	Gamma-aminobutyric acid
GAD4	Glutamate decarboxylase 4
GO	Gene ontology
HANZE	Historical analysis of natural hazards in Europe
H^+-ATPase	ATP phosphohydrolase (H^+-exporting)
HESI	Heated Electrospray Ionization
HPLC	High-Performance Liquid Chromatography
IAA	Indoleacetic acid
ICP-OES	Inductively coupled plasma optical emission spectroscopy
IPR	N6-isopentenyladenosine
JA	Jasmonic acid
JAIle	jasmonic acid-isoleucine
KEGG	Kyoto encyclopaedia of genes and genomes
KOH	Potassium hydroxide
LDH	Lactate dehydrogenase
mRNA	Messenger ribonucleic acid
MRM	Multiple Reactions Monitoring
MS	Mass Spectrometry

MS2	Tandem mass spectrometry
NaAc	Sodium Acetate
NASA	National Aeronautics and Space Administration
NIR	Nitrite transporters
NMR	Nuclear magnetic resonance
NO	Nitric oxide
NRT	Nitrate transporters
PA	Phaseic Acid
PCA	Principal Component Analysis
PCR	Polymerase Chain Reaction
PDC	Pyruvate decarboxylase
PDL	Plant available phosphorus
PPC4	Phosphoenolpyruvate carboxylase 4
PTFE	Polytetrafluoroethylene
RPKM	Number of reads per kilobase million
ROS	Reactive oxygen species
RNA	Ribonucleic acid
SA	Salicylic Acid
SUS	Sucrose synthase
SUT1	Sucrose transport protein SUT1
SWT	Soil water tension
SWEET	Sugars will eventually be exported transporters
TCA	Tricarboxylic acid cycle
TF	Transcription factor
TOC	Total organic carbon
TPI	Triosephosphate isomerase
tZR	*trans*-zeatin riboside
UPLC	Ultra-Performance Liquid Chromatography
UHPLC	Ultra-High-Performance Liquid Chromatography
Vario EL III C/H/N	Elementar Analyser vario
VWC	Volumetric water content
WHC	Water holding capacity

10. AFFIRMATION

I hereby declare, under penalty of perjury, that this thesis is the result of my own work and has been written solely using the references and resources mentioned. Any direct or indirect quotations from published sources have been appropriately indicated. This dissertation has not been previously submitted for academic evaluation or any other purposes. Additionally, I declare that no criminal record and no preliminary investigations are pending against me.

Hiermit versichere ich unter Strafandrohung wegen Meineids, dass diese Arbeit das Ergebnis meiner eigenen Arbeit ist und ausschließlich unter Verwendung der angegebenen Quellen und Ressourcen verfasst wurde. Jegliche direkten oder indirekten Zitate aus veröffentlichten Quellen wurden korrekt angegeben. Diese Dissertation wurde zuvor nicht zur akademischen Bewertung oder für andere Zwecke eingereicht. Zusätzlich erkläre ich, dass ich weder vorbestraft bin noch, dass gegen mich Ermittlungsverfahren anhängig sind.

_____ _____

Date / Datum Signature of the applicant / Unterschrift des Antragstellers

11. ACKNOWLEDGEMENTS

First, I would like to express my gratitude to my parents, Angela and Carlos, for their great support throughout my professional career and for helping me achieve all my goals.

I would also like to thank Dr. Mohammad-Reza Hajirezaei for providing me with the opportunity to work on this project over the past four years.

A special thanks goes to Prof. Dr. Nicolaus von Wirén for his support and contributions to my scientific education, as well as for his constructive criticism and unwavering motivation.

I extend my sincere gratitude to Bianka Jacobi and Dr. Britt Leps for their incredible support during these years and for making my time at IPK much smoother.

I am also deeply grateful to Dr. Yudelsy A. Tandrón-Moya and Prof. Dr. Davide Francioli for our extensive brainstorming sessions, data analysis, interpretation, and continuous motivation.

For the excellent technical assistance during these years, I am deeply thankful to Nicole Schaefer, Melanie Ruff, Barbara Kettig, Heike Nierig and Dagmar Böhmert. I also thank my former colleagues Dr. Markus Meier and Dr. Vanessa Paffrath for providing me with my first insights into the working group and the PhD Board. Additionally, I express my gratitude to all the VolCorn members, for their contribution with the progress and success of the project. For their best support in the greenhouse-experiments, I am grateful to the gardener team leaded by Enk Geyer.

I am grateful to Prof. Dr. Philipp Franken and Prof. Dr. Edgar Peiter for agreeing to evaluate this thesis.

Last but not least, I would like to thank all my colleagues form the Molecular Plant Nutrition group, especially Dr. Diana Heuermann, Dr. Mikel Rivero-Marcos, Dr. Anja Hartmann, and Dr. Ricardo-Fabiano Giehl for their willingness to share ideas and knowledge. My gratitude also goes to Jorge García, Rodolfo Augusto Maniero, and Gabriel Oliveira Ragazzo, for the best company during my stay at IPK.

12. CURRICULUM VITAE

Geeisy Angela Cid Valdés

Date of birth: December 17th, 1992

Place of birth: Ciego de Avila, Cuba

Education

09/2010-07/2015: **Chemical engineering** at the Central University "Marta Abreu", Santa Clara, Cuba (Diploma thesis on "Evaluating the use of additives in the crude PCNm1400 employed in the steam generation system of the Central Rum Industry")

10/2015-04/2018: **M.Sc. Plant biotechnology** at the University "Maximo Gomez", Ciego de Avila, Cuba (Master thesis on "Establishement of an extraction process for obtaining bioactive anthraquinones from *Morinda royoc* roots with scaling-up criteria")

06/2018-12/2018…… **Research internship** on "Antimicrobial activity of bioactive natural products against plant pathogens" at the Kompetenzzentrum Obstbau-Bodensee, Ravensburg, Baden-Württemberg, Germany.

06/2019-present……. **PhD Biological science** on "Unveiling metabolomic and transcriptomic responses to waterlogging in spring wheat at different developmental stages" supervised by Prof. Dr. Nicolaus von Wirén. Leibniz Institute of Plant Genetics and Crop Plant Research, Department of Physiology and Cell Biology, Molecular Plant Nutrition Group.

Participation in Courses and Workshops

02/2020: VOC's: from volatile sampling to data processing. German Centre for Integrative Biodiversity Research (iDiv). Halle-Jena-Leipzig, Germany

06/2022-09/2022: Workshop on "Metabolomics dedicated to deciphering plant responses to climate change". France-Germany.

07/2022: STARGATE training school in: Image Analyses for plant phenotyping: Wageningen University Research, Netherlands.

03/2023: de.NBI. Spring School 2023. Data management.

Publications

Francioli D, **Cid G**, Kanukollu S, Ulrich A, Hajirezaei MR, Kolb S. 2021. Flooding Causes Dramatic Compositional Shifts and Depletion of Putative Beneficial Bacteria on the Spring Wheat Microbiota. Frontiers in Microbiology 12

Francioli D, **Cid G**, Hajirezaei MR, Kolb S. 2022. Leaf bacterial microbiota response to fooding is controlled by plant phenology in wheat (*Triticum aestivum* L.). Nature. Scientific Reports 12.

Francioli Davide, **Geeisy Cid**, Mohammad-Reza Hajirezaei, and Steffen Kolb. 2022. Response of the wheat mycobiota to flooding revealed substantial shifts towards plant pathogens. Frontiers. Plant Science

Geeisy Cid, Davide Francioli, Steffen Kolb, Yudelsy Antonia Tandron Moya, Nicolaus von Wirén, Mohammad-Reza Hajirezaei. Elucidating the systemic response of wheat plants under waterlogging based on transcriptomic and metabolic approaches. Journal of Experimental Botany (in process).

Geeisy A. Cid Valdés

Nachterstedt, May 29th, 2023